AN ABSTRACT OF THE DISSERTATION OF

Matthew J. Quinn for the degree of Doctor of Philosophy in Microbiology presented on December 5, 2011.

Title: Molecular and Genetic Assessment of Selected Antiporters and Methyl-Accepting Chemotaxis Proteins in *Vibrio cholerae*

Abstract approved:

Claudia C. Häse

The pathogen *Vibrio cholerae* uses cations as a primary currency of virulence and environmental persistence, using gradients of those cations to move, acquire nutrients, and control virulence gene expression. An understanding of the overlapping roles of bioenergetics and chemotaxis in the virulence and environmental survival of *V. cholerae* issues from a large body of prior work, but the interplay of each component is not yet clearly understood. To this end, the activity of the antiporters Vc-NhaP1, Vc-NhaA, and Vc-NhaB was assayed, as was the sodium transporting respiratory pump NQR, and environmental stimuli were paired with potential motility-linked sensors. The Vc-NhaP1 antiporter was found to be a $K^+(Na^+)/H^+$ antiporter essential for *V. cholerae* growth at low environmental pH. Deletion of the *V. cholerae nhaP1* gene caused growth inhibition when external potassium was either limited (100 mM and below) or in excess (400 mM and above). This growth defect was most

apparent at mid-logarithmic phase, after 4-6 hours of culturing. Using a pH-sensitive GFP protein, cytosolic pH was shown to be dependent on K^+ in acidic external conditions in a Vc-NhaP1-dependent manner. When functionally expressed in an antiporterless *E. coli* strain and assayed in everted membrane vesicles, Vc-NhaP1 operated as an electroneutral alkali cation/proton antiporter, exchanging K^+ or Na^+ ions for protons within a broad pH range (7.25 to 9.0). These data establish the putative *V. cholerae* NhaP1 protein as a functional $K^+(Na^+)/H^+$ antiporter of the CPA-1 family that is required for bacterial pH homeostasis and growth in an acidic environment. Further, a model system comprised of a *V. cholerae* strain lacking both the *nqr* operon and the ORFs of *Vc-nhaA* or *Vc-nhaB* was generated and tested with and without lactate. These strains, along with the single mutants of *nqr*, *Vc-nhaA*, and *Vc-nhaB*, were assessed for aerobic growth as a function of media pH and cation concentration (Na^+, Li^+, or K^+). Loss of Vc-NhaA and, to a lesser extent, Vc-NhaB, was better observed when NQR was absent but lactate was added to facilitate replenishment of the quinone pool. Loss of Vc-NhaA in this background inhibited growth most at basic pH under increasing Na^+ and Li^+ conditions, and loss of Vc-NhaB in this background inhibited was most severe in acidic conditions in the presence of 0-100 mM Na^+ or Li^+. We also observed the growth inhibition of Vc-NhaA in the absence of NQR and in the presence of lactate and 100-450 mM Li^+, which has not been previously reported. These growth defects were restored upon expression of the cognate antiporter gene on an inducible expression vector. Lastly, potential chemotaxis stimuli were correlated with cognate methyl-accepting

chemotaxis protein (MCP) receptors. The homology of MCP sensory domains among *Vibrionaceae* demonstrated a subset were unique to *V. cholerae*. Of these unique MCPs, transposon insertion in VC0098 significantly reduced chemotaxis swarm diameter towards Na^+ and K^+. Additionally, the MCP VCA0663 was shown, by transposon mutagenesis and complementation, to direct chemotaxis towards N-acetyl-glucosamine. Additional observations are described concerning the chemotaxis defects incurred by transposon mutagenesis of MCPs *in vitro* towards mucin, bile, or L-serine. MCP strains were also tested *in vivo* for 4 and 24 hours in the infant mouse model of infection. None of the observed chemotaxis defects showed complete loss of chemotaxis by transposon mutagenesis, in line with the hypothesis that the large number of MCPs encoded by *V. cholerae* result in redundant chemotaxis sensory functions. These findings add to the understanding of how bioenergetics and chemotaxis interact within *V. cholerae*, a foundation from which the bacterium can be understood and, eventually, controlled.

Molecular and genetic assessment of selected antiporters and methyl-accepting chemotaxis proteins in *Vibrio cholerae*

by

Matthew J. Quinn

A DISSERTATION

submitted to

Oregon State University

in partial fulfillment

of the requirements for

the degree of

Doctor of Philosophy

Presented December 5, 2011

Commencement June 2012

Doctor of Philosophy dissertation of Matthew J. Quinn presented December 5, 2011.

APPROVED:

Major Professor, representing Microbiology

Chair of the Department of Microbiology

Dean of the Graduate School

I understand that my dissertation will become part of the permanent collection of Oregon State University libraries. My signature below authorizes release of my dissertation to any reader upon request.

Matthew J. Quinn, Author

ACKNOWLEDGEMENTS

The author expresses sincere appreciation to the following individuals, with whose support this work was made possible. Claudia Hase has been a constant source of expertise, guidance, and motivation, which has informed every facet of this research. Thanks must be given to the patience, understanding, and insight of the committee members: Gitali Indra, Malcolm Lowry, Walt Ream, and Mahfuz Sarker. Pavel Dibrov has patiently, but relentlessly, challenged every aspect of the author's understanding of bioenergetics, holding it to the highest of standards, for which the author is sincerely grateful. Similarly, Andrew Camilli was a source of inspiration and innovation, who spared valuable time to mentor the author. Yusuke Minato has been an exceedingly constant source of advice and support, for which no debt of sake can repay him. The author is also grateful to Jonathan Sun and Wyatt Faulkner for their unflagging diligence and willingness to engage in challenging research. Special mention must go to the author's scientific mentors: Carol Forward, who initiated this journey over 20 years ago by leading the author through Science Olympiad competitions and *ad hoc* fetal pig dissections; Ken Ward, who encouraged the author to pursue an advanced degree; Janine Trempy, whose levelheaded and earnest advice was heeded and welcomed; Linda Bruslind, who was a mentor of exceptional caliber; and Marcus Beck, who shared his passion and enthusiasm for teaching with the author, as well as the occasional glass of scotch. Kathy Quinn deserves special recognition for her unequalled motivation, inspiration, love, and support in this endeavor, and all others. Vincie Burnham has also been a constant and genuine source of love and

support. Jonathan Quinn gave love and support as only a brother could, colored by antagonism but overflowing with earnestness and honest affection. Most importantly, Delfina Homen's love, advice, support, encouragement, and epically delicious baking goods were a shining light in the darkest moments.

CONTRIBUTION OF AUTHORS

Erin Lind assisted with creating the mutants of *V. cholerae* strain O395N1 ΔnhaP1 and O395N1ΔnhaA, as well as the plasmids used for mutagenesis of the genes *nhaP1*, *nhaA*, and *nhaB*. Jonathan Sun assisted with data collection for Figures 2.1, 2.4, and 2.5. Wyatt Faulkner assisted with data collection for Figures in Chapter 3. EmilyKate McDonough assisted with data collection for Figure 4.4, supervised by Dr. Andrew Camilli.

TABLE OF CONTENTS

TABLE OF CONTENTS (Continued) Page

TABLE OF CONTENTS (Continued) Page

TABLE OF CONTENTS (Continued) Page

TABLE OF CONTENTS (Continued) Page

LIST OF FIGURES

LIST OF FIGURES (Continued)

LIST OF TABLES

Molecular and Genetic Assessment of Selected Antiporters and Methyl-Accepting Chemotaxis Proteins in *Vibrio cholerae*

1. General Introduction: *Vibrio cholerae*, bioenergetics, and motility

1.1. Background

Cholera has been a major cause of enteric disease throughout human history, the disease being known long before the discovery of its causative agent, *Vibrio cholerae*. Though ancient Greek and Sanskrit historical records may indicate cholera-like disease, it was not until 1854 that direct microscopic observation of the etiological bacterium was made by Filippo Pacini. The epidemiological studies of Whitehouse and Snow during the London cholera outbreak of 1854 found a correlation between drinking water from a single contaminated pump and disease incidence. Cholera incidence still correlates to contaminated drinking water, but since Snow's time several food borne vectors of cholera have been discovered, and together these two mechanisms are the most common means of acquiring cholera. Cholera is currently in its seventh pandemic, which has not abated in almost 50 years.

Like most enteric pathogens, *V. cholerae* is transmitted via the fecal-to-oral route. Left untreated, cases requiring hospitalization have a mortality rate of roughly 50% (Sack*, et al.*, 2004). Treatment via rehydration therapy is simple to administer, but many people still lack access to such modest healthcare. The global rate of cholera incidence is estimated to be over 100,000 people per year (Enserink), with a range of approximately 20,000 to 120,000 cases between 1995 and 2005 (Griffith*, et al.*, 2006). These reported cases represent only cases requiring hospitalization, so the true extent of cholera is almost certainly under-estimated. Endemic outbreaks are usually seasonal, as the bacterium has adapted to warm brackish waters in temperate estuarine environments (Singleton*, et al.*, 1982; Singleton*, et al.*, 1982; Miller*, et al.*,

1984). This niche underscores the link between pathogenesis and biology, as the adaptations the bacterium has made to dynamic changes in salinities allow it to exploit both the host and its reservoir. Unfortunately, while progress is being made in treatment and quick identification and containment of outbreaks, increased global warming coupled with the lack of infrastructure in impoverished nations will make *V. cholerae* a continuing threat to human health. For these reasons, it is imperative that the physiological and biochemical needs of *V. cholerae* be studied, to better understand potential means of controlling the bacterium and, thus, the disease for which it is named.

1.2. Classification and Characterization

Vibrio cholerae is a Gram-negative, oxidase positive, facultatively anaerobic, comma-shaped bacterium of the class Gammproteobacteria and the family Vibrionaceae. *Vibrio* species have a single polar flagellum which is sheathed by the outer membrane and can rotate at over 100,000 rpm (Magariyama, *et al.*, 1994) with a speed of over 60 μm per second (Atsumi, *et al.*, 1992; Atsumi, *et al.*, 1996). It can also be found in a biofilm state after colonization of the human intestine (Faruque, *et al.*, 2006), or in association with chitinous carapaces of copepods (Tamplin, *et al.*, 1990) or other plankton, or from water near endemic areas (Alam, *et al.*, 2006; Alam, *et al.*, 2007). The metabolism and virulence of *V. cholerae* is intertwined with salinity and pH, both of which the bacterium has adapted to utilize (Hase and Mekalanos, 1998; Hase and Mekalanos, 1999).

Over 200 serogroups of *V. cholerae* exist, and though many of these serogroups can cause mild diarrhea, only the O1 and O139 serogroups have been linked with cholera. It should be noted that some strains of the O1 and O139 serogroups do not cause cholera; therefore, serogroup identification is not conclusive evidence of cholera. Epidemic strains of the O1 and O139 serogroups contain both the CTX phage and the toxin co-regulated pilus (TCP). The CTX phage encodes the cholera toxin (in one or more loci), which is the causative agent of profuse diarrhea which is the hallmark symptom of cholera. TCP serves both as an adhesion factor *in vivo* and as the receptor for the CTX phage particle. These two factors are often enough for local clinicians to diagnose and treat cholera. However, a more detailed assessment of the serogroup, serotype, or biotype is important for an epidemiological study of how the disease spreads over distance and time.

The term "biotype" distinguishes two strains of *V. cholerae* which react with the same antiserum, referred to as classical and El Tor. Both biotypes bear the O1 serotype, and can be subcategorized into the subtypes Inaba, Ogawa, and Hikojima. The classical biotype of *V. cholerae* is presumed to have been the dominant biotype for much of the recorded history of cholera. At the outset of the seventh pandemic in 1961 the El Tor biotype predominated, though it had been documented as early as 1905; it also bears the O1 serotype, but can be differentiated from the classical biotype by several microbiological tests, discussed below. In 1992 a new serogroup of *V. cholerae* was isolated in India and Bangladesh, which became known as *V. cholerae*

O139 Bengal. It has since spread to pandemic proportions, and can currently be found alongside the O1 serotype, primarily in and near the Indian subcontinent.

V. cholerae is primarily categorized based on its oligosaccharide ("O") somatic antigen of LPS (reviewed in (Chatterjee and Chaudhuri, 2003)). The other bacterial antigenic determinants (flagellar and capsular) do not elicit a significant unique immune response, and so are not used in identification. Though there are over 200 documented serogroups of *V. cholerae*, only the O1 and O139 serogroups have been shown to cause cholera. The O1 serogroup identifies both the classical and El Tor biotypes, and the O139 serogroup applies to V. *cholerae* O139 Bengal isolates.

The reaction of *V. cholerae* to biochemical assays can differentiate the biotypes. The classical biotype can be distinguished from the El Tor biotype by simple microbiological tests (Kaper, *et al.*, 1995). El Tor strains can agglutinate chicken erythrocytes, give a positive Voges-Proskauer test, and sometimes exhibit hemolysis, whereas classical strains do not. Classical strains are inhibited by a 50U polymyxin B disk and are susceptible by lysis to the Classical IV bacteriophage (Mukerjee, *et al.*, 1963) and the FK bacteriophage (Takeya, *et al.*, 1981) while El Tor strains are not susceptible.

1.3. Distribution and Pandemics

Cholera has been described as a human health concern since ancient times, though it is difficult to track its epidemiology prior to microbiological observations. It is endemic to the Indian subcontinent, but when it began to spread past that to

pandemic proportion the Western world took notice. There have been seven pandemics of cholera in more recent times, the first six of which originated in the Indian subcontinent. Some uncertainty exists in regard to the exact dates of the pandemics; the dates given herein are compiled from Wilson (Wilson, 1984). The first pandemic began in 1817 and ended in 1823, and at its peak it had spread past Southeast Asia to the Middle East, the Caucuses and the Black Sea. The second pandemic lasted from 1826 to 1837, during which the pandemic spread to Western Europe and the Americas for the first time due to increased international travel, poor sanitary conditions, and an incomplete knowledge of the etiology of the disease. The mass deaths occurring in London and Paris during 1831 were met with confusion and anger, as the bacterial nature of the disease was not yet understood (Higgins, 1979). During the third pandemic, which lasted from 1846 to 1862, Dr. John Snow conducted his famous epidemiological assessment of the Broad Street well, which established that cholera during that outbreak was associated with drinking water. The fourth pandemic (1864-1875) struck the Americas again, notably affecting pioneers traveling west (Kaper*, et al.*, 1995). The fifth pandemic lasted from 1883 to 1896, during which Robert Koch correlated presence of the bacterium in stool samples of cholera victims to infection while studying cholera in Egypt and Calcutta (Koch, 1884). While Koch was recognized as the discoverer of the etiological agent of cholera, almost thirty years beforehand the Italian scientist Filippo Pacini correlated the disease with *V. cholerae* when he published his observations of the bacterium in association with intestinal mucosa of cadavers which had died of cholera ((Bentivoglio and Pacini,

1995) and reviewed in (Franceschini, 1971)). The sixth pandemic was the first of the 20th century, lasting from 1899-1923, but almost 40 years lapsed before the seventh pandemic erupted.

In 1961, the O1 El Tor biotype surfaced on Indonesia, which marked the beginning of the seventh pandemic (the spread of which is reviewed in (Barua, 1992)). Being more amenable to an asymptomatic state, it was carried and disseminated wider than the O1 classical strains. It spread into India and Iran by 1965, to the horn of Africa by 1970, and into most of sub-Saharan Africa by 1971. By 1991, the pandemic had spread to South America, where it had not been reported for nearly 100 years. The primary biotype causing cholera in South America was El Tor. One possible reason for the spread is the shift in oceanic currents linked with the El Niño climate change. The spread of cholera to a non-endemic area due to global warming is predicted, based on several factors discussed in section 1.4.5.

A new cholera-causing serogroup (O139 Bengal) also appeared in Bangladesh (Albert, *et al.*, 1993) and India in 1991 (Ramamurthy, *et al.*, 1993). It was the first time that a non-O1 serogroup was documented to have caused the disease (Hisatsune, *et al.*, 1993). With a novel O-antigen structure and the addition of a capsule of similar structure to the new O-antigen, O139 capitalized on the lack of immunity even in previously (O1) infected individuals. Currently, outbreaks can be caused by either the classical, El Tor, or Bengal strains. The evolution of these *V. cholerae* strains in relation to each other and their effect on human health will be of profound interest and important to observe in coming years.

1.4. Factors Affecting Outbreaks

While food, water, and horizontal transmission each plays an important role in the initiation or continuance of a cholera outbreak, the severity of an outbreak correlates with proper socio-economic, immune, and environmental conditions. The socio-economic variable is best represented by inadequate infrastructure, as measured by a diminished capacity to provide fresh water or sewage treatment, or when populations increase to levels that overwhelm previously adequate infrastructure. Access to proper health care is another socio-economic metric of cholera prevention. Immunity plays a large part in susceptibility to *V. cholerae* in endemic areas; the corollary is that immunological naïve persons (usually the very young) are the most at risk.

Variation in *V. cholerae* pathogenicity, coupled with immunological variance between people ensures that asymptomatic carriers can continue to shed the bacterium in their stool over a wide temporal and geographical range until conditions favorable for an outbreak arise. *V. cholerae* is also adapted to cause outbreaks under optimal environmental factors, such as water temperature and salinity. The association of *V. cholerae* with copepods also seems to be seasonal and to correlate with outbreaks. Ultimately, the severity of an outbreak can then be traced to an optimization of the following conditions: infrastructure; immunity; mobility of infected persons and persistent infection; environmental conditions; and global warming.

1.4.1. Infrastructure. Access to clean water and adequate sanitation is one of the best methods to prevent cholera. The size of the outbreak correlates to the degree

of sanitation, which can be measured by proper sewage treatment, adequate water treatment, and population density. These factors were used to predict incidence of disease at the state level during the Latin America outbreak of 1991-1992 (Sepulveda, *et al.*, 1992). The relevance of this metric to outbreaks in refugee camps and after natural disasters is obvious. The recent earthquakes in Pakistan and Haiti both precipitated cholera outbreaks due, in large part, to the damaged infrastructure in underdeveloped areas.

One of the worst and most recent outbreaks, in Zimbabwe in 2008, resulted in an estimated 4200 deaths and over 100,000 cases. The WHO could only estimate these numbers because political and socioeconomic conditions prevented an accurate epidemiological assessment (Nelson, 2009). A post-conflict outbreak among refugees returning to Juba, Sudan in 2007 led to a cholera outbreak affecting 3157 people with a case fatality rate (CFR) of 2% (Organization, 2009). During the Iraq war in 2007, Khwaif et al (Khwaif, *et al.*) assessed the extent of an outbreak of *V. cholerae* El Tor serotype Inaba infection and reported 4667 cases nationwide with a CFR in Bagdad of 2.2%. In 1994, refugees fleeing the Rwandan genocide into Zaire were victims of a cholera outbreak which left approximately 12,000 people dead and an unknown number infected (Siddique, 1994; Siddique, *et al.*, 1995).

A particularly interesting case took place in 2000 in South Africa. The taxes on water supplies meant to encourage government reinvestment in infrastructure backfired when impoverished citizens of KwaZulu-Natal province refused to pay the higher rates and, instead, began drinking untreated water. The water was

contaminated with *V. cholerae* and caused an outbreak affecting 103,320 people (Sidley, 2001; Griffith, *et al.*, 2006). In addition, numerous smaller outbreaks have been documented and current information on outbreaks can be obtained from the ProMED database (www.promedmail.org).

The relation of these outbreaks to food is not well documented. Except in the case of the 2000 South African outbreak, even a linkage to contaminated water source is poorly documented. The only common theme to the outbreaks just mentioned is that they occurred when infrastructure was compromised, regardless of the source (natural disaster, forced migration, or socioeconomics).

1.4.2. Immunity. The introduction of a non-O1 serogroup which causes cholera is more prone to cause outbreaks in endemic areas of cholera simply because it will not be subject to the acquired immunity of the local population constantly re-exposed to the O1 serogroup. The O blood group of humans has also been shown to play a role in the effectiveness of cholera toxin to induce diarrhea and will be discussed later in this chapter (section 1.5.5). Lastly, sub-clinical infections and asymptomatic carriers play an important role in the spread and maintenance of an outbreak.

1.4.3. Mobility of infected persons and persistent infection. Reference to cholera as a "waterborne" disease has two meanings. The traditional meaning implies that *V. cholerae* infects a person through drinking contaminated water or indirectly using water as a vehicle to contaminate the food or object which becomes directly infectious. The second meaning refers to mobility of the disease via waterways, either

by ocean or river travel. In the modern sense, this meaning must be expanded to include air travel. Long survival times of *V. cholerae* in both stool of asymptomatic carriers, as well as on contaminated foods, provides the mechanism for dispersal. Not all infections with virulent *V. cholerae* strains result in life-threatening diarrhea. A subset of those people will be colonized for a varying degree of time and will continue to shed the bacteria in their stool. When these carriers handle food under an unsanitary condition, they can become foci for outbreaks (Albert, *et al.*, 1997). Thus, asymptomatic carriers represent and important route by which a disease with such a short incubation period and quick pathogenesis can spread to pandemic proportions.

The two virulence factors of *V. cholerae* most involved in dissemination are cholera toxin and toxin co-regulated pilus (TCP). TCP mediates attachment to the intestinal epithelia during infection, which will be discussed in more detail in section 1.6.2. It is also known that cholera toxin induction in classical strains is reduced at 37^{o}C (Miller and Mekalanos, 1988; Gardel, *et al.*, 1994), an apparent contradiction medically but perhaps useful to the bacterium from an epidemiological perspective. These two virulence factors may account for the ability of asymptomatic carriers to disseminate the infection.

Studies of dissemination have shown that the biliary tract may play an important role. In the rabbit system, both classical and El Tor strains survived in experimentally infected gall bladders for fifteen weeks (Sayamov, 1963). "Cholera Dolores", a human carrier documented by Azurin et al. (Azurin, *et al.*, 1967), was able to shed El Tor bacteria for 4 years. The bacteria were found to inhabit the biliary tract.

Cholera toxin levels were not increased in El Tor strains exposed to bile (Gupta and Chowdhury, 1997), but were increased in a classical strain exposed to bile (Hung and Mekalanos, 2005). The difference was attributed to differences in the *ctx* promoter which allowed different expression levels of cholera toxin in classical and El Tor. Hung et al. (Hung, *et al.*, 2005) also demonstrated that bile induces biofilm formation, which enhances resistance to the bacteriocidal effects of bile. Incidentally, biofilms of *V. cholerae* were shed in rice water stool, and such inocula showed enhanced infectious ability (Faruque, *et al.*, 2006).

A recent statistical study of historical outbreak data kept by sanitary commissioners of the British East Indian province of Bengal (1891-1940) revealed some surprising trends which support a role for the asymptomatic carrier (King, *et al.*, 2008). The authors adapted epidemiological models to best describe the data observed, and discovered that the model that best fit the data predicted that acquired immunity lapsed after only several months rather than the previously estimated period of 3-10 years. The short immunity may decrease the susceptible population during an outbreak, thus stopping the outbreak relatively quickly in an affected locale while simultaneously allowing a second outbreak to occur within one year. The model also predicts a very high degree of asymptomatic or mildly infected individuals, on the order of 99%. This has been observed for El Tor infections but not for classical infections (Bart, *et al.*, 1970), which presumably was the biotype causing the infections recorded by the sanitary commissioners.

1.4.4. Environmental Conditions. Survival of *V. cholerae* outside the body is associated with many conditions. A review by Pollitzer et al. (Pollitzer, *et al.*, 1959) associated enhanced survival of *V. cholerae* with intermediate salinities, lower temperature, high organic content, near neutral pH, absence of light, and a lack of competing microbes. In association with many foods, *V. cholerae* shows increased resiliency at colder temperatures (Felsenfeld, 1965). Venkatraman and Ramakrishnan (Venkatraman, 1941) showed that *V. cholerae* survived for 198 days in a 2% sea salt solution. Building on this, El Tor was shown to increase its survival time in seawater from 10-13 days at 30-32^{o}C to 58-60 days at 5-10^{o}C (Pesigan, *et al.*, 1967). It was further shown that raw seafood contaminated experimentally with stool from cholera patients could produce vibrios for 2-4 days at ambient temperature (30-32^{o}C) and for 4-9 days when refrigerated (5-10^{o}C).

Infectivity and survivability are two different concepts, which is evident when considering that the seasonal nature of cholera infection in endemic countries is correlated to surface seawater temperature (Pascual, *et al.*, 2000). Notably, other conditions, such as a nutrient source, are required for the bacterium to thrive. The environmental nutrient source is likely copepods and the plankton they feed on, and during infection the bacterium naturally acquires nutrients from the infected person. Colder temperatures simply permit *V. cholerae* persistence until an infectious opportunity arises. The persistence of El Tor is often greater than that of classical O1, which is one factor explaining why the pandemic that started nearly 50 years ago has not yet ended.

The environmental link between *V. cholerae* and copepods must be discussed further, given the important role copepods play either as a direct or indirect food source for humans and the central role such food has just been shown to play in cholera infection (Colwell, 1996). Kaneko and Colwell reported that *Vibrio* spp. reached their maximum annual levels in US coastal waters in the summer, when surface water temperatures reached approximately 30^{o}C (Kaneko and Colwell, 1973). *In vitro* studies of *V. cholerae* O1 have shown that colonization of chitinous surfaces by the bacterium correlates with (a) increased temperature (optimum of 30^{o}C), (b) salinity of 1.5%, and (c) pH of 8.5 (Huq, *et al.*, 1984). These conditions are very similar to those found in endemic marine environments. Both classical and El Tor were directly observed to colonize the oral feeding area and egg sacs of the copepods *Acartia tonsa, Eurytemora affinis*, and *Scottolana*, as well as two more unidentified species from Bangladesh (Huq, *et al.*, 1983). Just one copepod can harbor 10^4 *V. cholerae* on its surface (Colwell, 1994).

Copepods thrive in the wake of primary production associated with phytoplankton blooms (Kiørboe, 1994). The bacteria pass up the food chain, colonizing each successive trophic level. Shellfish become colonized by consuming *V. cholerae*-bearing planktonic crustaceans (Hood and Ness, 1982; Hood, *et al.*, 1983). Thus colonized, crustaceans or fish become the vehicle for initial, if not sustained, human infection. The link between copepods and *V. cholerae* O1 in Bangladesh over the period 1987-1990 was established by biweekly fluorescent antibody detection of attached vibrios to adult copepods, juvenile copepods, nauplii copepods, cladocerans,

or zooplankton from pond and river water (Colwell, 1996). Using a stepwise logistic model, the increase in copepods was best correlated with the increase in *V. cholerae* prevalence, with correlation of the following additional variables being measured and ruled out: air and water temperature, pH, dissolved oxygen tension, water chemistry (bromine, calcium, carbon dioxide, chloride, NaCl, color, conductivity, copper, fluoride, water hardness, iodine, iron, manganese, phosphorous, nitrate, silicates, sulfates), blue green algae, chladocerans, colonial algae, diatoms, dinoflagellates, green algae, and volvox.

A novel preventative method capitalizes on the association of *V. cholerae* with plankton in the environment (Colwell, *et al.*, 2003). The fibers of sari cloth contain 20 μm pores which are large enough to catch plankton but not planktonic bacteria, yet simple filtration using sari cloth reduced cholera incidence by 38-52%. Such methods underscore the importance of understanding the life cycle of cholera in the environment, which in the case of sari cloth filtration takes advantage of the association of the bacterium and plankton in the environment. A more subtle conclusion is that water contamination leading to cholera may really be two-fold, being contaminated with plankton which, in turn, are contaminated with *V. cholerae*.

1.4.5. Global Warming. Any increase in global temperature will affect the distribution of disease outbreaks and cholera has been used to model such changes (Colwell, 1996). Satellite imagery in conjunction with epidemiological data points to a link between sea surface temperatures and cholera outbreaks in Bangladesh (Colwell, 1996; Pascual, *et al.*, 2000). The increase in temperature may affect cholera

environmental outgrowth directly or indirectly by altering nutrient availability and metabolic activity favorable to plankton blooms which, in turn, could permit cholera outgrowth (Huq, *et al.*, 1983; Huq, 1984; Tamplin, *et al.*, 1990; Kiørboe, 1994). Whatever the cause, the correlation is important in that sea surface temperatures will rise as global temperatures rise, which may encourage cholera to become endemic in countries in which it is not currently endemic. An example of such spread is the El Niño weather pattern, which is described as an increase in central Pacific sea surface temperature of 0.5^{o}C averaged over 3 consecutive months (NOAA, 2005). The increased temperature causes ocean currents to stagnate and prevent cold water from upwelling off the western coast of South America. The spread of the seventh pandemic to South America in 1991 also correlated with an El Niño event during the same time. Later environmental sampling also linked *V. cholerae* presence with El Niño conditions (Gil, *et al.*, 2004).

1.5. Clinical Features

V. cholerae may cause a range of diarrheal symptoms, but the most clinically significant and deadly is cholera gravis. The primary clinical characteristic of cholera gravis is the large quantity of watery diarrhea it produces. It is often called “rice water stool” due to the presence of mucus and epithelia which give the watery stool a slightly milky and textured appearance. Infection persists for between 2 and 5 days. Patients may continue to shed bacteria for some time after symptoms subside, as

mentioned previously, noteworthy because *V. cholerae* isolated from rice water stool is more infectious (Faruque, *et al.*, 2006).

1.5.1. Infectious Dose. Because cholera is easily treated when adequate healthcare is available, human volunteers provide valuable insight into the dynamics such as the infectious dose of disease. Such volunteer studies indicate that the infectious dose is 10^7-10^{11} when orally administered without bicarbonate (to neutralize stomach acidity (Cash, *et al.*, 1974)), but is as low as 10^4 when delivered under conditions which enhance the ability of the bacterium to survive passage into the intestine. Such conditions include co-administration with bicarbonate (Levine, 1980), with food, or in the VBNC state (Huq, 1984; Colwell, *et al.*, 1996)).

1.5.2. Incubation Period. The incubation period of cholera is 6-48 hours (Finkelstein, 1996). In a controlled laboratory study, volunteers given 10^4 cells of *V. cholerae* O1 El Tor developed mild diarrhea (0.6-1.5 L) by a mean onset of 36.5 hours while those given 10^6 cells (n = 9 of 10 symptomatic) developed 0.4-13.1 L of diarrhea beginning 25.5 hours after infection (Levine, 1981). When given 10^4 CFU of *V. cholerae* O139 with 2 g of sodium bicarbonate, a separate group of volunteers manifested cholera symptoms in 48-50 hours (Morris, *et al.*, 1995). The disease lasts up to 5 days without antibiotics and 2 to 3 days with antibiotics (Sack, *et al.*, 2004).

1.5.3. Symptoms. The most prominent feature of cholera is the sudden and painless onset of profuse watery diarrhea (Carpenter, 1971). Stool can be passed at the rate of 0.5-1.0 liter per hour (Sack, *et al.*, 2004) and tends to be most severe at the onset of the disease. The severe diarrhea over the course of an infection can rapidly

dehydrate the patient and is often the cause of death if left untreated. Patients tend to remain lucid throughout infection, as the dehydration does not inhibit higher brain functions. Other symptoms may include vomiting, acidosis, cramps, and circulatory collapse (Keen and Bujalski, 1992). Carpenter (Carpenter, 1971) reviewed the classical symptoms of cholera in severe patients. The patient may be cyanotic or have sunken eyes and cheeks, a scaphoid abdomen, poor skin turgor, a weak or absent peripheral pulse, tachycardia, tachypnea, or low to unmeasurable blood pressure. Low grade fever or mild hypothermia may also occur. In a 1996 study, classical biotype infection had a higher incidence of lower body temperature and slightly more stool than did O139 infection (Dhar*, et al.*, 1996).

1.5.4. Prognosis. Patients who develop cholera gravis are subject to a mortality of 50% or more if they do not receive medical care. However, evidence suggests that these patients represent only a fraction of people infected. Most people infected with *V. cholerae* do not develop symptoms of cholera gravis. Thus a CFR of less than 1.0% is a nominal value for populations affected by pandemic cholera. Due to the sometimes rapid onset and duration of the disease, some patients will die before medical care is sought, and this inherent speed leads to a CFR greater than 0. However, the disease is highly survivable when hospitalization is available. Therefore, human volunteer studies are regularly conducted and approved by institutional review boards.

1.5.5. Blood Group O. Barua and Paguio (Barua and Paguio, 1977) first noted the correlation between disease severity and blood group O in 1975 in the Philippines,

and further studies corroborated this (Chaudhuri and DasAdhikary, 1978; Clemens, *et al.*, 1989; Faruque, *et al.*, 1994; Swerdlow, *et al.*, 1994). In Peru, it was observed that the O blood group was strongly associated with severe cholera, which was measured by more diarrheal stools, higher likelihood to report vomiting and muscle cramps, and an eightfold increase in need for hospitalization as compared to other blood groups (Swerdlow, *et al.*, 1994). In each case, the etiological agent was *V. cholerae* El Tor. A correlation also exists between the O blood group and increased severity of disease caused by O139 as measured by stool production (Cohen, *et al.*, 1999). The molecular explanation for this observation is that the B subunit of cholera toxin can bind to the unique side chains of the A and B blood groups but not the O blood group. When the A or B blood group antigens are expressed on the intestinal lumen surface (about 80% of the population) they bind the cholera toxin B subunit and prevent it from interacting with the GM1 ganglioside and catalyzing pore formation or A subunit translocation across the membrane (see section 1.6.1 and (Holmner, *et al.*)). Thus, cholera toxin is unimpeded when not in association with A or B blood groups and is free to initiate the secretory diarrhea characteristic of cholera.

1.5.6. Treatment. Cholera is treated with a combination of intravenous fluid replacement or oral rehydration solution (ORS) coupled with antibiotic treatment when available (Keen and Bujalski, 1992). Treatment begins with an initial physiological assessment of dehydration as categorized by mild fluid loss (5% body weight), moderate fluid loss (7% body weight), or severe fluid loss (10% body weight) (Benenson, 1990). An intravenous or oral fluid replacement regimen then commences

to replace the quantity of fluid estimated to be lost. This can be a crude estimate when applied to adults, as osmotic fluctuations are better tolerated in adults. In children, the estimate must be more precise, as they are prone to brain damage when serum sodium concentrations reach 160-170 mEq/L (Carpenter, 1971). Where available, a "cholera cot" is used in affected countries, which provides a hole in the bed through which stool may pass into a collecting bucket. Antibiotics may be co-administered to reduce the duration of dehydration, though antibiotic resistance is always a concern.

1.5.7. Antibiotic Susceptibilities. The seventh pandemic cholera began shortly after the widespread usage of antibiotics due largely to the susceptibility of *V. cholerae* to tetracycline. Importantly, antibiotic treatment leads to a lower requirement of saline or ORS, which is often in limited supply in outbreaks as the lack of infrastructure associated with many outbreaks may limit the means by which ORS is acquired. The resistance of *V. cholerae* to antibiotics was originally noted in O139 isolates. However, the resistance is now commonly found in El Tor isolates as well. The antibiotic resistance of *V. cholarae* is mediated by the SXT mobile genetic element. It is one type of integrating conjugative element (ICE) which inserts into the bacterial chromosome but can be spread by conjugation (reviewed by Burrus (Burrus, *et al.*, 2006)). The SXT element was originally responsible for resistance to sulfamethoxazole, trimethoprim, chloramphenicol, and streptomycin (Waldor, *et al.*, 1996; Hochhut, *et al.*, 2001). However, the pattern of antibiotic use in an area selects for variants of this element tailored to protect the bacterium against antibacterial agents used locally. To illustrate this, genetic analysis of an SXT element from an El

Tor serotype Ogawa isolate from India showed resistance to ampicillin, polymixin B, co-trimoxazole, trimethoprim, streptomycin, spectinomycin, furazolidone, tetracycline, ciprofloxacin and naladixic acid (Kumar*, et al.*).

1.5.8. Vaccines. Because of the quick mortality associated with cholera, prevention via a vaccine has been a goal of health care researchers since shortly after Koch's discovery. Many vaccines have been attempted: parenteral, killed whole cell vaccines (Azurin*, et al.*, 1967; Mosley*, et al.*, 1972; Mosley*, et al.*, 1973); a vaccine derived from a modified cholera toxin (Lycke, 2005); Peru-15 (CholeraGarde), a live-attenuated oral cholera vaccine (Qadri*, et al.*, 2007); and an oral whole cell recombinant B subunit vaccine, Dukoral® (Dorlencourt*, et al.*, 1999; Legros*, et al.*, 1999). One of the most recent vaccines contains a mixture of formalin- or heat-killed serotypes of *V. cholerae* El Tor, classical, or Bengal (Kanungo*, et al.*, 2009). However, an effective vaccine has been elusive. In most cases, protection from a vaccine is lost within several years (Graves*, et al.*). Even immunity from prior exposure in endemic areas can subside within months, as discussed earlier, and, therefore, a short time span for immunity is expected. The value of vaccination, even with such short periods of efficacy, lies in herd immunity. The challenge, then, is the cost of repeated immunization on the scale of so many at-risk people per year, as individuals in endemic countries usually cannot afford such treatment (Enserink).

1.6. Virulence Factors

The primary virulence factors of *V. cholerae* are the cholera toxin (CT) and the toxin co-regulated pilus (TCP) while the primary regulator of toxicity is the ToxT transcriptional regulator. Other factors which also contribute to pathogenicity include hemagglutanins, biofilm formation, capsule, accessory toxins in addition to CT, bioenergetics (discussed further in Chapters 2 and 3), and motility (discussed further in Chapter 4).

1.6.1. Cholera Toxin. Cholera toxin (CT) was first hypothesized to exist by Koch (Koch, 1884). CT was discovered separately in 1959 by De et al. (De, 1959) and Dutta et al. (Dutta, *et al.*, 1959) and purified by Finkelstein and LoSpalluto (Finkelstein and LoSpalluto, 1969). CT is an A-B type toxin comprised of five B subunits with each unit containing 103 amino acids together having a mass of 11.6 kDa, and one A subunit which is proteolytically cleaved by host proteases into two peptides (A_1 being 195 amino acids, and A_2 being 45 amino acids) linked by a disulfide bond (Lonnroth and Holmgren, 1973; Spangler, 1992; Burnette, 1994; Zhang, *et al.*, 1995; Zhang, *et al.*, 1995). The B subunits form a pore in a target membrane, which allows the A subunit to enter the cytosol where the disulfide bond is broken and the A_1 peptide diffuses to its cytosolic target (the G_s protein) which controls adenylate cyclase activity. The cell surface receptor for B subunit binding is the GM_1 ganglioside expressed on intestinal epithelial cells (King and Van Heyningen, 1973; Pierce, 1973). The neuraminidase of *V. cholerae* aids infection by converting higher order gangliosides to GM_1 (Holmgren, *et al.*, 1975).

The primary effect of CT is to stimulate adenylate cyclase, resulting in an overexpression of cyclic-AMP (Sahyoun and Cuatrecasas, 1975). The $G_{s\alpha}$ protein target normally functions by binding GTP and activating adenylate cyclase. When GTP is cleaved to GDP, it inactivates the $G_{s\alpha}$ protein to which it is bound. However, the A1 subunit of CT was found to be the catalytically active portion of the toxin (Kassis*, et al.*, 1982). It can transfer the ADP-ribose moiety from NAD^+ to an arginine residue on the $G_{s\alpha}$ protein (Moss and Vaughan, 1977) and lock it in the active state to continually activate adenylate cyclase. The increase in concentrations of cAMP increases the activity of protein kinase A, which phosphorylates regulatory proteins that lead to increased chloride ion leakage in crypt cells and inhibitions of chloride and sodium ion uptake in villus cells. The resulting osmolyte accumulation in the lumen causes dehydration of host tissue that is in addition to the direct physiological effects of the ionic imbalance caused by sodium, potassium, and chloride ion leakage. When the purified toxin was given to human volunteers, a dose of 5 μg caused 1-6 L of diarrhea and a higher dose of 25 μg caused more than 20 L of diarrhea (Finkelstein, 1996).

CT production is regulated by ToxR (Champion*, et al.*, 1997) and ToxT (Brown and Taylor, 1995). The CT open reading frame is encoded as part of a lysogenic filamentous phage called CTXϕ, which targets *V. cholerae* and uses TCP as a receptor for binding the virion (Waldor and Mekalanos, 1996). The phage can exist as a self-replicating plasmid, or it can integrate into the chromosome as a prophage (Waldor and Mekalanos, 1996). The core region of the phage includes (upstream of

ctxA and *ctxB*) *zot*, *ace*, *orfU*, and *cep* (Baudry, *et al.*, 1992; Pearson, *et al.*, 1993; Trucksis, *et al.*, 1993) and upstream of this core region is RS2 encoding the *rstR*, *rstA*, and *rstB* genes (Sharma, *et al.*, 1997). Flanking the RS2-core region, on either side, is the RS1 region, which is identical to the RS2 with the addition of *rstC* (Chun, *et al.*, 1999; Faruque, *et al.*, 2002). As a prophage it integrates into the chromosome at *attRS* sites.

1.6.2. Toxin Co-regulated Pilus. TCP is a Type IV pilus which is expressed as long filaments on the surface of *V. cholerae* cells (Taylor, *et al.*, 1987) and has been shown to be an intestinal colonization factor in mice (Taylor, *et al.*, 1987) and in human volunteers (Herrington, *et al.*, 1988). It is encoded on the vibrio pathogenicity island (VPI, (Karaolis, *et al.*, 1998)). A mutation in the *tcpA* gene (the major subunit of the pilus) was shown to inhibit biofilm formation on chitinous surfaces, implying that TCP also has a role in the environmental phase in regulating biofilms (Reguera and Kolter, 2005).

1.6.3. ToxR Regulation. CT and TCP are controlled by the transcriptional regulator ToxT. The expression of ToxT, in turn, is regulated by the membrane proteins ToxR and TcpP, the latter of which is controlled by AphAB (Kovacikova and Skorupski, 1999; Kovacikova, *et al.*, 2004). ToxR seems to be expressed constitutively (Beck, *et al.*, 2004), though a recent report found that AphB controls ToxR expression in El Tor. Transcription of *aphA* is inversely linked to cell density via HapR (Kovacikova and Skorupski, 2002). Both AphA and AphB bind to the promoter of *tcpP* and initiate transcription given the appropriate environmental signals

(Kovacikova, *et al.*, 2004). TcpP, together with ToxR, ToxS (which maximizes the expression of ToxR-mediated *ctx* (Miller, *et al.*, 1989)), and TcpH (which prevents degradation of TcpP and, thus, regulates its activity post-translationally (Beck, *et al.*, 2004)), increase expression of ToxT (Hase and Mekalanos, 1998; Krukonis and DiRita, 2003; Childers and Klose, 2007). ToxT is part of the vibrio pathogenicity island (VPI), together with TcpP and TcpH, and known to regulate expression of itself, *ctxAB*, *tcpA*, *acf*, and *mshA*, among other proteins (Brown and Taylor, 1995; Hsiao, *et al.*, 2006), all of which contain the "toxbox" in their promoter (yrTTTTwwTwAww) (Withey and DiRita, 2006). While the expression of AphA and AphB are linked to quorum sensing, the signals they and ToxR and TcpP respond to help integrate cell density and environmental signals to enhance virulence factor expression. It should be noted that strain to strain variation is inherent because of the multiple levels of gene regulation described for these virulence factors. In short, such variation depends on the relative contribution of each of these factors relative to one another.

1.6.4 Hemagglutinins (HA). The mannose-sensitive HA (MSHA) has primarily been found in El Tor isolates (Jonson, *et al.*, 1991). It is a thin and flexible Type IV pilus (Jonson, *et al.*, 1991; Jonson, *et al.*, 1994). Lack of MSHA in a transposon mutant was linked to attenuation in mice (Finn, *et al.*, 1987). MSHA has been shown to mediate nutrient attachment, biofilm formation, and chitin utilization in aquatic environments (Watnick, *et al.*, 1999; Chiavelli, *et al.*, 2001; Meibom, *et al.*, 2004; Moorthy and Watnick, 2004). Interestingly, TcpJ catalyzes the degradation of

the MshA protein, suggesting that TCP and MSHA are optimized for different life stages with TCP for human infection and MSHA for environmental persistence (Hsiao, *et al.*, 2008). It was also noted that overexpression of *mshA* inhibited mouse colonization (Hsiao, *et al.*, 2008). It has been reported that ToxT, which is upregulated during infection, repressed MSHA (Hsiao, *et al.*, 2006). These observations are consistent with a model predicting that MSHA is important for environmental persistence. Another hemagglutanin, the mannose/fucose-resistant-HA (MFRHA) was first cloned by Franzon and Manning (Franzon and Manning, 1986). Loss of MFRHA led to attenuation in mice (Franzon, *et al.*, 1993), but its exact role in pathogenesis is not well defined.

The HA/protease (HAP) is a soluble metalloenzyme which cleaves fibronectin, mucin, and lactoferrin (Finkelstein, *et al.*, 1983). Loss of the *hapA* gene does not lead to attenuation (Finkelstein, *et al.*, 1992). It was hypothesized to be a "detachase" associated with the later stages of infection, specifically dissociation and escape from the intestine (Finkelstein, *et al.*, 1992). Its expression is regulated by HapR (Jobling and Holmes, 1997) which is in turn regulated by RpoS (Nielsen, *et al.*, 2006), an alternative sigma factor which responds to high cell density. Thus, it is likely that HAP degrades the intestinal mucus when bacteria sense that escape is warranted, as a function of increased cell density, lack of nutrients, and a mounting host immune response.

1.6.5. Ace, zot, cep. Accessory cholera enterotoxin (Ace) was originally identified as a protein capable of increasing short circuit current in Ussing chambers

(Trucksis, *et al.*, 1993). It was later shown to be part of the CTX phage (Waldor and Mekalanos, 1996), being 61% similar to gene VI of the Pseudomonas filamentous phage Pf1 (an M13 phage). Gene VI of M13 is a small hydrophobic protein involved in virion particle assembly. Similarly, the zonula occludens toxin (zot) was originally observed to increase the permeability of intracellular tight junctions (Fasano, *et al.*, 1991). However, discovery of the CTX phage showed that *zot* is similar to gene I of M13 phages, which is a membrane associated protein that aids in filamentous phage assembly. The core-encoded pilus (*cep*) gene encodes a protein that enhances colonization in mice (Pearson, *et al.*, 1990) but not in humans (Tacket, *et al.*, 1993) and its role in the CTX phage is not well understood.

1.6.6. Bioenergetics. The sodium cycle has also been linked to *V. cholerae* virulence through the influence of NQR on ToxT, though it is undoubtedly crucial for environmental persistence as well. In *V. cholerae*, the sodium cycle intertwines closely with respiration. The concept of an Na^+ cycle provides a convenient conceptual framework within which to examine the role of bioenergetic in virulence. This work, of course, builds on the seminal work of Peter Mitchell (Mitchell, 1961), whose work concerning the creation and use of a proton motive force (PMF) allows us to ask questions regarding the role of sodium within this system.

Research into the mechanism of sodium-linked oxidative phosphorylation began in the pre-genomic era with the discovery that *Propionigenium modestum*, a Gram negative anaerobic bacterium which inhabits aquatic mud and human saliva (Hilpert, *et al.*, 1984), phosphorylates ADP to ATP using a sodium electrochemical

gradient rather than a proton gradient (Kluge, *et al.*, 1992). This is an ingenious mechanism for salt water organisms and some extremophiles to energize major physiological functions under conditions when the PMF could bot be maintained at an adequate level; because a gradient of sodium energy is used rather than just proton energy, the resulting gradient is called sodium motive force (SMF). The primary danger of a sodium gradient lies in the osmotic balance which a living cell must maintain. By linking ATP synthesis to an influx of sodium ions (which are in abundance extracellularly in sea water), the cell must extrude those ions readily or the SMF will diminish and ATP synthesis, along with metabolism, will stall. Thus, microbes which utilize SMF must be able to maintain the gradient as it uses it; in *P. modestum*, a major mechanism of sodium homeostasis is the Na^+-motive decarboxylase, which couples the energy released through catabolism to Na^+ export (Bott, *et al.*, 1997), which maintains the SMF in a saline environment and enables ATP synthesis, as previously described. Similar Na^+-linked ATPases have been observed in environmental microbes such as *D. maritima* (Popova, *et al.*, 2005); such an ATPase has also been hypothesized to exist in several other genomes, based on conserved motifs in published genome sequences (Dzioba, *et al.*, 2003), as in *P. marinus* SS120 (Dufresne, *et al.*, 2003). *V. cholerae* was similarly thought to utilize the SMF by coupling NQR with a Na^+-translocating F_0F_1 ATPase, but it actually does not (Dzioba, *et al.*, 2003). Though it is also a marine microbe, *V. cholerae* spends part of its life cycle in the intestinal lumen of those it infects, and for a significant portion of time must traverse a low-sodium environment. In fact, because it is still dependent

on sodium, the massive diarrhea caused by the eponymous toxin merely increases the salt concentration to levels to which *V. cholerae* is accustomed, making the diarrhea an accidental but deadly side effect of a survival mechanism. Therefore, the use of SMF and PMF in *V. cholerae*, while overlapping, must be more nuanced.

One of the better studied components of the *V. cholerae* electron transport system is the Na^+-pumping NADH:quinone oxidoreductase (Hase and Barquera, 2001). By transferring electrons from NADH to ubiquinone (coenzyme Q) using cofactors such as FAD, FMN, and riboflavin (Barquera*, et al.*, 2002; Bogachev*, et al.*, 2002; Barquera*, et al.*, 2004), the complex of 6 subunits cooperate to pump sodium ions across the membrane from the cytosol into the periplasm. In contrast, the cytochrome cbb3 cluster of the C-Family exports protons, and that only through one channel (rather than 2 in mitochondrial cytochrome ccb_3) (Hemp*, et al.*, 2007). Thus, oxidation of NADH in *V. cholerae* generates a proton motive force and maintains the sodium gradient; the reasons for this are potentially tied to the combined marine/pathogenic environments this bacterium encounters.

The Na^+-pumping NADH:quinone oxidoreductase is a complex of proteins encoded by a six gene operon in many bacteria, termed *nqrABCDEF*. A recent publication showed the membrane topologies of each of the *V. choleae* NQR subunits and their consequent cellular locations based on PhoA and GFP fusions, a study needed because transmembrane prediction software gave sometimes conflicting predictions of membrane spanning regions, and the knowledge of membrane localization was needed to know the position of redox centers relative to the plane of

the membrane (Duffy and Barquera, 2006). NqrA was shown to be completely soluble (no transmembrane regions); NqrB, NqrD, and NqrE contained 9, 6, and 6 transmembrane helices, respectively; NqrC contained 2 transmembrane domains, and at each terminus, with the bulk of the subunit facing into the cytoplasm; and NqrF contained only one transmembrane helix at the N terminus. The importance of this study was in localizing the redox active prosthetic groups, which until recently were incompletely characterized (Duffy and Barquera, 2006).

Electron transfer in the NQR complex differs in several important ways from electron transfer in mitochondrial Complex I. While both systems use NADH as an electron donor, the accepting FAD prosthetic group (NqrF) accepts only one electron at a time; these are passed, in order, to a 2Fe-2S cluster (NqrF), an FMN prosthetic group and a separate FMNH prosthetic group in NqrB and NqrC, and a covalently bound ubiquinone-8 (Turk, *et al.*, 2004). Like mitochondrial Complex I, NQR of *V. cholerae* passes electrons to ubiquinone, but because it passes them individually, so NQR never fully reduces ubiquinone. Therefore, the ubisemiquinone radicals are prone to superoxide generation, and this indeed happens in the periplasm; superoxide increased in proportion to NADH concentration, in a manner which HQNO dissipated (by blocking quinol binding sites, preventing electrons from ever passing to ubiquinone) and cyanide increased (by blocking ubiquinone oxidation by quinol oxidase or cytochrome bc_1) (Lin, *et al.*, 2007). Further, the rate at which superoxide was produced was dependent on the concentration of cytoplasmic sodium. The production of extracellular superoxide linked to electron transport (in turn linked to

sodium pumping) seems counterintuitive at first glance. It may be a trait which aids in pathogenesis, or it could act as an indiscriminate defense mechanism against other microbes, both cases made possible because *V. cholerae* encodes a catalase. Superoxide production through NQR could be an antimicrobial mechanism used by *V. cholerae* during infection, representing another mode by which NQR can affect the virulence of *V. cholerae*.

The link between NQR and virulence is therefore difficult to ascertain. Because respiration is channeled through NQR in *V. cholerae*, which couples respiration to Na^+ content of the cell, individual cells could asses metabolic capacity indirectly, as a function of Na^+ content or turgidity, or directly via the quinone pool and ATP production. Transposon insertion into the NQR operon led to constitutive expression of TCP, as well as increased ToxT expression (as measured by a ToxT:LacZ fusion) when cells were cultured in acidic media (Hase and Mekalanos, 1998; Hase and Mekalanos, 1999). Therefore, virulence gene expression may be linked to loss of NQR-dependent Na^+ regulation, or through a stagnating quinone pool (and concomitant reduction of ATP synthesis) interpreted by the cell as a starvation state.

NQR is, of course, central to any discussion of bioenergetics in *V. cholerae* and, by extension, virulence. However, it is but one pump out of many that are encoded in the genome that have either been shown experimentally, or hypothesized by sequence similarity, to contribute to sodium homeostasis. These transporters, as well as their highest ranked HMM-designated protein family, are listed in Table 1.1.

The antiporters listed therein theoretically permit a proton dependent F_0F_1 ATPase coupled to SMF via electron transport (in the case of NQR) to be moderated by a combined sodium and proton gradient. *V. cholerae* has ten putative antiporters, five of which have now been characterized.

The first antiporter described in *V. cholerae* was NhaA (Vimont and Berche, 2000), which is an electrogenic antiporter as it transmits two protons into the cell for every sodium ion it pumps out. NhaA is most active at pH 8.5. NhaR regulates *nhaA* transcription in *E. coli* (Rahav-Manor, *et al.*, 1992) and *V. cholerae* (Williams, *et al.*, 1998). *V. cholerae nhaR* was found to restore tolerance of the *E. coli ΔnhaR* strain towards lithium (which tends to use the same channels as sodium and is much more toxic, making it a useful screen) at pH 7.6, and the deletion mutant lost the parent's ability to survive 150 mM NiCl at pH 9.5. This suggests that NhaR controls the expression of genes regulating lithium (and ostensibly sodium) balance, one of which is active at pH 9.5.

The second antiporter, NhaD, first described in 2002 as a homologue of Ec-NhaD (Dzioba, *et al.*, 2002), was activated at pH 7.75 and is electroneutral. NhaD specifically acidified medium containing inverted *E. coli ΔnhaAΔnhaB* inverted vesicles expressing *V. cholerae nhaD* in the presence of lactate, which was inhibited by NaCl. The maximum activity, as measured by dequenching of acridine orange in the same assay system, was found to be pH 8.0. The half-maximal response at pH 8.0 of these inverted vesicles was 1.1 mM, which is twice that of *E. coli nhaA* (Gerchman, *et al.*, 1993). NhaD could function to acquire Na^+ and expel H^+ at slightly basic pH,

replenishing the Na^+ pool so NQR can function, or NhaD could be linked to virulence gene regulation (Dibrov, 2005).

Lastly, Vc-NhaB needed to be characterized by expression in EP432 and in a *V. cholerae* strain lacking NhaA or NhaB, as a Na^+ or Li^+-related phenotype arising from single mutagenesis was masked by the residual activity of, presumably, NhaA (Herz*, et al.*, 2003). Vc-NhaB rescued the antiporterless strains at pH 7.0 in the presence of 400 mM Na^+ and 200 mM Na^+, respectively. Further, it was found that Vc-NhaB could not be functionally expressed in vesicles of EP432, prohibiting further *in vivo* biochemical assessment. Still other *nha* genes have yet to be characterized, the study of which will undoubtedly elucidate the complex interplay of bacteria with host and environment as it transitions between the two.

1.6.7. Motility. The characteristic single polar flagellum of *V. cholerae* makes the bacterium capable of high speed motility, which can be used diagnostically to identify the highly motile cells in stool of infected persons. *V. cholerae* uses this motility to pierce the mucus lining of the intestine and presumably to localize within the distal portion of the small intestine (Butler and Camilli, 2004). Such motility is obviously specific towards signals the bacterium can sense and move towards. The sensors dedicated to motility are methylating chemotaxis proteins (MCPs), a highly conserved class of transmembrane sensory proteins of which *V. cholerae* has 45 paralogues (Heidelberg*, et al.*, 2000; Boin*, et al.*, 2004). When active, each MCP induces the autophosphorylation of the cytosolic intermediate CheA2 (Gosink*, et al.*, 2002), which phosphorylates CheY3 in turn (Hyakutake*, et al.*, 2005), which direct the

flagellum to rotate counter-clockwise (to move forward) (Bren and Eisenbach, 2001). Methylation of the MCPs by CheR dulls the sensitivity of the sensor to its ligand (Springer and Koshland, 1977), which halts the phosphorylation cascade and causes the flagellum to spin clockwise and allows the bacterium to reorient, which in *V. alginolyticus* involve. When flagella were locked in a counterclockwise rotation, rendering motile bacteria incapable of responding to a chemotaxis sensory input, infectivity of the cells in an animal model was greatly increased (Butler and Camilli, 2004). Recently, inhibition of the flagellum regulatory cascade was shown to inhibit transcription of a novel hemagglutinin (*frhA*) in a c-di-GMP dependent manner (Syed, *et al.*, 2009). Clearly, the role of motility in *V. cholerae* virulence deserves further research, and a clear goal of such research is assigning stimuli to MCP sensors.

V. cholerae possesses 45 MCPs, whereas *E. coli*, which is used as a model of bacterial motility, contains but 5 MCPs (Wadhams and Armitage, 2004). Given what is already known about the intersection of virulence and motility in *V. cholerae*, it is worth investigating the ligand/MCP pairings of such a complex network of motility inputs to elucidate which contribute specifically to virulence. Three MCPs in *V. cholerae* have already been implicated in virulence, but their cognate ligands are unknown (Alm and Manning, 1990; Everiss, *et al.*, 1994; Harkey, *et al.*, 1994; Shikuma and Yildiz, 2009); a fourth MCP is known to sense a chitin oligomer (Meibom, *et al.*, 2004), and a fifth is known to sense the O_2 concentration (presumably by sensing the NADH content of the cell), but their role in virulence is unknown (Boin and Hase, 2007). Aerotaxis is an intriguing potential virulence factor, as the intestine

is normally anaerobic, so motility through the intestinal mucus to the epithelial surface (the cells of which are oxygenated) may well be directed, in part, by aerotaxis. Upon colonization, *V. cholerae* also experiences a transient increase in $\Delta\psi$ before initiating the transition to a biofilm (and, hence, a non-motile lifestyle) (Van Dellen, *et al.*, 2008), which may represent one more potential chemotaxis stimulus important for the environmental or virulent state.

The list of possible chemoattractants is long, though previously published work suggests that list can be narrowed to disease-related stimuli such as mucin (Freter and O'Brien, 1981), bile (Freter and O'Brien, 1981), N-acetyl-glucosamine (Meibom, *et al.*, 2004), and cations (Shikuma and Yildiz, 2009). Recent work shows that a strain lacking the transcriptional regulator OscR is defective in chemotaxis in soft agar swarm plates supplemented with NaCl (Shikuma and Yildiz, 2009). Interestingly, this strain also had diminished expression of two MCP genes, VC1967 (two-fold decrease) and VCA0988 (five-fold decrease) in response to sodium when analyzed by gene array analyses. Notably, the authors claim that OscR senses osmolarity, but assay only one cation (sodium), so the list of potential effectors should include other cations such as potassium and lithium. Recently, a double mutant of two MCPs (*tcpI* and *acfB*) was shown to be significantly more reduced in intestinal colonization than either single mutant (Chaparro, *et al.*, 2010). This demonstrates both that MCPs can be linked directly to intestinal colonization ability and that the great number of MCPs implies a redundancy of sensor/effector output function, as hypothesized. Clearly, the field of motility in *V. cholerae* must be studied in more

depth to better understand how motility governs virulence. MCPs will be discussed in much more detail in Chapter 4.

1.7. Study Objectives

Potassium/proton antiport activity has also been demonstrated in the *Vibrio* species *V. alginolyticus* (Tokuda, *et al.*, 1981; Nakamura, *et al.*, 1984), *V. parahaemolyticus* (Radchenko, *et al.*, 2006), and recently in *V. cholerae* (Resch, *et al.*, 2010). In *V. alginolyticus*, such activity has been shown to participate in regulation of cytoplasmic pH in acidic media (Nakamura, *et al.*, 1984; Nakamura, *et al.*, 1992). Although a K^+/H^+ antiporter was implicated in cytoplasmic pH maintenance in *V. alginolyticus*, the responsible ion transporter has not been identified. Many *Vibrio* species have three paralogues of NhaP (Table 1), a family of bacterial cation/proton antiporters identified by amino acid homology that generally pump Na^+ or K^+ (Resch, *et al.*, 2010). The NhaP2 homologue from *V. cholerae* was recently shown to have K^+/H^+ antiport activity in the parent as well as *E. coli* strains, showing also a unique response to Li^+ and strong *in vitro* activity (Resch, *et al.*, 2010). The *V. cholerae* NhaP2 antiporter was found to be a K^+/H^+ antiporter most active at low pH (6.0) which is indispensable for the growth of *V. cholerae* at extracellular potassium concentrations of 400 mM or greater in acidic media, removing excess of internal K^+ from the cytoplasm at the expense of ΔpH (Resch, *et al.*, 2010). The NhaP2 protein from *V. parahaemolyticus* was similarly shown to be involved in K^+/H^+ antiport at high concentrations of potassium when expressed ectopically in *E. coli* (Radchenko, *et*

al., 2006). As the NhaP2 antiporter is only one of three putative NhaP paralogues in *V. cholerae* identified by sequence similarity, we intend to also characterize the role of the other putative NhaP proteins, beginning with Vc-NhaP1, to assess their relative contribution to the overall cytoplasmic ion homeostasis.

Further examination of sodium ion homeostasis *in vivo* focused on the interaction of NhaA, NhaB, and NQR. Though the field of bacterial antiporter research is well characterized, the precise genetic mechanisms of environmental Na^+/H^+ and Li^+/H^+ resistance have not been fully described in *V. cholerae*. Specifically, Herz, *et al.*, (2003) found that the contribution of NhaA, NhaB, and NhaD to sodium or lithium tolerance of *V. cholerae* could only be observed upon chemical inhibition of NQR. A genetic assessment of this interaction was necessary to confirm these results by creating double antiporter/NQR mutants. Succesful creation of the strains O395N1ΔNQRΔnhaA and O395N1ΔNQRΔnhaB allowed an assessment of the relative contribution of NhaA, NhaB, and NQR to sodium and lithium toxicity, as a function of pH, in *V. cholerae*. These double mutants will also be useful as a background in which to test the function of as-yet uncharacterized antiporters of *V. cholerae*.

Lastly, of the 45 dedicated motility sensors in *V. cholerae*, MCPs, only two MCPs had been assigned stimuli prior to this study (see section 1.6.7), chitin (mediated by the MCP at locus VC0449) and oxygen (indirectly sensed by the MCP at locus VCA0658, termed Aer-2). The chemotactic response profiles of the remaining 43 MCPs have been largely uncharacterized. Utilizing a defined transposon library

containing insertions in each MCP of *V. cholerae*, a comprehensive assessment of transposon-mediated loss of function in defined media was possible. It was necessary and possible to assess which MCPs mediated chemotaxis in that media towards selected chemoattractants, including L-serine, N-acetyl-glucosamine (oligomerization of which forms chitin), mucin, bile salts, sodium, and potassium.

1.8. Tables

Table 1.1. *V. cholerae* proteins associated with generation or utilization of the SMF. When known, the gene name is indicated next to its locus tag. Match values represent the chance of a false positive identity; queries returning no value are rendered as 0.

Locus	HMM Description	HMM Accession	Match Value
VC2290 (NqrF)	Na^+-translocating NADH:quinone oxidoreductase (NQR), multi-subunit	TIGR01941	0
VC2291 (NqrE)		TIGR01940	1.7e-159
VC2292 (NqrD		TIGR01939	2.8e-158
VC2293 (NqrC)		TIGR01938	2.1e-144
VC2294 (NqrB)		TIGR01937	1.4e-285
VC2295 (NqrA)		TIGR01936	0
VC0549 (OadC)	Na^+-translocating oxaloacetate decarboxylase (OAD), multi-subunit	TIGR01195	3.9e-22
VC0550 (OadA)		TIGR01108	0
VC0551 (OadB)		TIGR01109	1e-165
VC1627 (NhaA)	Na^+/H^+ antiporter NhaA	TIGR00773	1.1e-278
VC1901 (NhaB)	Na^+/H^+ antiporter NhaB	TIGR00774	0
VC2037 (yqkI)	Na^+/H^+ antiporter NhaC-type	TIGR00931	7.1e-205
VCA0213 (NhaC2)	Na^+/H^+ antiporter family	PF03553	1e-109
VCA0193 (NhaC3)	Na^+/H^+ antiporter, putative	PF03553	1.1e-61
VC1131 (NhaC4)	Membrane protein, putative	PF03553	1.1e-122
VCA1015 (NhaD)	Na^+/H^+ antiporter NhaD	TIGR00775	1.8e-222
VC0389 (NhaP1)	Transporter, CPA-2 family	PF00999	2.6e-70
VC2703 (NhaP2)	Transporter, CPA-2 family	PF00999	7.2e-72
VC0689 (NhaP3)	Transporter, CPA-2 family	PF00999	1.3e-26
VCA0152 (MrpF)	Na^+/H^+ antiporter subunit	PF03334	2.8e-28
VCA0153 (MrpE)	Multiple resistance and pH regulation protein F	PF04066	8.6e-25
VCA0154 (MrpD)	Na^+/H^+ ion antiporter subunit	PF01899	1.5e-08
VCA0155 (MrpC)	NADH-ubiquinone/plastoquinone	PF00361	1.8e-47
VCA0156 (MrpB)	NADH-ubiquinone/plastoquinone oxidoreductase	PF00420	1.9e-15
VCA0157 (MrpA)	NADH-ubiquinone/plastoquinone	PF00361	2.2e-66
VC0784	Sodium:alanine symporter family	PF01235	1e-165
VC0795 (citS)	Citrate carrier protein, CSS family	TIGR00783	1.1e-195

VC1235	Transporter, DAACS family	PF00375	5.3e-103
VC1422	Sodium:alanine symporter family	PF01235	5.7e-170
VC2356	Sodium:alanine symporter family	PF01235	4.4e-232
VC2705	Transporter, solute:sodium symport (SSS) family	PF00474	2.4e-27
VCA0036	Transporter, DAACS family	PF00375	3.1e-139
VCA0041	Sodium/glutamate symporter	PF03616	5.8e-251
VCA0667	Transporter, solute:sodium symport (SSS) family	PF00474	5.3e-25
VCA1071 (putP)	Sodium:proline symporter	TIGR02121	0
VC0650	MATE efflux family protein	TIGR00797	2.2e-25
VC1540	MATE efflux family protein	TIGR00797	1.3e-166
VC1631	MATE efflux family protein	TIGR00797	1.5e-51
VC2671	MATE efflux family protein	TIGR00797	8.2e-48
VCA0989	MATE efflux family protein	TIGR00797	1.9e-36
VC1008 (MotY)	OmpA family	PF00691	1.5e-30
VC2601 (MotX)	N/A	---	---

NhaP1 is a $K^+(Na^+)/H^+$ Antiporter Required for Growth and Internal pH Homeostasis of *Vibrio cholerae* at Low Extracellular pH

Matthew J. Quinn, Craig T. Resch, Jonathan Sun, Erin J. Lind, Pavel Dibrov, and Claudia C. Häse

Manuscript accepted with minor revisions for publication in *Microbiology*, November 22, 2011.

2.1. Abstract

Vibrio cholerae has adapted to a wide range of salinity, pH and osmotic conditions, enabling it to survive passage through the host and persist in the environment. Among the many proteins responsible for bacterial survival under these diverse conditions, we have identified Vc-NhaP1 as a $K^+(Na^+)/H^+$ antiporter essential for *V. cholerae* growth at low environmental pH. Deletion of the *V. cholerae nhaP1* gene caused growth inhibition when external potassium was either limited (100 mM and below) or in excess (400 mM and above). This growth defect was most apparent at mid-logarithmic phase, after 4-6 hours of culturing. Using a pH-sensitive GFP protein, cytosolic pH was shown to be dependent on K^+ in acidic external conditions in a Vc-NhaP1-dependent manner. When functionally expressed in an antiporterless *E. coli* strain and assayed in everted membrane vesicles, Vc-NhaP1 operated as an electroneutral alkali cation/proton antiporter, exchanging K^+ or Na^+ ions for protons within a broad pH range (7.25 to 9.0). These data establish the putative *V. cholerae* NhaP1 protein as a functional $K^+(Na^+)/H^+$ antiporter of the CPA-1 family that is required for bacterial pH homeostasis and growth in an acidic environment.

2.2. Introduction

Vibrio cholerae is a Gram-negative pathogen which causes cholera, a dangerous disease that remains a public health concern (Enserink, 2010). As it transitions between the infectious state and its environmental reservoir, the bacterium encounters a dynamic range of osmotic and pH conditions. During human infection, *V. cholerae* produces the potent enterotoxin, cholera toxin, which promotes accumulation of Na^+ and Cl^- ions in the host intestinal lumen and, in turn, causes rapid osmotic dehydration of host tissue and profuse diarrhea. In the environment, *V. cholerae* is found in many coastal and estuarine waters where it is exposed to severe periodic changes in salinity, pH and osmolarity as variable ratios of brackish and fresh water are mixing at different rates (Singleton, *et al.*, 1982; Singleton, *et al.*, 1982; Miller, *et al.*, 1984). Thus, both the pathogenic and environmental lifestyles of this organism require that *V. cholerae* can adapt to rapidly shifting osmolarities, ionic strengths and pH values. These lifestyles require that *V. cholerae* possess adequate molecular mechanisms to adapt to such environmental challenges.

A number of *V. cholerae* proteins have been described that generate, maintain, or use a transmembrane gradient of cations such as Na^+ (Hase, *et al.*, 2001). These proteins are predicted to help the bacterium survive hypo- and hyperosmolar states in addition to exploiting the Na^+ gradient for solute transport, pH regulation, and motility. For example, the NQR complex couples Na^+ export to electron transport, resulting in the generation of a sodium motive force that can then be used for various types of membrane work (Tokuda and Unemoto, 1981; Tokuda and Unemoto, 1982;

Zhou, *et al.*, 1999). The *V. cholerae* NhaA antiporter mediates Na^+/H^+ exchange and thus regulates sodium ion homeostasis at pH 8.5, conditions which are not unusual for seawater in areas where *V. cholerae* is endemic (Vimont and Berche, 2000). The NhaD antiporter from *V. cholerae* expressed in *E. coli* sub-bacterial vesicles was shown to be a specific sodium/proton antiporter most active at pH 8.0 (Dzioba, *et al.*, 2002), whereas the *V. cholerae* Mrp complex is an electrogenic cation/proton exchanger of broad specificity, exchanging Na^+, K^+, and Li^+ with maximum of activity at pH 9.0-9.5 (Dzioba-Winogrodzki, *et al.*, 2009). Several membrane systems exploit the transmembrane Na^+ gradient generated by primary (e.g., NQR) or secondary (e.g., NhaA) sodium pumps to drive nutrient acquisition and motility (see (Hase, *et al.*, 2001)). The Na^+ ions which consequently accumulate in the bacterial cytoplasm are then again expelled by antiporters or NQR, resulting in internal cation homeostasis within dynamic external environments.

Potassium/proton antiport activity has also been demonstrated in the *Vibrio* species *V. alginolyticus* (Tokuda, *et al.*, 1981; Nakamura, *et al.*, 1984), *V. parahaemolyticus* (Radchenko, *et al.*, 2006), and recently in *V. cholerae* (Resch, *et al.*, 2010). In *V. alginolyticus*, such activity has been shown to participate in regulation of cytoplasmic pH in acidic media (Nakamura, *et al.*, 1984; Nakamura, *et al.*, 1992). Although a K^+/H^+ antiporter was implicated in cytoplasmic pH maintenance in *V. alginolyticus*, the responsible ion transporter has not been identified. Many *Vibrio* species have three paralogues of NhaP (Table 1), a family of bacterial cation/proton antiporters identified by amino acid homology that generally pump Na^+ or K^+ (Resch,

et al., 2010). The NhaP2 homologue from *V. cholerae* was recently shown to have K^+/H^+ antiport activity in the parent as well as *E. coli* strains, showing also a unique response to Li^+ and strong *in vitro* activity (Resch, *et al.*, 2010). The *V. cholerae* NhaP2 antiporter was found to be a K^+/H^+ antiporter most active at low pH (6.0) which is indispensable for the growth of *V. cholerae* at extracellular potassium concentrations of 400 mM or greater in acidic media, removing excess of internal K^+ from the cytoplasm at the expense of ΔpH (Resch, *et al.*, 2010). The NhaP2 protein from *V. parahaemolyticus* was similarly shown to be involved in K^+/H^+ antiport at high concentrations of potassium when expressed ectopically in *E. coli* (Radchenko, *et al.*, 2006). As the NhaP2 antiporter is only one of three putative NhaP paralogues in *V. cholerae* identified by sequence similarity, we intend to also characterize the role of the other putative NhaP proteins, beginning with Vc-NhaP1, to assess their relative contribution to the overall cytoplasmic ion homeostasis.

Here, we report the detailed characterization of the putative *V. cholerae* NhaP1 protein, encoded by VC0389 (NP#230338.1). We performed growth analysis of a defined in-frame *V. cholerae nhaP1* deletion mutant and compared the ability of the parental strain and its isogenic mutant strain to regulate cytoplasmic pH. We also assayed key biochemical features of the Vc-NhaP1 protein heterologically expressed in an *E. coli* strain lacking three major cation/proton antiporters. The presented results represent the first detailed physiological and biochemical analyses of a NhaP1-type of antiporter.

2.3. Materials and Methods

2.3.1. Bacterial Strains and Culture Conditions. The Na^+/H^+ antiporter-deficient strain of *E. coli* TO114 [F l IN (*rrnD-rrnE*) *nhaA*::Km^R *nhaB*::Em^R *chaA*::Cm^R] was kindly provided by H. Kobayashi (Faculty of Pharmaceutical Sciences, Chiba University, Chiba, Japan) (Radchenko, *et al.*, 2006). For routine cloning and plasmid construction, DH5α (*supE*44 *hsdR*17 *recA*1 *endA*1, *gyrA*96 *thi*-1 *relA*1) (U.S. Biochemical Corp.) or TOP10 [F- *mcr*A Δ(*mrr-hsd*rms-*mcr*BC) Δ80*lacZ*ΔM15 Δ*lac*X74 *rec*A1 *ara*D139 Δ(*ara leu*) 7697 *gal*U *gal*K *rps*L (Str^R) *end*A1 *nup*G] (Invitrogen) was used as the host. *V. cholerae* strain O395N1 was used in this study (Mekalanos, *et al.*, 1983), which is a classical Ogawa strain with a deletion in the *ctxA* gene (O1 classical biotype; Sm^R, Δ*ctxA*1). If not otherwise indicated, TO114 cells were grown aerobically at 37 °C in LBK medium [modified L broth in which NaCl was replaced with KCl (Padan, *et al.*, 1989)] supplemented with 100 μg/mL ampicillin, 30 μg/mL kanamycin, 34 μg/mL chloramphenicol, 100 μg/mL erythromycin, and 0.05% (w/v) arabinose. *V. cholerae* cells were grown aerobically at 37°C in LB supplemented with 100 μg/mL streptomycin, 100 μg/mL ampicillin, and 0.02% (w/v) arabinose, unless otherwise indicated. Cytoplasmic pH experiments were conducted in K100 media, a minimal salts medium with K^+, and K0 media, in which K+ salt were replaced with Na^+ salts (Epstein and Kim, 1971); cytoplasmic pH was measured in pH media (150 mM choline chloride and 60 mM Bis-Tris propane [BTP] adjusted to pH 6.0, 6.5, or 7.2).

2.3.2. Cloning and Expression of Vc-NhaP1. Sequence data for *V. cholerae* were obtained from the Institute of Genomic Research (http://www.jcvi.org). Cloning was performed as described before (Resch, *et al.*, 2010). The putative *Vc-nhaP1* ORF was amplified by high-fidelity polymerase chain reaction (PCR), using chromosomal DNA of *V. cholerae* O395N1 as a template and directly cloned into the pBAD-TOPO vector (Invitrogen) under the arabinose-induced promoter (P_{BAD}), yielding pVc-NhaP1. The following primers were used for cloning: forward primer VcNhaP1expF, 5'-GAGGAATAATAAATGTCCGTCTACTACACTTG-3'; and reverse primer VcNhaP1expR, 5'-TTAGTGTTGTTGTTCTTGCTG –3'. The forward primer was designed to achieve expression of the native enzyme without addition of the N-terminal leader sequence usually introduced by this vector. The primer contains an in-frame stop codon and a translation re-initiation sequence, which consists of a ribosome-binding site and the first ATG of the protein. In the reverse primer, the native stop codon of *Vc-nhaP1* was maintained. Using these primers, the *nhaP1* ORF was amplified by polymerase chain reaction as described previously. Briefly, 1 unit of Platinum PCR Supermix High Fidelity DNA polymerase (Invitrogen) was used to amplify the approximately 1.3 kb fragment corresponding to *Vc-nhaP1*, a portion of which was run on a gel to confirm the amplicon size. The remainder of the PCR mixture was purified using the QIAquick PCR Purification Kit (Qiagen), and was then introduced into the pBAD-TOPO vector using the manufacturer's protocol (Invitrogen). Transformants were screened by PCR for the correct orientation by using a forward primer for the plasmid (pBAD Forward) and the 3' expression primer for

the gene. Plasmid extractions were performed using the QIAprep Spin Miniprep Kit (Qiagen) and the fidelity of the PCR was confirmed by DNA sequencing at the Oregon State University Center for Genome Research and Biocomputing core lab facility. This pVc-NhaP1 construct was then introduced into *E. coli* TO114 by chemical transformation and into *V. cholerae* O395N1Δ*nhaP1* by electroporation as described previously (Hamashima, *et al.*, 1995).

2.3.3. Chromosomal Deletion of the Vc-nhaP1 Gene. Chromosomal deletion of the *Vc-nhaP1* gene was conducted by homologous recombination. The defined mutant construct was made using overlap extension PCR (Ho, *et al.*, 1989). A 1 kb fragment upstream of the start codon was amplified from genomic DNA by PCR using the following primer pair: 1, 5'- GGGGGGGATCCGCATTCTGAAATGCGTGAAAG-3'; and 2, 5'- GACTGACTGACTGACTGACTCATTCTCTTCTCAGTGTGTGTAACAATTTG-3'. A 1 kb fragment downstream of the stop codon was amplified from genomic DNA by PCR using the following primer pair: 3, 5'-AGTCAGTCAGTCAGTCAGTCTAATCTCCGTTGTTTAATCGACAAAC-3'; and 4, 5'-GGGGGGAGCTCAAGTTCGGAATTGATAAGCGC-3'. The DNA products of these two PCRs are able to anneal together due to complementary sequences engineered into the primers 2 and 3 and were used as a template for a third PCR using primers 1 and 4, resulting in a 2 kb PCR product encompassing 1 kb upstream of the start codon and 1 kb downstream of the stop codon with the gene itself removed. This PCR product was cloned into suicide vector pWM91 (Metcalf, *et al.*, 1996) by restriction sites engineered into the primers 1 and 4, and the mutant allele was introduced into the

chromosome of *V. cholerae* O395N1 following conjugation with the *E. coli* strain hosting the vector. Using sucrose selection as previously described (Metcalf*, et al.*, 1996), the in-frame deletion of the ORF was introduced into the chromosome of *V. cholerae* strain O395N1. This mutant strain (O395N1Δ*nhaP1*) along with its isogenic parent (O395N1) and O395N1Δ*nhaP1*/pVc-NhaP1 overexpressing the *V. cholerae nhaP1* gene *in trans* and O395N1/pBAD24 were used to assess the function of Vc-NhaP1.

2.3.4. Analysis of Growth Phenotypes. For growth analysis of *V. cholerae* strains, LBB medium (non-cationic L broth) was supplemented with antibiotics, arabinose, and varying concentrations of NaCl, KCl, LiCl, $MgCl_2$, $CaCl_2$, $CuCl_2$, $FeCl_3$, or L-proline. The initial pH of the media was adjusted with HCl to 6.0, 7.2, or 8.5 and buffered by the addition of 60 mM BTP. Cells were inoculated into 200 μL of liquid medium in 96-deep well plates (Whatman) at an initial optical density at 600 nm absorbance (A_{600} OD) of 0.05 and grown at 37°C for 18 h with vigorous aeration. Growth was then measured as the A_{600} OD of the bacterial suspension at 600 nm by scanning the plates on a BioRad iMark microplate absorbance reader. All experiments were repeated at least three times in triplicate.

2.3.5. Measurement of Cytoplasmic pH in vivo. Cells of O395N1 and O395N1Δ*nhaP1* were transformed with pMMB1311 (encoding GFPmut3b, a pH sensitive GFP) (Kitko*, et al.*, 2009), yielding strains MJQ0121 and MJQ0122, respectively. Potassium-depleted cells for the pH recovery experiments were obtained essentially as described (Kroll and Booth, 1981; Kroll and Booth, 1983). The strains

were cultivated overnight in K100 medium (Epstein and Kim, 1971), containing 46 mM K_2HPO_4, 23 mM KH_2PO_4, 8 mM $(NH_4)_2SO_4$, 400 μM $MgSO_4$, 6 μM $FeSO_4$, 1 mM Na-citrate, 1 mg/L thiamine, 2 g/L glucose and supplemented with 100 μg/mL streptomycin and 100 μg/mL ampicillin at 37°C. Cells were pelleted and resuspended to A_{600} OD 0.5 in K0 medium (Epstein and Kim, 1971), in which all potassium salts were substituted by sodium ones. Further, cells were allowed to grow in K0 medium to A_{600} OD 1.0 and placed on ice, pelleted at 2200 rpm at 4°C for 5 minutes and resuspended at A_{600} OD 0.4 in the pH assay buffer, containing 50 mM choline chloride and 60 mM BTP (pH 6.0). K^+-depleted cells were dispensed in 200 μL aliquots in a 96 well plate, and a baseline reading was taken using a Tecan plate reader (excitation/emission at 480nm/525 nm) at 37°C. Glucose (at final concentration of 1 mM) was added at t=0 to energize cells. After 10 minutes, KCl was added to experimental wells (final concentration of 0-100 mM) and 20 mM benzoate was added to calibration wells to collapse ΔpH, thus equalizing internal pH to external pH, to correlate emission values to internal pH. Data were collected for a further 10 minutes. All measurements were performed in triplicates in each of three independent experiments. Errors are stated as standard error of the mean (SEM; n = 3), and where necessary significance of the results was assessed by Student's t-test. For the comparison of steady-state pH_{in} values, the potassium-, sodium-, or choline-loaded cells were prepared using the method of cation replacement advanced by Unemoto and colleagues (Nakamura, *et al.*, 1982). Briefly, mid-log cultures were pelleted, resuspended in 0.4 M chloride salt of a desired cation containing 50 mM

diethanolamine hydrochloride at pH 8.5, and incubated at room temperature for 10 min. Then cells were pelleted by centrifugation, and the treatment was repeated. After that, cells were pelleted again, washed twice and resuspended in 0.4 M chloride salt of a desired cation with 50 mM BTP-HCl (pH 6.0). Prepared cation-loaded cells were assayed immediately. Steady-state pH_{in} levels were recorded as described above for 10 min.

2.3.6. Isolation of Membrane Vesicles for Assay of Antiporter Activity. Antiporter activity was measured in inside-out membrane vesicles isolated from the Δ*nhaA*, Δ*nhaB*, Δ*chaA* strain of *E. coli* TO114 transformed with pVc-NhaP1 or pBAD24. These transformants were grown in LBK medium containing 100 mg/ml ampicillin, 30 mg/ml kanamycin, 34 mg/ml chloramphenicol, 100 mg/ml erythromycin and 0.05% arabinose. Cells were harvested at an O.D. (600 nm) of 1.0 to 1.2, then washed three times in buffer containing 140 mM choline-chloride, 10% (w/v) glycerol and 20 mM Tris-HCl, pH 7.5, and then lysed using a French Press, essentially as described previously (Resch, *et al.*, 2010). The unbroken cells were pelleted, the supernatants were ultracentrifuged at 184,000 × *g* for 90 min at 4°C, and isolated vesicles were resuspended in the same buffer. For Δψ measurements, vesicles were isolated in the above buffer, but choline-chloride was replaced with 280 mM sorbitol.

2.3.7. Measurement of Transmembrane ΔpH. For ΔpH measurements, aliquots of vesicles containing approximately 200 mg of total protein were added to 2 ml of buffer containing 140 mM choline chloride, 5 mM $MgCl_2$, 10% (w/v) glycerol, 4 mM acridine orange and 50 mM BTP-HCl adjusted to the indicated pH. Measurement

of K^+/H^+, Na^+/H^+ and Li^+/H^+ antiporter activities were performed by using the acridine orange fluorescence dequenching assay (Dzioba*, et al.*, 2002; Dzioba-Winogrodzki*, et al.*, 2009; Resch*, et al.*, 2010). Briefly, respiration-dependent ΔpH was generated by the addition of 20 mM Tris-D-lactate and the resulting quenching of acridine orange fluorescence was monitored in a Shimadzu RF-1501 spectrofluorophotometer (excitation at 492 nm and emission at 528 nm). The detected antiport activities were expressed as percent restoration of lactate-induced fluorescence quenching in response to the addition of 10mM of NaCl, LiCl or KCl at the indicated concentrations. Each experiment was carried out in duplicate from separate isolations of membrane vesicles. The background activity measured in "empty" vesicles at every pH tested in separate control experiments is subtracted from the levels obtained in Vc-NhaP1 containing vesicles to yield the data shown.

2.3.8. Measurement of Transmembrane Δψ. Inside-out membrane vesicles (Resch*, et al.*, 2010) were isolated from TO114 cells transformed with pVc-NhaP1 or pBAD24 and assayed for Δψ in chloride-free, potassium-free buffer at pH 7.5. Vesicles were mixed with 20 mM of diethanolamine for 5 min prior to the addition of 8 mM of the Δψ-sensitive dye Oxonol V. Excitation and emission were measured at 595 nm and at 630 nm, respectively.

2.3.9. Materials. All chemicals were purchased from Sigma-Aldrich or Fisher Scientific. Restriction endonucleases and DNA-modifying enzymes were purchased from Invitrogen, MBI Fermentas, or New England Biolabs.

2.4. Results

2.4.1. Distribution of nhaP *genes in various* Vibrio *species.* *In silico* analyses revealed that, of the several putative antiporters encoded in the *V. cholerae* genome, three (Vc-NhaP1, Vc-NhaP2, and Vc-NhaP3) are paralogues of each other (Table 1, also see (Dzioba-Winogrodzki, *et al.*, 2009)). These proteins have homologues in other *Vibrio* species as well, and three other *Vibrio* species (*V. parahaemolyticus*, *V. alginolyticus*, and *V. mimicus*) encode homologues of all three NhaP paralogues (Table 1). Additionally, NhaP1 is at least 85% identical to genes in the following sequenced *Vibrio* genomes: *V. cholerae* (2740-80, V52, TM 11079-80, TMA21, RC 385, V51, 623-29, LMA-3894-4, MZO-2, RC 27, CT 5369-93), *V. mimicus* (VM573, MB 451, VM603, VM223), *Vibrio species* (RC 586, AND4, Ex25, RC 341, MED222), *V. harveyi* (1DA3, HY01, ATC BAA 1116), *V. vulnificus* (YJ016, CMCP6, MO6-24/O), *V. furnisii* (NCTC 11218), *V. parahaemolyticus* (AQ 3810, RIMID 2210633, K5030, AN-5030, Peru-466, AQ4037), *V. metschnikovii* (CIP 69.14), *V. alginolyticus* (40B), *V. orientalis* (CIP 102891), *V. brasiliensis* (LMG 20546), *V. coralyticus* (ATCC BAA-450), *V. splendidus* (12B01, LGP 32), *V. harveyi* (ATCC BAA 1116), *V. fischeri* (ES 114), and *V. sinaloensis* (DSM 21326). These data show that the *nhaP1* genes are widely conserved among different *Vibrio* species.

2.4.2. Growth properties of the V. cholerae *Δ*nhaP1 *mutant.* Deletion of *Vc-nhaP2* shows a growth deficiency phenotype specifically in growth media containing 400-500 mM K^+ at pH 6.0 (Resch, *et al.*, 2010). For comparison, we measured the effect of pH and K^+ on growth yield in the ΔVc-*nhaP1* mutant. After 18 hours of

aerobic growth O395N1Δ*nhaP1*, unlike the parent strain, showed markedly lowered growth yield in the media supplemented with K^+ at pH 6.0, with the most severe growth deficiencies observed at 0-100 mM and 400-600 mM of added K^+ (Fig. 1A). Complementation *in trans* with the *V. cholerae nhaP1* gene in the arabinose-inducible pBAD system restored the growth phenotype of the parent strain almost completely (Fig. 1A) and the level to which complementation restored the growth phenotype increased as the arabinose concentration was increased (data not shown). No difference in growth was observed between the parent and O395N1Δ*nhaP1* growing in K^+ media at pH 7.2 or 8.5 (Fig. 1 B-C). When these experiments were performed with Na^+ or Li^+ added instead of K^+, no growth defects were found in O395N1Δ*nhaP1* at high concentrations of added Li^+ or Na^+ (Fig. 1 D-I). Of note, the growth defect related to the deletion of *nhaP1* persisted in acidic medium at low concentrations of added Na^+ (Fig.1D). These experiments demonstrate that deletion of Vc-*nhaP1* leads to an inhibited growth phenotype in acidic media (pH 6.0) in two situations: (i) low concentrations of alkali cations or (ii) in the presence of high concentrations of K^+. Standard osmolytes, sucrose (up to 500 mM) and proline (up to 50 mM), were also assayed as possible substitutions for alkali cations. While proline did not affect the growth of the O395N1Δ*nhaP1* mutant at any concentration used, sucrose improved it to some extent, elevating the growth yield for 18 hours from A_{600}=0.400 in the original LBB medium to approximately 0.850 in the same medium supplemented with 300 mM sucrose. It therefore never reached the growth yields typical for the wild type (of app. 1.300-1.400, see Fig. 1A). At concentrations exceeding 400 mM, sucrose

inhibited the growth yield. Thus, the inhibited growth of O395N1Δ*nhaP1* at low ionic strength may be attributed to impaired osmoregulation, but only partially.

To further characterize the growth deficiency revealed in O395N1Δ*nhaP1* growing at pH 6.0 for 18 hours (Fig. 1 A,D), dynamics of growth was monitored by taking the A_{600} OD readings every 60 minutes (Fig. 2). Interestingly, at 100-400 mM K^+ (Fig. 2 C-E) growth of O395N1Δ*nhaP1* was clearly triphasic, whereas O395N1 and O395N1Δ*nhaP1*/pVc-NhaP1 exhibited biphasic growth phenotypes only at 500 mM KCl (Fig. 2F). When grown over a range of NaCl concentrations, no apparent differences were noted in the O395N1Δ*nhaP1* strain compared to O395N1 (Fig. 2 H-N). However, a reduced fitness of O395N1Δ*nhaP1* compared to O395N1 or O395N1Δ*nhaP1*/pVc-NhaP1 was noted in the absence of added NaCl (Fig. 2 H), as expected.

2.4.3. Cytoplasmic pH homeostasis in the V. cholerae *Δ*nhaP1 *mutant strain.*

In an attempt to assess the physiological function of Vc-NhaP1 at the biochemical level, we investigated the possible effect of Vc-NhaP1 on homeostasis of cytoplasmic pH. First, the ability to recover cytoplasmic pH values were measured in K^+-depleted bacteria by using a pH-sensitive GFP maintained on the pMMB1311 plasmid, which has been used before in *E. coli* (Kitko, *et al.*, 2010) and *B. subtilis* (Kitko, *et al.*, 2009). After a baseline reading, KCl or NaCl was added to final concentrations of 0 mM, 1 mM (KCl), 10 mM, or 100 mM (NaCl), and readings were taken every 2 minutes for a further 10 minutes. Relative absorbance values were calibrated to pH readings with a standard curve for each experiment (data not shown). At external pH

6.0, K^+-depleted cells of both O395N1 and O395N1Δ*nhaP1* were unable to build up and maintain the pH gradient across the membrane in the choline-Cl medium even in the presence of glucose: internal pH was stable at 6.0 for at least 10 minutes (Fig. 3A). The addition of 10 mM KCl swiftly raised the cytoplasmic pH in cells of O395N1 and O395N1Δ*nhaP1* after approximately 3 minutes, while up to 100 mM NaCl did not raise the cytoplasmic pH significantly even after 10 minutes (Fig. 3B). Noticeably, the pH response to added KCl in O395N1Δ*nhaP1* was significantly less pronounced than in O395N1 (Fig 3A). In a parallel series of experiments, cells were loaded with different cations as described in Materials and Methods, and the steady-state pH_{in} levels were recorded for 10 minutes after addition of glucose at external pH 6.0. As Fig. 3C shows, the pH homeostasis was totally lost in the Na^+-loaded cells of both O395N1 and O395N1Δ*nhaP1*, while the K^+-loaded cells demonstrated internal pH values much closer to the physiological ones. As could be expected from data shown in Fig. 3A, elimination of functional Vc-NhaP1 resulted in somewhat lower intracellular pH (7.1 *versus* app. 7.5 in the wild type). When cells of O395N1 and O395N1Δ*nhaP1* were loaded with choline-Cl, they lost pH homeostasis irrespectively of the presence of Vc-NhaP1 (data not shown).

2.4.4. Ion specificity and pH profile of Vc-NhaP1 activity. To directly measure antiport activity, we expressed Vc-NhaP1 in cells of the antiport-deficient (Δ*nhaA*, Δ*nhaB*, Δ*chaA*) *E. coli* strain TO114. Inside-out membrane vesicles from TO114/pVc-NhaP1 and "empty" TO114/pBAD24 cells were analyzed for cation/H^+ antiport activities by the standard acridine orange fluorescence dequenching technique and

expressed as percent restoration of lactate-induced fluorescence quenching. The pH of the assay buffer in this system represents cytosolic pH. When assayed in inside-out membrane vesicles by the addition of 10 mM of KCl, Vc-NhaP1 demonstrated modest but measurable activity in the cytosolic pH range 7.0 to 9.5 with a relatively broad optimum at cytosolic pH 7.25 to 8.0 (Fig. 4, squares). When assayed with 10 mM NaCl, Vc-NhaP1 showed a somewhat higher activity from cytosolic pH 7.0 up to the apparently optimal pH of 8.5, with approximately 15% of dequenching (Fig. 4, circles). No activity was detected at or below pH 6.5 with any of the probed cations. Like Vc-NhaP2, Vc-NhaP1 did not show any Li^+/H^+ antiport activity at any of the tested pH values (Fig. 4, triangles). Neither Mg^{2+} nor Ca^{2+} were found to be substrates of Vc-NhaP1 (data not shown). These *in vitro* kinetic data obtained in the inside-out membrane vesicle model suggest that Vc-NhaP1 is a cation/proton antiporter with K^+ and Na^+ specificity.

2.4.5. Electroneutrality of Vc-NhaP1. To probe whether Vc-NhaP1 mediates electrogenic or electroneutral antiport, inside-out membrane vesicles were isolated from TO114 cells transformed with pVc-NhaP1 or pBAD24 and assayed for $\Delta\psi$ in chloride-free, potassium-free buffer. Vesicles were loaded with diethanolamine prior to the addition of Oxonol V in order to maximize the magnitude of the respiration-generated $\Delta\psi$, and again energized by lactate. The subsequent addition of either K^+ (Fig. 5A, upper traces) or Na^+ (Fig. 5A, lower traces) resulted in no detectable depolarization, indicating that the cation/H^+ antiport by Vc-NhaP1 is electroneutral, with one alkali exchanged cation per one proton. Addition of the

protonophore CCCP short-circuited the membrane for H^+ and thus completely dissipated the respiratory $\Delta\psi$ (the last addition in each trace of Figure 5A). Valinomycin in the presence of potassium may be used instead of CCCP to dissipate $\Delta\psi$ (the last addition in the left trace of Figure 5B).

It was important to make sure that under the experimental conditions used the sensitivity of the method was sufficient to register *electrogenic* antiport by a partial depolarization resulting from the operation of an antiporter exchanging more than $1H^+$ per each alkali cation. To this end, inside-out membrane vesicles were also isolated from TO114/pBVA cells expressing the electrogenic Vc-NhaA, which we cloned in *E. coli* and characterized previously (Resch, *et al.*, 2010). Upon the addition of Na^+, these vesicles demonstrated very fast and deep depolarization followed by a slower partial re-polarization that apparently reflects activization of the respiratory H^+ pumping in response to the Vc-NhaA-mediated ion currents (Figure 5B, the right trace). This behavior is typical for an electrogenic antiporter such as NhaA and differentiates it from electroneutral Vc-NhaP2 (Resch, *et al.*, 2010) and Vc-NhaP1 (Fig. 5A). In another positive control for the experiments with Vc-NhaP1 shown in Fig.5, an artificial rather than natural electrogenic cation-proton exchanger was used. "Empty" TO114/pBAD24 vesicles were pre-treated with high (5.0 μM) concentration of nigericin, an artificial ion exchanger that acts as an electrogenic antiporter at concentrations exceeding 1.0 μM (Gómez-Puyou, 1977; Guffanti, *et al.*, 1998). The addition of potassium to the nigericin-treated vesicles after energization by lactate caused detectable depolarization (not shown). Taken together, these $\Delta\psi$ measurements

strongly suggest that, like Vc-NhaP2 (Resch, *et al.*, 2010) and in contrast to Vc-NhaA, Vc-NhaP1 catalyzes the electroneutral ion exchange of one K^+ or Na^+ ion per $1H^+$.

2.5. Discussion

Cation-proton antiporters are found across all domains of life, typically serving to maintain cytosolic ion and pH homeostasis as well as turgor pressure (Bakker and Mangerich, 1981; Zilberstein, *et al.*, 1982; Nakamura, *et al.*, 1984; Csonka, 1989; Nakamura, *et al.*, 1992; Corratge-Faillie, *et al.*, 2010). Not surprisingly, there are many examples of antiporters of different kinds that co-exist in the membranes of microorganisms exposed to dynamic changes of the ionic composition in the environment, of which many have been described in *V. cholerae* (Miller, *et al.*, 1984; Vimont and Berche, 2000; Hase, *et al.*, 2001; Dzioba-Winogrodzki, *et al.*, 2009). Here, we describe biochemical and some physiological properties of an uncharacterized antiporter, Vc-NhaP1, one of the three NhaP paralogues predicted by the genomic screen of *V. cholerae* (see Table 1 and (Resch, *et al.*, 2010; Resch, *et al.*, 2010)). This sub-group of *V. cholerae* antiporters is especially interesting because (i) antiporters of NhaP-type in general have diverse cation selectivities, which is manifested in a variety of physiological functions (Resch, *et al.*, 2010), and (ii) as this work and (Resch, *et al.*, 2010) show, these closely related paralogues indeed differ biochemically, thus offering a rare opportunity to identify structural determinants of their cation specificity and to obtain insights into the events in the ion-binding cavity

using site-directed mutagenesis prior to crystallographic analysis. We are currently working in this direction.

Our analysis of growth phenotype of the Vc-*nhaP1* deletion mutant revealed that Vc-NhaP1 is essential for growth of *V. cholerae* at low pH under two distinct conditions: when concentration of external K^+ exceeds 300 mM (Fig. 1A and Fig. 2); and when concentration of alkali cations in the medium is minimal (Fig. 1A, D and Fig.2). The former feature, i.e. coping with the high potassium load, is common for Vc-NhaP2 (Resch, *et al.*, 2010) and Vc-NhaP1 (this work). It suggests that both antiporters are co-operating to keep the cytoplasmic concentration of K^+ under toxic levels, by using a relatively high ΔpH (normally existing on the membrane of cell growing in acidic media (Padan, *et al.*, 1981)) to expel K^+ in an electroneutral manner (see (Resch, *et al.*, 2010) for extended analysis); elimination of either antiporter by chromosomal deletion leads to the dramatically lowered growth yield at pH 6.0 and $[K^+]>300$ mM. In both cases, introduction of the corresponding gene *in trans* complemented the mutant phenotype (Fig. 1-2 and data in (Resch, *et al.*, 2010)).

The second growth phenotype of the Vc-*nhaP1* deletion mutant, a growth defect observed under minimal alkali cation load at pH 6.0, is unique to Vc-NhaP1. Apparently, this phenotype could not be explained by a simple assumption that in the low-cation environmentVc-NhaP1 mediates a $K^+(Na^+)/H^+$ antiport that removes the excess of H^+ from the cytoplasm in exchange for external alkali cations, because in this case electroneutral Vc-NhaP1 would move ions against both thermodynamic driving forces, ΔpH and ΔpK. Operating in the opposite direction, Vc-NhaP1 would

mediate externally directed K^+ flux and thus alleviate the hypo-osmotic stress (Csonka, 1989). One may notice here that protons that Vc-NhaP1 brings into the cytoplasm in this case would be promptly removed by respiratory chain. However, our attempts to prove the idea about a role of Vc-NhaP1 in osmo-protection were not entirely successful, because external proline did not rescue the Vc-*nhaP1* deletion phenotype and sucrose improved the growth only partially. Therefore, we also examined a possible involvement of Vc-NhaP1 in pH regulation (see below).

Of note, deletion of Vc-*NhaP1* shows a dissimilar response to Li^+ as compared to deletion of Vc-*NhaP2* (Resch, *et al.*, 2010). While the elimination of functional Vc-NhaP2 renders cells much more *resistant* to external Li^+ due to the prevention of Vc-NhaP2-dependent hetero-ion $Li^+/K^+(Na^+)$ exchange (see (Resch, *et al.*, 2010)), deletion of Vc-*nhaP1* does not affect the lithium resistance of *V. cholerae* cells in any way (Fig. 1G-I), indicating that Vc-NhaP1, in contrast to its NhaP2 paralogue, cannot bind Li^+ ion at all.

The above phenotypic analysis indicates that (a) Vc-NhaP1 is able to exchange protons for K^+ and, probably, Na^+, but not Li^+ ions; (b) in acidic low-cation media, Vc-NhaP1 possibly affects intracellular osmolarity and/or pH; and (c) Vc-NhaP1-dependent ion exchange is most probably electroneutral, so that Vc-NhaP1 can only expel alkali cations when cells have sufficiently high transmembrane ΔpH (cytoplasm more alkaline, as it happens in acidic growth media) and, *vice versa*, chemical transmembrane gradient of a substrate cation (ΔpK or ΔpNa) is required to change intracellular pH.

To check these predictions, we first examined the cation selectivity and electrogenicity of Vc-NhaP1 using the experimental model of inside-out TO114 membrane vesicles containing the heterologously expressed antiporter. As expected, Vc-NhaP1 did not exchange Li^+ for H^+ (Fig. 4, triangles), but both K^+ and Na^+ were the substrates of antiport (Fig. 4, squares and circles, respectively). For K^+, Vc-NhaP1 has a broad pH optimum at 7.5-8.5, while Na^+/H^+ antiport peaked at pH 8.0-8.5 (experimental pH in the model of inside-out vesicles corresponds to the cytoplasmic pH *in vivo*). Unfortunately, modest levels of observed activity (app. 16% of dequenching with Na^+ and no more than 11% with K^+) precluded accurate assessment of affinities of Vc-NhaP1 for its substrate cations. At this moment, it is not entirely clear why the activity of Vc-NhaP1 is considerably lower than that of Vc-NhaP2 when expressed and assayed under exactly the same conditions (Vc-NhaP2 was observed to have 50% of dequenching at pH 8.0 with K^+ (Resch, *et al.*, 2010)), but preliminary immunodetection probes with the V5-tagged variants of Vc-NhaP1 and Vc-NhaP2 indicate that this is due to the intrinsic properties of Vc-NhaP1 rather than problems with its expression and/or targeting (C. Resch, unpublished observations). As Fig. 5A shows, neither K^+/H^+ nor Na^+/H^+ antiport *via* Vc-NhaP1 disturb $\Delta\psi$ on the vesicular membrane, indicating the electroneutral character of both processes. This also is in accord with the observed phenotype of O395N1Δ*nhaP1*, which is evident under acidic but not neutral or alkaline growth conditions, i.e. only where the ΔpH on the membrane (more acidic outside) is of a considerable magnitude (Padan, *et al.*, 1981).

Further, we assessed whether Vc-NhaP1 contributes to the control of cytoplasmic pH in acidic external medium. Data presented in Fig.3 suggest that (a) potassium rather than sodium ions are necessary for the pH homeostasis in *V. cholerae* at external pH 6.0 and (b) functional Vc-NhaP1 contributes to both efficiency of pH_{in} recovery (Fig. 3A) and the resulting steady-state level of pH_{in} (Fig. 3C). It is important to note that the regulation of pH_{in} in these experiments showed a clear dependence on K^+ supplied externally (Fig. 3A) or internally (Fig. 3C) in a Vc-NhaP1-dependent manner, and not when Na^+ was supplied either externally (Fig. 3B) or internally (Fig. 3C). The capacity of Vc-NhaP1-mediated Na^+ export (Fig. 4), while greater than the antiporter's capacity for K^+ export, may be obscured *in vivo* by residual Na^+ export from either NQR, NhaB, or other Na^+ transporters. Whatever capacity NhaP1 has for Na^+ transport, it is clear that K^+ (and not Na^+) supplied internally or externally regulate pHin in *V. cholerae*. All these observations support the idea that, at acidic pH_{out} and moderate concentrations of external K^+, Vc-NhaP1 somehow attenuates the cytoplasmic pH by mediating flux of K^+. Elimination of functional Vc-NhaP1 apparently disturbs the homeostasis of cytoplasmic pH under acidic conditions. Of note, O395N1Δ*nhaP1* retained some capacity for K^+-dependent regulation of cytoplasmic pH (Fig. 3A,C), implying that other components of K^+ homeostasis in *V. cholerae*, namely Vc-NhaP2 and Vc-NhaP3, may partially compensate for the loss of Vc-NhaP1. Further studies will be required to determine the precise contributions of each NhaP paralogue to the regulation of cytoplasmic pH in *V. cholerae*. Curiously, data in Fig. 3, especially Fig. 3C clearly suggest that the

K^+ transport mediated by Vc-NhaP1 helps to *alkalinize* the cytoplasm of *V. cholerae*. At this moment, one can only speculate about the molecular mechanism underlying this effect: indeed, as discussed above, electroneutral Vc-NhaP1 in low-ionic acid media should rather let external protons into the cell in exchange for abundant internal K^+. While our data clearly show a dependence of pH_{in} regulation on presence of Vc-NhaP1, export of protons into acidic media is thermodynamically unfavorable; therefore, Vc-NhaP1 is necessary for pH_{in} regulation in *V. cholerae*, but it either has other undiscovered pleiotropic functions or, more likely, it cooperates with other transporters or antiporters. To resolve this paradox, extensive studies will be required, including the construction and analysis of double and triple mutants bearing the deletions of *nhaP* paralogues, possibly in conjunction with the elimination of selected H^+ and Na^+ pumps, as well.

Cytoplasmic pH is normally tightly regulated over a wide range of extracellular cation concentrations in many bacteria. Cells of *E. coli* maintain a cytosolic pH of 7.4-7.8 when grown in media ranging from pH 5.6-8.5 (Slonczewski, *et al.*, 1981), similar to cells of *V. alginolyticus*, which maintain a cytosolic pH of 7.6-7.8 in media ranging from pH 6.0-9.0 (Nakamura, *et al.*, 1992). Sodium-proton antiport has been linked to cytosolic pH homeostasis in *E. coli* at alkaline extracellular pH (Zilberstein, *et al.*, 1982). Studies in *E. coli* (Bakker and Mangerich, 1981; Kroll and Booth, 1981; Slonczewski, *et al.*, 1981; Zilberstein, *et al.*, 1982; Kroll and Booth, 1983) and *V. alginolyticus* (Tokuda, *et al.*, 1981; Tokuda and Unemoto, 1981; Hamaide, *et al.*, 1983; Nakamura, *et al.*, 1984; Nakamura, *et al.*, 1992) showed that K^+

is necessary for regulating cytosolic pH under acidic external conditions. As shown in Table 1, *V. alginolyticus,* like *V. cholerae,* has three *nhaP* paralogues. Data presented in this communication suggest that Vc-NhaP1 could play a role in moderating cytosolic pH when external pH is low. Loss of Vc-NhaP1 resulted in somewhat reduced capacity to control cytosolic pH as well as hypersensitivity to high [K^+] in an acidic environment. It is possible that the primary functions of NhaP-type ion exchangers in *Vibrio* spp. are pH attenuation and protection against K^+ in acidic media.

During growth curve experiments, a slight biphasic growth was observed in O395N1Δ*nhaP1*/pVc*nhaP1* and O395N1/pBAD24 cells exposed to 500 mM K^+, but not in the uncomplemented mutant (Fig. 2F). Our previous work has shown the importance of Vc-NhaP2 under these conditions (Resch*, et al.*, 2010), so it appears that these two paralogues augment each other at high K^+ concentrations. Therefore, this biphasic growth might have been caused by a regulated change in the expression levels of NhaP2 and/or NhaP3 in response to high (app. 0.5M) extracellular K^+ concentrations. However, our preliminary measurements of *nhaP* paralogue transcripts in O395N1 by qRT-PCR as a function of [K^+] or [Na^+] at pH 6.0 show no correlation between paralogue expression and [K^+] or [Na^+] (data not shown). As loss of NhaP1 caused no change in growth inhibition by any of the cations tested at 7.2 and higher, as compared to the parent, expression of NhaP paralogue was not measured. The physiological relevance of NhaP paralogues in *V. cholerae* is intriguing, as such high levels of K^+ are not expected to be encountered normally; environmentally, *V.*

cholerae is presumably exposed to app. 7 mM KCl in seawater (Webb, 1939) and the intestine (Watten, *et al.*, 1959). It is conceivable, however, that a battery of three NhaP paralogues expelling K^+ might be critical for *V. cholerae* passing acidic and K^+-rich gastric barrier.

2.6. Acknowledgments

The authors would like to thank Dr. Yusuke Minato for helpful discussions, and Dr. Joan L. Slonczewski for the kind gift of pMMB1311. This research was supported by grants from the National Institutes of Health (no. AI-063121-02) and the Natural Sciences and Engineering Research Council of Canada (no. 227414-04).

2.7. Tables and Figures

Table 2.1. Homology of monovalent cation:proton antiporter-2 (CPA2) family antiporters (HMM PF00999) of *Vibrio* species predicted from bioinformatic analyses. Locus: Gene (and name, where available). Antiporter type: Most similar *V. cholerae* homologue. HMM Match: Match value to the HMM CPA2 motif. VC identity: amino acid identity to the closest *V. cholerae* CPA2 family paralogue. Species: Vibrio species.

Locus	***Antiporter type***	**V. cholerae *identity***	***Species***
VC0389 (Vc-NhaP1)	(CPA2) family antiporter (HMM PF00999, HMM Match 2.6e-70)	N/A	*V. cholerae*
VC2703 (Vc-NhaP2)	(CPA2) family antiporter (HMM PF00999, HMM Match 7.2e-72)	N/A	
VC0689 (Vc-NhaP3)	(CPA2) family antiporter (HMM PF00999, HMM Match 1.3e-26)	N/A	
VMD_33930	VC-nhaP1-type antiporter	423/443 (95%)	
VMD_05140	VC-nhaP2-type antiporter	557/571 (98%)	*V. mimicus*
VMD_04400	VC-nhaP3-type antiporter	581/599 (97%)	
VV2961	VC-nhaP1-type antiporter	385/431 (89%)	*V. vulnificus*
VV0696	VC-nhaP3-type antiporter	444/598 (74%)	
V12G01_14609	VC-nhaP1-type antiporter	365/418 (87%)	
V12G01_00925	VC-nhaP2-type antiporter	481/578 (83%	*V. alginolyticus*
V12G01_02860	VC-nhaP3-type antiporter	421/589 (71%)	
V12B01_10612	VC-nhaP1-type antiporter	381/426 (89%)	*V. splendidus*
V12B01_01622 (CvrA)	VC-nhaP2-type antiporter	418/582 (72%)	
VP2718	VC-nhaP1-type antiporter	387/443 (87%)	
VP2867	VC-nhaP2-type antiporter	485/571 (85%)	*V. parahaemolyticus*
VPA0277	VC-nhaP3-type antiporter	421/587 (72%)	

Figure 2.1. Growth deficiency in Δ*nhaP1*. Growth yields of O395N1/pBAD24 (♦), O395N1Δ*nhaP1*/pVc-NhaP1 (black symbols: ■ = KCl, ● = NaCl, ▲ = LiCl), and O395N1Δ*nhaP1*/pBAD24 (gray symbols: ■ = KCl, ● = NaCl, ▲ = LiCl) were determined in LB-based media supplemented with selected cations. A_{600} OD values (y-axis) of *V. cholerae* cultures were measured after 18 hours of aerobic growth in the presence of 0-600 mM (x-axis) of either KCl (A-C), NaCl (D-F), or LiCl (G-I). All media were buffered to the indicated pH with 60 mM BTP. Plasmid gene expression was induced by addition of 0.02% arabinose. Plotted are the averages of three separate experiments, each performed in triplicate. Bars show the standard deviation.

Figure 2.1.

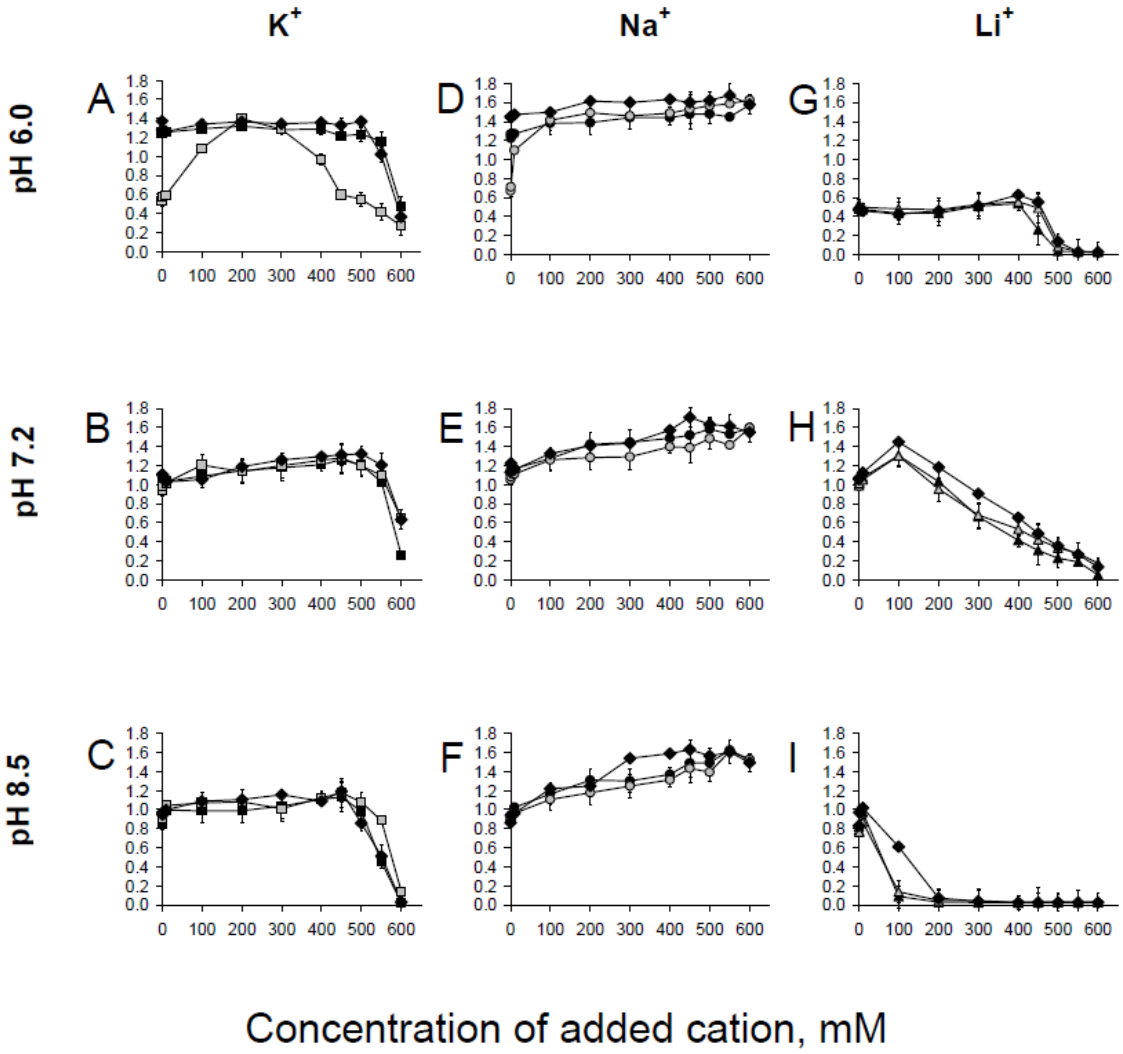
K+
Na+
Li+
pH 6.0
pH 7.2
pH 8.5
A
B
C
D
E
F
G
H
I
0.0
0.2
0.4
0.6
0.8
1.0
1.2
1.4
1.6
1.8
0
100
200
300
400
500
600
Concentration of added cation, mM

Figure 2.2. The Δ*nhaP1* growth dynamics at different [K^+] and [Na^+]. Growth of *V. cholerae* strains was measured every hour as OD at 600 nm in LB-based media supplemented with 0, 100, 200, 300, 400, 500 and 600 mM KCl (A-G) or the same concentrations of NaCl (H-N) and buffered with 60 mM BTP at pH 6.0. Gene expression was induced by the addition of 0.02% arabinose to all media. Growth of O395N1/pBAD24 (♦), O395N1Δ*nhaP1*/pBAD24 (■ = KCl, panels A-G; ● = NaCl, panels H-N), and O395N1Δ*nhaP1*/pVc-*NhaP1* (■ = KCl, panels A-G; ● = NaCl, panels H-N) is shown. Plotted are the averages of three separate experiments, each performed in triplicate.

Figure 2.2.

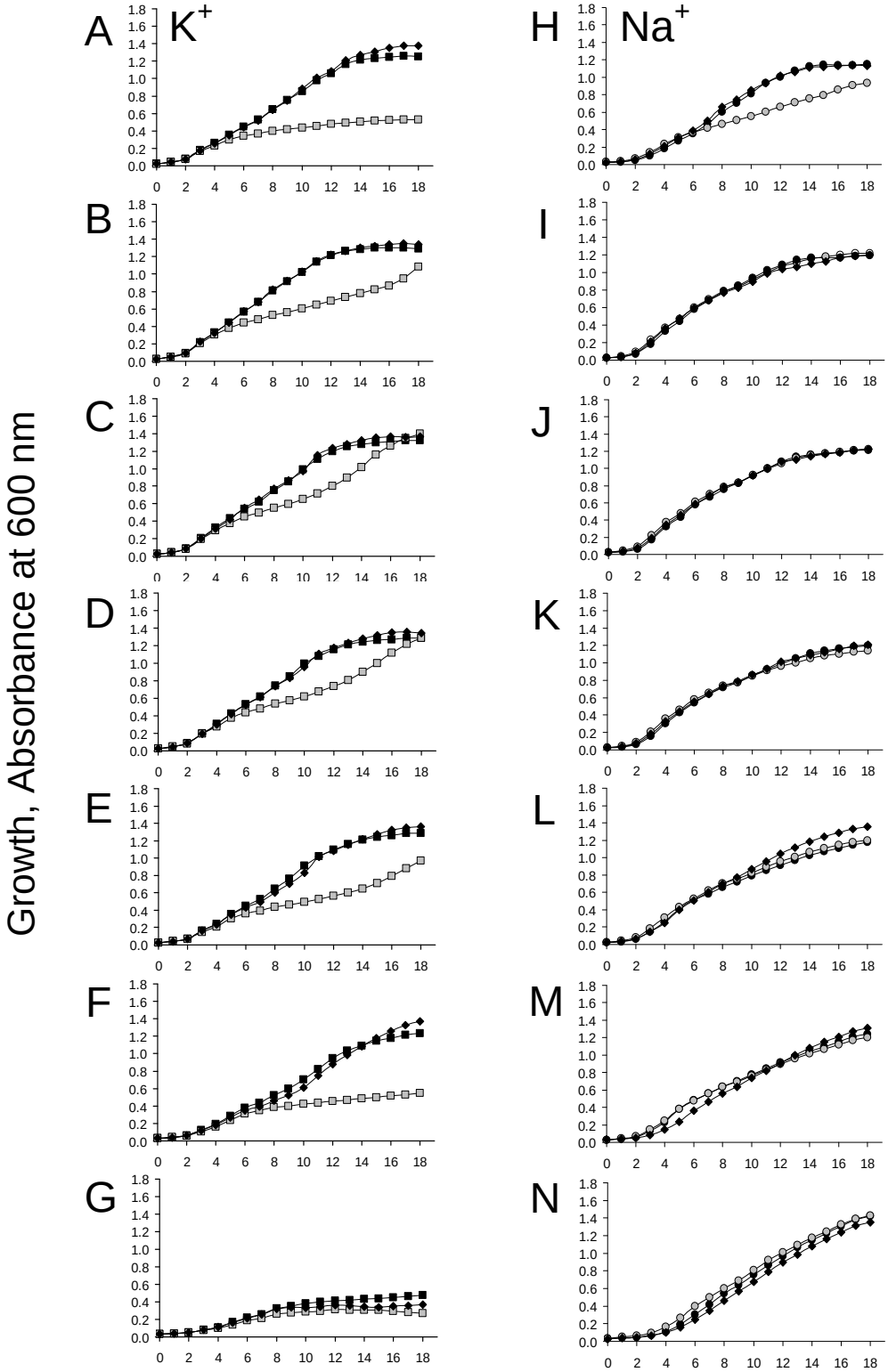

Figure 2.3. Vc-NhaP1 as a K^+/H^+ antiporter contributes to the cytoplasmic pH homeostasis in acidic media. Cytoplasmic pH was measured using pGFPmut3b in K^+-depleted cells of O395N1 (diamonds) and O395N1Δ*nhaP1* (squares for K^+ and circles for Na^+) in response to K^+ (**Panel A**) added at a final concentration of 0 mM (light gray), 1 mM (dark gray), or 10 mM (black), or in response to Na^+ (**Panel B**) at a final concentration of 0 mM (light gray), 10 mM (dark gray), or 100 mM (black); cations were added at t = 10 minutes. **Panel C**: Steady-state levels of internal pH in cells of O395N1 (filled bars) and O395N1Δ*nhaP1* (hatched bars) loaded with K^+, Na^+, or choline. The pH of the experimental buffer is 6.0 in all cases. 1 mM glucose was added to energize the cells. Plotted are the averages of three separate experiments over a ten minute period, each performed in triplicate. Bars show the standard deviation. See the text for further details.

Figure 2.3.

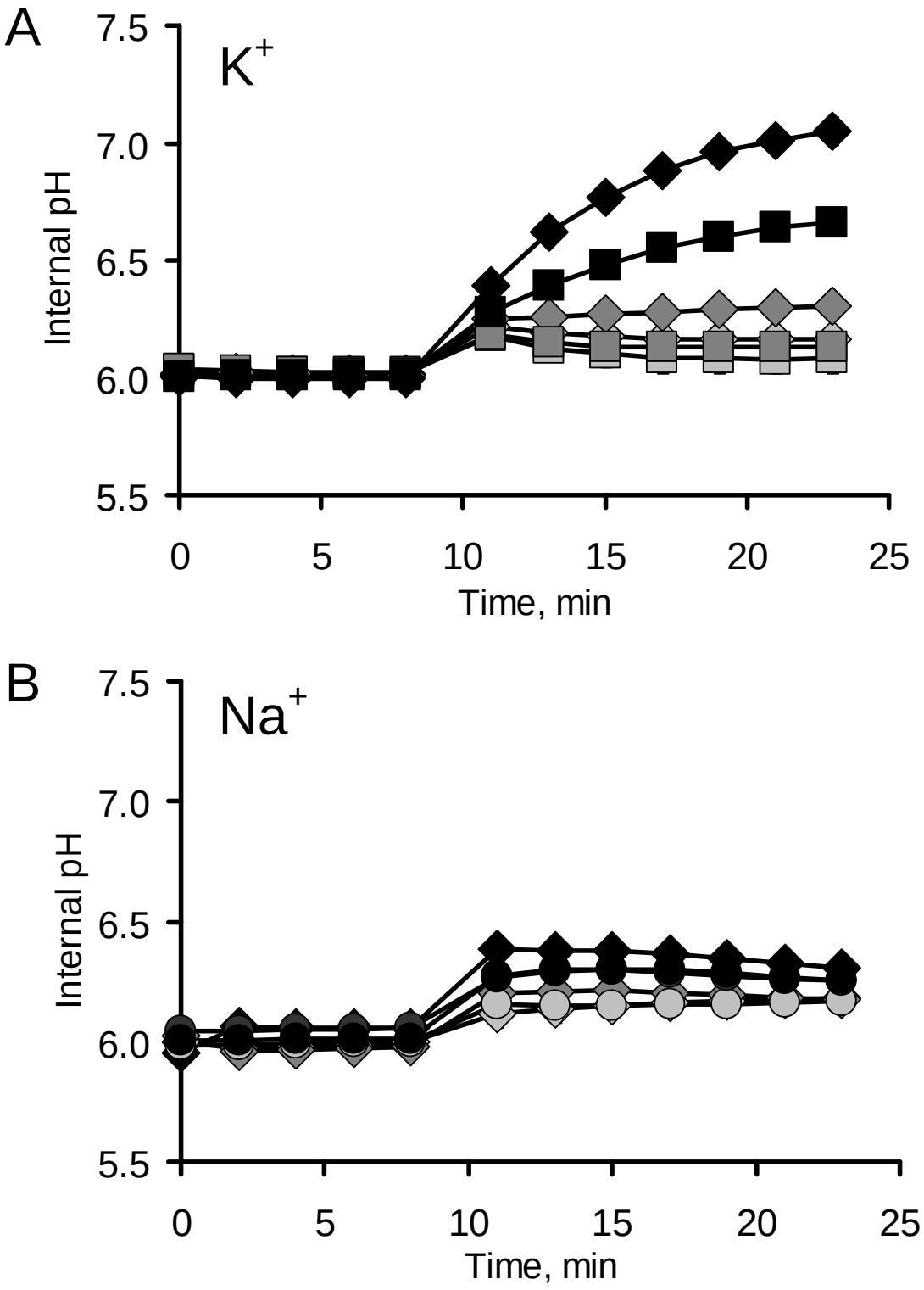
A
K+
Internal pH
7.5
7.0
6.5
6.0
5.5
0
5
10
15
20
25
Time, min
B
Na+
Internal pH
7.5
7.0
6.5
6.0
5.5
0
5
10
15
20
25
Time, min

Figure 2.3, continued.

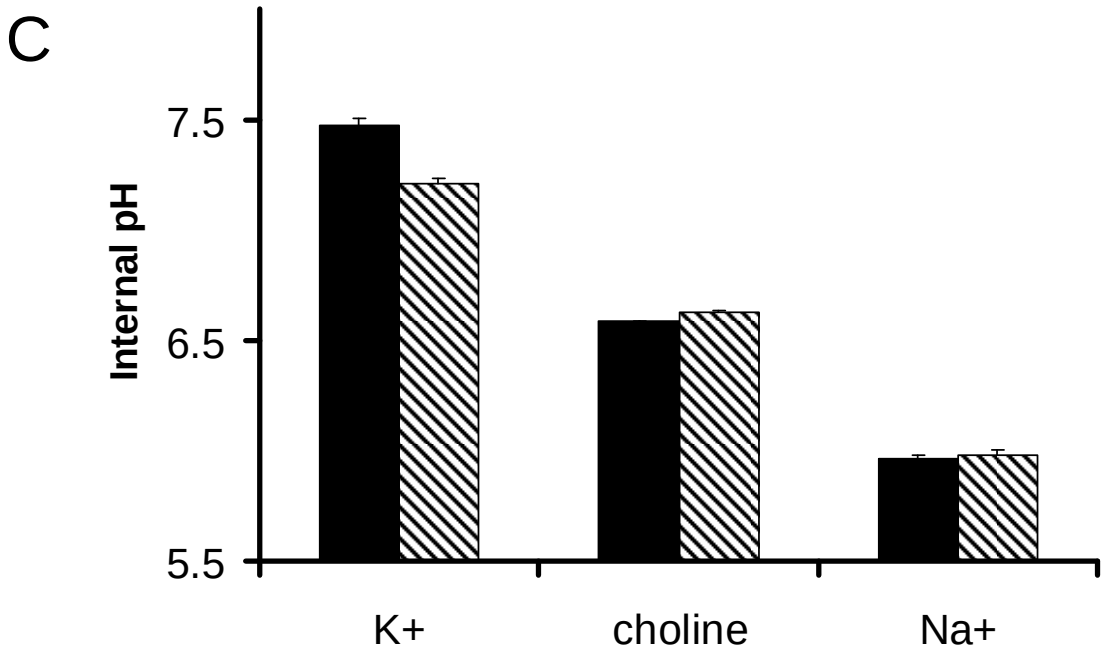

Figure 2.4. Cation specificity and pH profiles of Vc-NhaP1 activity. The antiporter was functionally expressed in *E. coli* T0114 and assayed for cation/H^+ antiport in inside-out membrane vesicles prepared as described in Materials and Methods. 10 mM of NaCl (circles), KCl (squares), or LiCl (triangles) were used to access the Vc-NhaP1 activity. Antiport activity is expressed as a percentage of the de-quenching of acridine orange. For each probe cation and specified pH, the background activity was measured in "empty" TO114/pBAD24 vesicles and subtracted from the activity measured in Vc-NhaP1 vesicles to yield the data plotted here. In all cases, this background activity did not exceed 10% of dequenching. All measurements were done in triplicates; standard deviation is shown.

Figure 2.4.

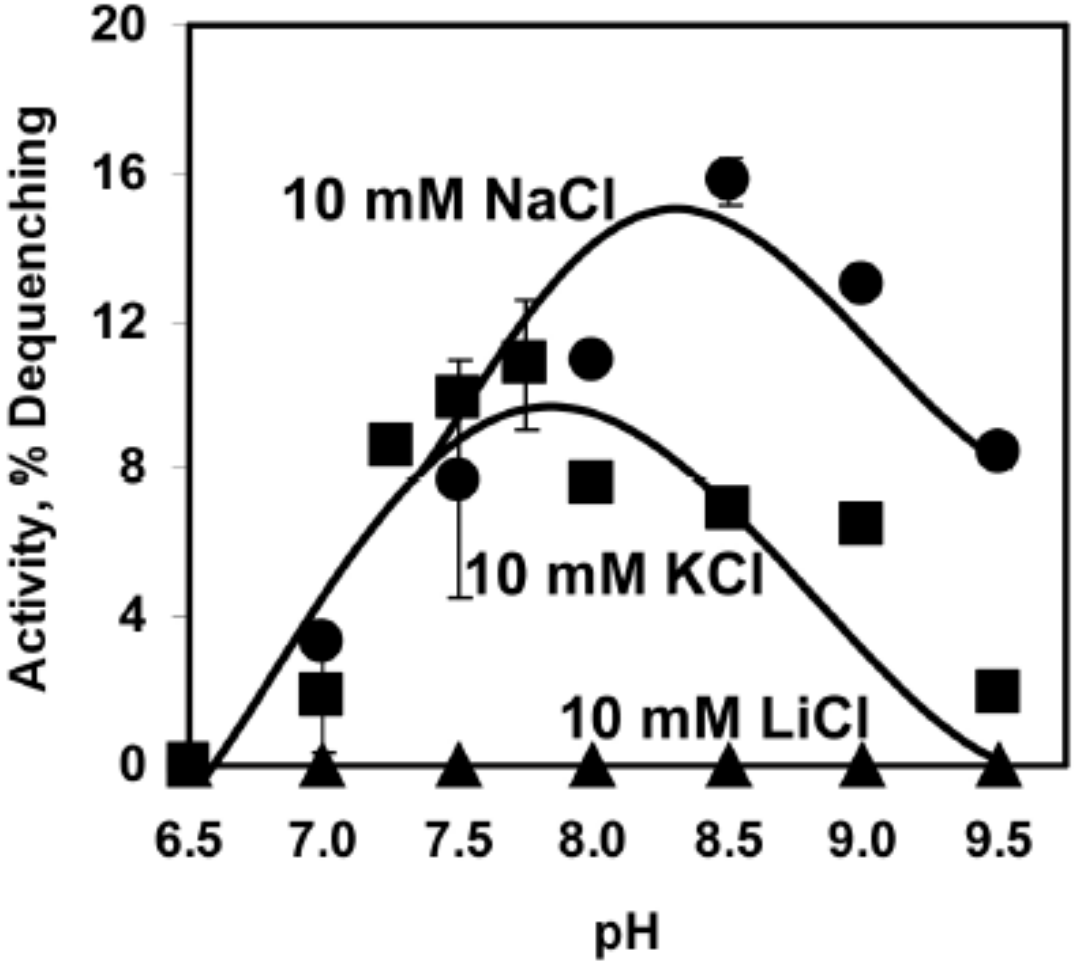
20
16
12
8
4
0
Activity, % Dequenching
10 mM NaCl
10 mM KCl
10 mM LiCl
6.5
7.0
7.5
8.0
8.5
9.0
9.5
pH

Figure 2.5. Probing the electrogenicity of Vc-NhaP1. Inside-out membrane vesicles were isolated from TO114 cells transformed with pVc-NhaP1 or pBAD24 and $\Delta\psi$ was assayed at pH 7.5 in sorbitol-based medium containing no K^+ or Cl^- (**Panel A**). Vesicles were mixed with 20 mM of diethanolamine for 5 min prior to the addition of Oxonol V and respiration-dependent formation of the transmembrane electrical gradient was initiated by the addition of 20 mM Tris-D-lactate. After steady-state $\Delta\psi$ was reached, cation/H^+ antiporter activity was initiated by the addition of 10 mM K_2SO_4 (**Panel A**, upper traces; **Panel B**, left trace) or 10 mM Na_2SO_4 (**Panel A**, lower traces). Control addition of the protonophore CCCP (**Panel A**) or valinomycin in the presence of K^+ (**Panel B**, left trace) at the end of each trace completely dissipated respiratory $\Delta\psi$. As a positive control, the TO114 vesicles expressing the electrogenic Vc-NhaA [26] were also assayed under the same conditions (**Panel B**, right trace). Immediate partial depolarization upon addition of Na^+ in this case indicates electrogenic character of ion exchange catalyzed by Vc-NhaA.

Figure 2.5.

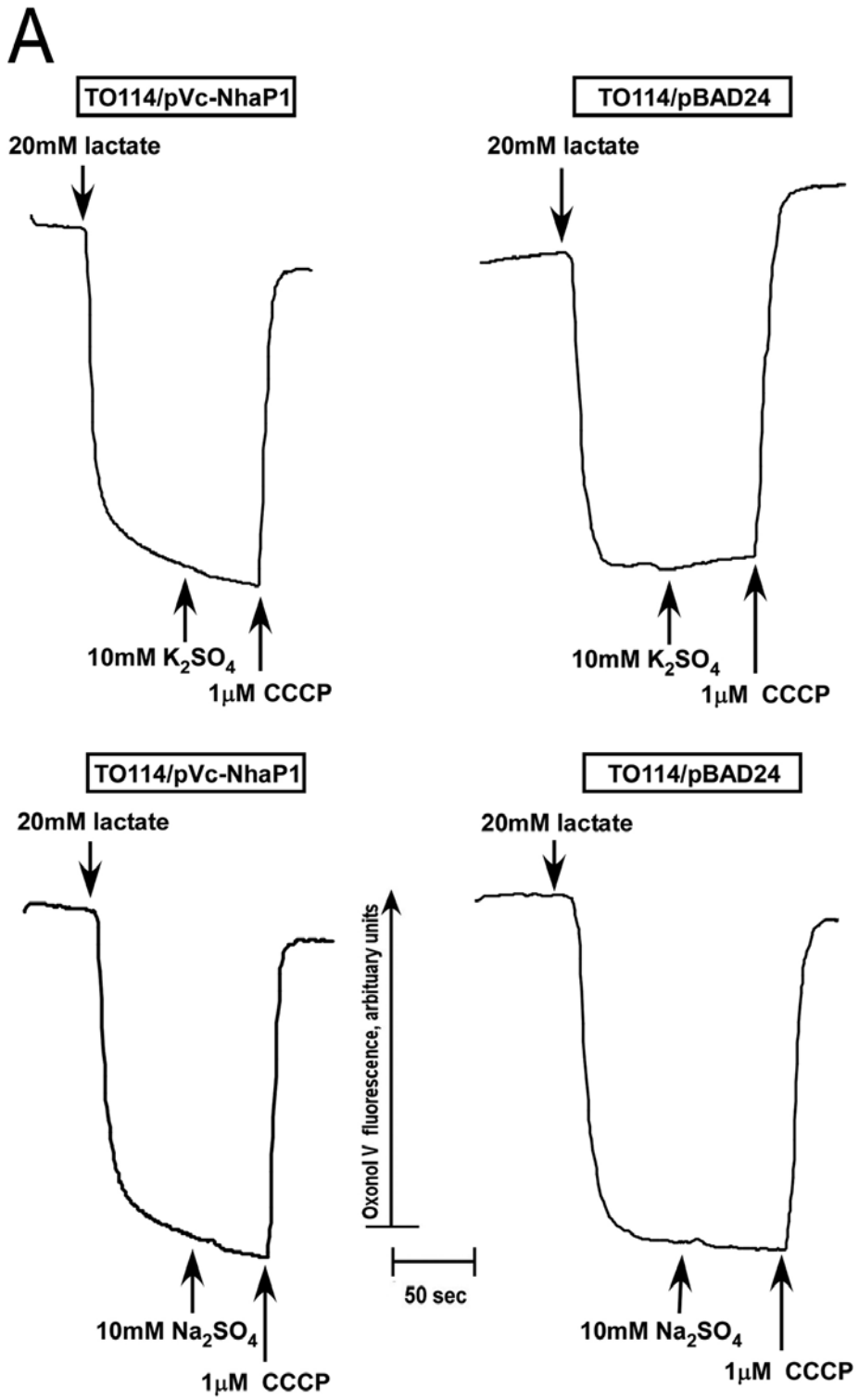
A
TO114/pVc-NhaP1
20mM lactate
10mM K_2SO_4
1μM CCCP
TO114/pBAD24
20mM lactate
10mM K_2SO_4
1μM CCCP
TO114/pVc-NhaP1
20mM lactate
10mM Na_2SO_4
1μM CCCP
Oxonol V fluorescence, arbituary units
50 sec
TO114/pBAD24
20mM lactate
10mM Na_2SO_4
1μM CCCP

Figure 2.5, continued.

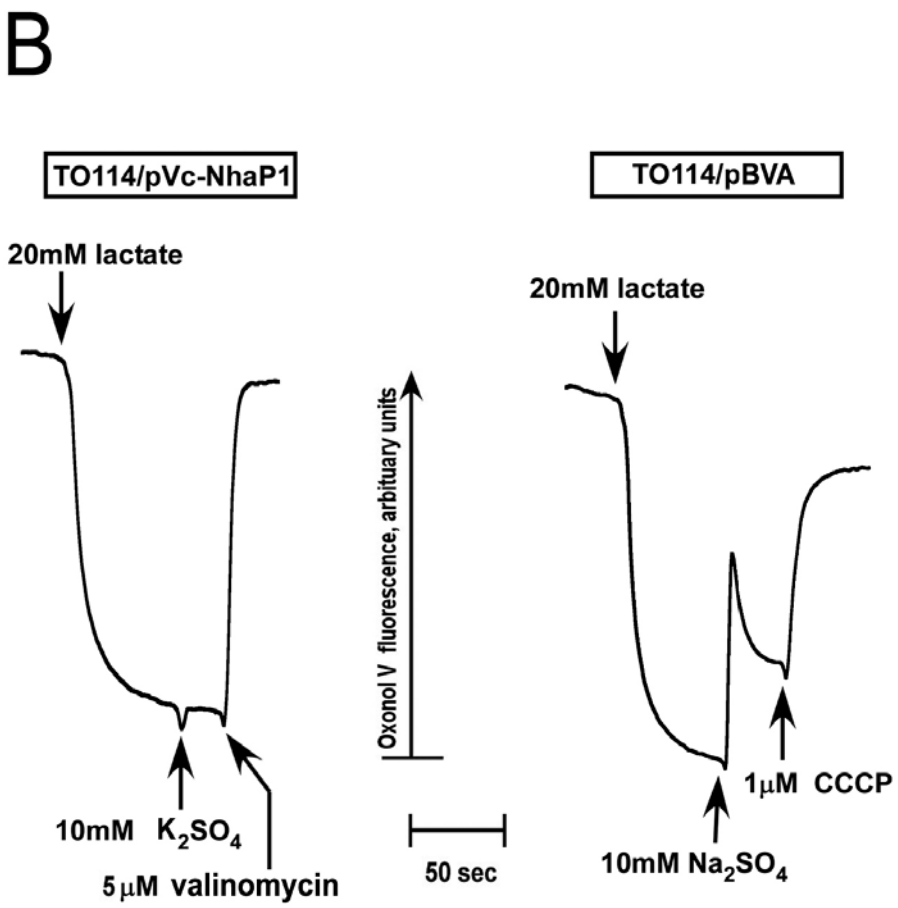

3. NhaA and NhaB of *Vibrio cholerae* Coordinate with NQR to Respond to Dynamic Sodium and Lithium Environments

Matthew J. Quinn, Wyatt Faulkner, Erin J. Lind, and Claudia Häse

3.1. Abstract

The human pathogen *V. cholerae* possesses many transporters, antiporters, and symporters to cope with a wide range of saline environments. Three of the major components of this regulatory network are NQR, Vc-NhaA, and Vc-NhaB. However, because of its central role in metabolism, the metabolic activity of NQR has previously been difficult to distinguish from its contribution to sodium motive forece (SMF) *in vivo*. Here, we describe the generation of a model system comprised of a *V. cholerae* strain lacking both the *nqr* operon and the open reading frames (ORFs) of *Vc-nhaA* or *Vc-nhaB* tested with and without lactate. These strains, along with the single mutants of *nqr*, *Vc-nhaA*, and *Vc-nhaB*, were assessed for aerobic growth as a function of media pH and cation concentration (Na^+, Li^+, or K^+). Loss of Vc-NhaA and, to a lesser extent, Vc-NhaB, was better observed when NQR was absent but lactate was added; lactate compensated, metabolically, for the loss of NQR but not osmotitcally. Loss of Vc-NhaA in this background inhibited growth most at basic pH under increasing Na^+ and Li^+ conditions, and loss of Vc-NhaB in this background inhibited was most severe in acidic conditions in the presence of 0-100 mM Na^+ or Li^+. We also observed the growth inhibition of Vc-NhaA in the absence of NQR and in the presence of lactate and 100-450 mM Li^+, which has not been previously reported. These growth defects were restored upon expression of the cognate antiporter gene on an inducible expression vector. The model system described herein will allow the further investigation of *V. cholerae* antiporters expressed *in situ*, allowing a better assessment of their contribution to bioenergetics.

3.2. Introduction

Vibrio cholerae is the etiological agent of cholera. Found worldwide, cholera is endemic to the Indian subcontinent, and specifically the estuarine and coastal waters which surround it (Enserink, 2010). Of the many factors which contribute to the virulence of *V. cholerae*, its environmental persistence ensures that it has an environmental reservoir from which future outbreaks originate. Therefore, understanding the effect of these environmental factors on the survival of *V. cholerae* is critical in managing this important human health problem.

V. cholerae survives the saline environment with a large genetic toolbox of transporters, antiporters, and symporters that generally work together to maintain a large ΔNa across the membrane (Table 1.1), preventing sodium (and lithium) toxicity as well as maintaining an energetic gradient by which nutrients can be imported (Hase and Barquera, 2001). Of these transporters, the best known are NQR, NhaA, and NhaB. NQR (NADH:quinone oxidoreductase) is a complex of proteins in the membrane which accept protons from NADH and transfer them to the quinone pool, in the process exporting sodium from the cytosol . In fact, NQR functions much like NADH oxidoreductase (Complex I of the oxidative respiratory chain), which occurs in most living things which respire oxidatively. It is interesting to note that *V. cholerae* lacks NADH oxidoreductase and funnels all electrons acquired by NADH to the quinone pool through NQR alone. NQR has also been implicated in the virulence of *V. cholerae*; deletion of the *nqr* operon or transposon insertion into the operon resulted in increased TCP production or ToxT expression (as measured by LacZ expression

coupled to the ToxT promoter) (Hase and Mekalanos, 1999). Therefore, the potential role of NQR in survival and virulence of *V. cholerae* underscores why this complex is of such interest to study.

Additionally, a wealth of research has been conducted into the role of the NhaA and NhaB antiporters of *E. coli*, *V. cholerae*, and several other bacteria. While these antiporters tend to share similar properties, they function uniquely in each bacterial species. EC-NhaA is an antiporter most active at pH 8 and above (Taglicht, *et al.*, 1991), with a transport ratio of $2H^+/1Na^+$ (Taglicht, *et al.*, 1993). It is expressed, similarly, at high pH in the presence of cytosolic Na^+ (Karpel, *et al.*, 1991; Shijuku, *et al.*, 2001). NhaA of *V. cholerae* complemented an *E. coli ΔnhaA* mutant (Vimont and Berche, 2000). Vesicles of EP432 (*E. coli ΔnhaAΔnhaB*) expressing VC-NhaA had an Na^+-activity profile with a maximum at approximately pH 8.0 (Herz, *et al.*, 2003). NhaB, on the other hand, seemed to be active mostly at acidic pH, as the *nhaB* mutant strain of *E. coli* HIT-1 showed no growth defect over the pH range 7.0-8.5 (Thelen, *et al.*, 1991; Schuldiner and Padan, 1993). It was noted that neither pH (7.0-8.5) nor Na^+ (0-200 mM) affected expression of NhaB as measured by *lacZ* expression governed by the EC-*nhaB* promoter (Sakuma, *et al.*, 1998). Pinner, et al., (Pinner, *et al.*, 1993) observed that *E. coli ΔnhaB* grew more slowly on agar plates having low pH and low (<10 mM Na^+). Recently, it was observed that AphB regulated *nhaB* expression under AKI conditions in *V. cholerae*. However, neither the single *nhaA* mutant nor a triple antiporter mutant (VC *ΔnhaAΔnhaBΔnhaD*) showed any growth inhibition in response to Na^+ at any pH; chemical inhibition of NQR by

HQNO, a quinone analog, was required to unmask the contribution of these antiporters to Na^+ regulation (Herz, *et al.*, 2003). The effect of HQNO on *nhaA*, *nhaB*, *and nhaD* was similarly observed in *V. parahaemolyticus* (Kuroda, *et al.*, 2005). However, the contribution of NQR to pH-dependent NhaA- and NhaB-mediated cation homestasis has not yet been demonstrated at the genetic level.

Lithium is often used as an experimental analog to sodium because it is toxic at concentrations 10x lower than sodium (Goldberg, *et al.*, 1988), thus disentangling sodium toxicity from osmotic stress. This is relevant to *V. cholerae* because the bacterium is so well adapted to saline environments, which are principally comprised of Na^+. NhaA- and NhaB-mediated resistance to Li^+ toxicity has also been shown in *E. coli* and *V. cholerae*, though less completely. Notably, NQR was not observed to export Li^+ in *V. parahaemolyticus*, as evidenced by the Na^+/H^+ antiporter mutants being sensitive to Li^+ but not Na^+ (Tokuda and Unemoto, 1982). Therefore, the primary exporters of Li^+ are expected to be antiporters, primarily NhaA, NhaB, and their homologues. In *E. coli*, a *ΔnhaA* strain grew in the presence of up to 200 mM LiCl; additionally, although the affinity of NhaA and NhaB to Li^+ was similar, the V_{max} of NhaB was 12 times lower than that of NhaA (Inaba, *et al.*, 1994). Expression of the *T. thermophilus* NhaA in EP432 resulted in Li^+ resistance at 87 mM Li^+ (Furrer, *et al.*, 2007). NapA of *E. hirae* expressed in vesicles of EP432 showed an apparent K_m of 0.1 mM Li^+ at pH 7.5 (Strausak, *et al.*, 1993). Loss of NhaA in *V. parahaemolyticus* resulted in sensitivity to Li^+ above 100 mM (Kuroda, *et al.*, 1994). A more detailed assessment of Li^+ toxicity in *V. parahaemolyticus* was later compiled

by Kuroda, et al. (Kuroda, *et al.*, 2005), who showed that the *ΔnhaA* mutant was resistant to 50 mM Li^+ but not 150 mM Li^+ at pH 8.5, while at pH 7.0 the same strain was sensitive only to 800 mM Li^+. Li^+/H^+ antiporter activity of VC-NhaA in EP432 peaked at pH 8.0 (Herz, *et al.*, 2003). The NhaB antiporter of several microbes studied to date contribute markedly less resistance to Li^+ toxicity. Pinner and colleagues found no change in Li^+ sensitivity upon deletion of *nhaB* in *E. coli* (Pinner, *et al.*, 1993), but later experiments showed a slight loss of resistance in the ΔnhaB strain (600 mM Li^+) as compared to the parent (700 mM Li^+) (Inaba, *et al.*, 1994). Interstingly, EC-NhaB was found to regulate cytosolic pH at high external pH (Shimamoto, *et al.*, 1994). Ectopic expression of the NhaB antiporter from *P. aeruginosa* in an antiporterless *E. coli* strain resulted in Li^+ resistance of 10-50 mM Li^+ (Kuroda, *et al.*, 2004). An isogenic mutant of *nhaB* in *V. parahaemolyticus* has not been tested; however, a *ΔnhaAΔnhaD* strain resisted 50 mM Li^+ at pH 8.5 and 500 mM Li^+ at pH 7.0 (Kuroda, *et al.*, 2005). In *V. cholerae*, heterologous expression of Vc-NhaB in everted EP432 membrane vesicles resulted in generally negative antiporter activity in response to Li^+ or Na^+, which the authors suggest is due to the protein being unstable during vesicle preparation (Herz, *et al.*, 2003).

Though the field of bacterial antiporter research is well characterized, the precise genetic mechanisms of environmental Na^+/H^+ and Li^+/H^+ resistance have not been fully described in *V. cholerae*. We have found that, similar to Herz, *et al.*, single mutants of NhaA and NhaB did not exhibit a marked growth defect in response to Na^+ or Li^+. We have built upon this work, and further shown that Na^+- and Li^+-dependent

phenotypes can only be seen in the absence of NQR activity, which we have done in a *ΔnqrA-F* background. Here we report that NhaB cooperated with NQR to achieve Na^+ resistance in a manner similar to the resistance provided by NhaA, with each antiporter having unique environmental pH activity profiles; further, we have observed unique pH profiles of susceptibility of *V. cholerae* lacking both NQR and either NhaA or NhaB to Li^+. Complementation with *Vc-nhaA* and *Vc-nhaB* showed the extent to which each antiporter contributed to *V. cholerae* survival when NQR-dependent Na^+ transport was inhibited but metabolism was not. Thus, this model system can be used to elucidate the function of other antiporters or symporters in *V. cholerae*.

3.3. Materials and Methods

3.3.1. Bacterial Strains and Culture Conditions. For routine cloning and plasmid construction, DH5α (*supE*44 *hsdR*17 *recA*1 *endA*1, *gyrA*96 *thi*-1 *relA*1) (U.S. Biochemical Corp.) or TOP10 [F- *mcr*A Δ(*mrr-hsd*rms-*mcr*BC) φ80*lacZ*ΔM15 Δ*lac*X74 *rec*A1 *ara*D139 Δ(*araleu*) 7697 *gal*U *gal*K *rps*L (Str^R) *end*A1 *nup*G] (Invitrogen) was used as the host. *V. cholerae* strain O395-N1 was used in this study (Mekalanos*, et al.*, 1983), which is the classical Ogawa strain with partial deletion of the *ctx*AB operon (O1 classical biotype; Sm^R, Δ*ctxA*1). If not otherwise indicated, *V. cholerae* cells were grown aerobically at 37 °C in LB supplemented with 100 μg/mL streptomycin. In frame deletion of the *nhaA*, *nhaB*, and *nqr* genes were constructed using the O395N1 strain, as described below. Unless otherwise noted,

complementation of *nhaA* and *nhaB* was performed in LBB supplemented with 100 µg/mL streptomycin, 100 µg/mL ampicillin, and 0.02% (w/v) arabinose.

3.3.2. Cloning and Expression of Vc-NhaA *and* Vc-NhaB. Sequence data for *V. cholerae* were obtained from the Institute of Genomic Research (http://www.jcvi.org). *Vc-nhaA* (VC1627, AAF94778.1) was amplified by high-fidelity polymerase chain reaction (PCR), using chromosomal DNA of *V. cholerae* O395-N1 as a template and directly cloned into the pBAD-TOPO vector (Invitrogen) under the arabinose-induced promoter (P_{BAD}), yielding pVc-NhaA. Primer pairs are listed in Table 3.1. The forward primer was designed to achieve expression of the native enzyme without addition of the N-terminal leader sequence usually introduced by this vector. The primer contains an in-frame stop codon and a translation re-initiation sequence, which consists of a ribosome-binding site and the first ATG of the protein. In the reverse primer, the native stop codon of *Vc-nhaA* was maintained.

Cloning of Vc-NhaB was accomplished similarly to that of Vc-NhaA. *Vc-nhaB* (VC1901, AAF95049.1) was amplified by high-fidelity PCR from chromosomal DNA template of *V. cholerae* O395-N1 and cloned into the pBAD-TOPO vector (Invitrogen) under the arabinose-induced promoter (P_{BAD}), yielding pVc-NhaB. Primer pairs are listed in Table 3.1.

3.3.3. PCR Conditions. Platinum PCR Supermix High Fidelity DNA polymerase (Invitrogen) was used to amplify the 1.2kb fragment corresponding to *Vc-nhaA* and the 1.6 kb fragment corresponding to *Vc-nhaB*. A hanging adenine was added via incubation of the DNA in the presence of 1 unit of Taq DNA polymerase

(Fermentas). A 5 μL aliquot of the PCR mixture was run on a gel to verify the product size, and the remaining PCR mixture was purified using the QIAquick PCR Purification Kit (Qiagen). The DNA was then introduced into the pBAD-TOPO vector using the manufacturer's protocol (Invitrogen). The ligation mixture was then used to transform TOP10 competent cells, which were then plated onto LB agar plates containing 100 μg/mL ampicillin and incubated overnight at 37 °C. Transformants were screened by PCR for the correct orientation by using a forward primer for the plasmid (pBAD Forward) and the 3′ expression primer for the gene. Transformants with the gene in the correct orientation were grown in LB broth containing 100 μg/mL ampicillin overnight at 37 °C, and plasmid DNA was isolated using the QIAprep Spin Miniprep Kit (Qiagen). The fidelity of the PCR was confirmed by DNA sequencing at the Oregon State University Center for Genome Research and Biocomputing core lab facility. The pVc-NhaA construct was then introduced into *V. cholerae* O395N1Δ*nhaA*Δ*nqr* by electroporation (Hamashima, *et al.*, 1995); the pVc-NhaB construct was similarly introduced into *V. cholerae* O395N1Δ*nhaB*Δ*nqr*.

3.3.4. Chromosomal Deletion of the Vc-nhaA *and* Vc-nhaB *Genes*.

Chromosomal deletion of the *Vc-nhaA* and *Vc-NhaB* genes was conducted by homologous recombination in the O395N1 and O395N1Δ*nqr* (Barquera, *et al.*, 2002) background. The in-frame deletion construct was made using overlap extension PCR (Ho, *et al.*, 1989). A 1 kb fragment upstream of the start codon, and a 1kb fragment downstream of the stop codon, was amplified from genomic DNA by PCR using the primer pairs outlined in Table 3.1. The 1 kb products of these two PCRs are able to

anneal together due to complementary sequences engineered into the primers and were used as a template for a third PCR using primers 1 and 4, resulting in a 2 kb PCR product encompassing 1 kb upstream of the start codon and 1 kb downstream of the stop codon with the gene itself removed. This was cloned into suicide vector pWM91 (Metcalf*, et al.*, 1996) by restriction sites engineered into the primers and introduced into the chromosome of *V. cholerae* O395-N1 following sucrose selection as previously described (Metcalf*, et al.*, 1996). This process results in an in-frame deletion of the VC1627 or VC1901 ORFs. The resulting mutant strains (VcΔnhaA, VcΔnhaB, VcΔNQR, VcΔnhaAΔNQR, VcΔnhaBΔNQR) along with its isogenic parent (VcWT) and VcΔnhaAΔNQR/pVc-NhaA overexpressing Vc-NhaA in trans (or VcΔnhaBΔNQR/pVc-NhaA overexpressing Vc-NhaB) were used to analyze growth phenotypes.

3.3.5. Analysis of Growth Phenotypes. For growth analysis of *V. cholerae* transformants, LBB medium (noncationic L broth) was supplemented with antibiotics, arabinose (see above), and varying concentrations of NaCl, LiCl, or KCl. The initial pH was adjusted to 6.5, 7.5, or 8.5 by the addition of 60 mM Bis-Tris propane (BTP) hydrochloride and subsequent titration to the indicated pH. Cells were inoculated at a starting optical density at 600 nm (OD_{600}) of 0.05 in 200 μL of liquid medium placed in 96-deep well plates (Fischer) and grown at 37 °C for 18 h with vigorous aeration. Growth was then measured as the OD of the bacterial suspension at 595 nm by scanning the plates on a BioRad iMark microplate absorbance reader. All experiments were repeated at least three times in triplicate.

3.3.6. Materials. All chemicals were purchased from Sigma-Aldrich or Fisher Scientific. Restriction endonucleases and DNA-modifying enzymes were purchased from Invitrogen, MBI Fermentas, or New England Biolabs.

3.4. Results

3.4.1. NhaA-dependent growth kinetics of O395N1. As antiporters generally exchange protons for cations, with optima specific to each antiporters, we hypothesized that in-frame deletion of the major antiporters *nhaA* or *nhaB* would be specific to a pH and cation optimum. Based on previous reports (Taglicht, *et al.*, 1991; Thelen, *et al.*, 1991; Taglicht, *et al.*, 1993; Kuroda, *et al.*, 1994; Vimont and Berche, 2000; Herz, *et al.*, 2003), we anticipated that the pH optimum for Vc-NhaA would be above 8.0 and its activity would correlate positively with Na^+ concentration. To test this hypothesis, O395N1 (black squares) and O395N1ΔnhaA (gray squares) were assayed for growth deficiency as a function of pH and Na^+ concentration (Figure 3.1). As expected, no difference in growth was observed after 18 hours. Because Vc-NQR can presumably compensate for the loss of Vc-NhaA, and inhibition of NQR by NQNO was previously observed to be necessary to see the effect of Vc-NhaA on Na^+ homeostasis (Herz, *et al.*, 2003), we measured the growth of the strains O395N1Δ*nqr* (black triangles) and O395N1Δ*nqr*Δ*nhaA* (gray triangles) in the presence of Na^+ at high pH (Figure 3.1). A modest but repeatable growth defect was observed in the O395N1Δ*nqr*Δ*nhaA* strain compared to the O395N1Δ*nqr* strain. Intriguingly, O395N1Δ*nqr* was modestly inhibited compared to the parent at every pH tested, and

colonies and LB agar plates appear smaller than the parent. Because NQR is the primary oxidizer of NADH from the TCA cycle in *V. cholerae*, which lacks a proton exporting *nuo* (Complex I of the electron transport chain), deletion of the *nqr* operon would be expected to impact respiration by depleting the quinone pool as well as disturbing Na^+ homeostasis. To determine whether the effect of NQR on growth was primarily related to respiration or Na^+ homeostasis, lactate was added to the growth media, which allowed lactate dehydrogenase to replenish the quinone pool directly (Figure 3.1). Addition of lactate restored most, if not all, of the growth inhibition observed in O395N1Δ*nqr*. O395N1Δ*nqr*Δ*nhaA* was less sensitive to addition of lactate, compared to O395N1Δ*nqr* or the parent. It was also observed that, at pH 7.5, O395N1Δ*nqr*Δ*nhaA* was sensitive to high concentrations of Na^+, mildly so at 200 mM and increasingly so above 400 mM; at pH 8.5, growth of O395N1Δ*nqr*Δ*nhaA* was arrested above OD_{595} of approximately 0.5 for any concentration of Na^+.

Each strain was also assayed for growth in response to Li^+ (Figure 3.2), as Li^+ is known to be an analog of Na^+ and poisonous to bacterial cells at lower concentrations. In line with previous observations (Vimont and Berche, 2000), 100 mM Li^+ inhibited O395N1Δ*nhaA* as compared to the parent at pH 8.5 (Figure 3.2) irrespective of lactate concentration. Interestingly, O395N1Δ*nqr* outgrew the parent in the presence of lactate. At pH 7.5, O395N1Δ*nhaA* was inhibited by 300-450 mM Li^+ as compared to the parent, irrespective of lactate concentration. Growth of O395N1Δ*nqr* was rescued by addition of lactate supplemented with 0-300 mM Li^+, as OD_{595} values increased from 0.3-0.6 without lactate to 0.9-1.1 with lactate. At pH 6.5,

very little difference between parent and O395N1Δ*nhaA* was observed in response to Li^+, though addition of lactate seemed to improve growth of both strains in the presence of 0-300 mM Li^+. Growth of O395N1Δ*nqr*Δ*nhaA* was reduced slightly compared to O395N1Δ*nqr* in the absence of lactate when supplemented by 0-450 mM Li^+. The addition of lactate made the reduced 18 hour growth of O395N1Δ*nqr*Δ*nhaA* even further as compared to O395N1Δ*nqr* in the presence of 100-500 mM Li^+. Intriguingly, O395N1Δ*nqr* was inhibited in growth compared to O395N1between 0-500 mM Li^+ in the presence and absence of lactate.

To probe whether the observed growth phenotypes were specific to Na^+ or were a result of osmotic dysregulation, strains were grown in media buffered to pH 6.5, 7.5, and 8.5 with the addition of 0-600 mM K^+ (Figure 3.3). O395N1 was largely unaffected by addition of K^+ in media buffered to pH 6.5-8.5. Addition of lactate did not change the 18 hour growth yield. Growth of O395N1Δ*nqr* was inhibited by all concentrations of K^+ at each pH tested in the absence of lactate, and upon the addition of lactate growth was restored to nearly that of the parent. At pH 8.5, O395N1Δ*nqr* Δ*nhaA* was inhibited slightly by 200-550 mM K^+ in the absence of lactate, but addition of lactate restored growth over this range while inhibiting growth in the presence of 0-10 mM K^+.

3.4.2. NhaB-dependent growth kinetics of O395N1. In experiments similar to those performed in Figures 3.1-3.3, the role of a *nhaB* chromosomal deletion in the survival of *V. cholerae* was also examined. Like *nhaA*, it was necessary to introduce a chromosomal deletion of *nhaB* in an O395N1Δ*nqr* background to observe any

physiological changes related to loss of NhaB *in vivo*. Loss of Vc-NhaB was found to be most physiologically important at pH 6.5 (Figures 3.4-3.6). A modest reduction in growth of O395N1Δ*nqr*Δ*nhaB* compared to O395N1Δ*nqr* was observed between 0-400 mM Na^+ in the absence of lactate, while a more robust growth inhibition was incurred in the presence of lactate and 0-100 mM Na^+ (Figure 3.4). Interestingly, deletion of *nhaB* led to increased growth due to moderate concentrations of lithium (Figure 3.5). Intriguingly, at in the absence of lactate at pH 6.5, K^+ was observed to inhibit growth of O395N1Δ*nqr*Δ*nhaB* from 0-200 mM K^+ and to slightly increase growth from 400-500 mM K^+ (Figure 3.6A). Growth of O395N1Δ*nqr*Δ*nhaB* at pH 6.5 was inhibited at low (0-10 mM) K^+ concentrations in the presence of lactate (Figure 3.6B). As seen in Figure 3.5, Li^+ inhibited O395N1Δ*nqr* growth even in the presence of lactate.

3.4.3. Complementation of double NQR-antiporter mutants. To observe the extent to which Vc-NhaA and Vc-NhaB contribute to Na^+ and Lit^+ homeostasis, we re-introduced the parental ORF expressed *in trans* on the inducible pBAD vector. O395N1Δ*nqr*Δ*nhaA* hosting pBAD-*Vc-nhaA* was grown in LBB buffered to pH 8.5 containing 0-600 mM Na^+ and Li^+ as well as LBB buffered to pH 6.5 and containing 0-600 mM Li+. O395N1Δ*nqr*Δ*nhaB* hosting pBAD-*Vc-nhaB* was grown in LBB buffered to pH 6.5 containing 0-600 mM Na^+ and Li^+. Both mutants were also transformed with pBAD24, an empty vector, to allow simultaneous comparison of induction in the same arabinose-containing media. OD_{595} was measured after 18 hours of aerobic growth, as before, and compared to the parent strain hosting the empty

vector. Growth of each strain is reported in Figure 3.7. As expected, expression of *Vc-nhaA in trans* in O395N1Δ*nqr*Δ*nhaA* resulted in up to 0.3 OD units increase in growth when compared to O395N1Δ*nqr*Δ*nhaA* hosting the empty vector in the presence of Na^+, with a maximum increase around 500 mM Na^+ (Figure 3.7A). A similar increase in growth was observed for the same complemented strain of O395N1Δ*nqr*Δ*nhaA* grown with 0-10 mM Li^+ (Figure 3.7B). The growth inhibition of O395N1Δ*nqr*Δ*nhaA* by Li^+ at pH 6.5 was restored by complementation to near-WT levels (Figure 3.7C).

Growth of O395N1Δ*nqr*Δ*nhaB* was best complemented by Vc-NhaB in the presence of 0-10 mM Na^+ (Figure 3.7D), though the growth of the complemented strain was modestly better than O395N1Δ*nqr*Δ*nhaB*pBAD24 across all Na^+ concentrations tested. A similar trend was observed for low (0-10 mM) concentrations of Li^+, but expression of Vc-NhaB in the O395N1Δ*nqr*Δ*nhaB* background seemed to slightly hinder growth in the presence of 100 mM Li^+ or more. The growth characteristics of the complemented strains are similar to those of O395N1Δ*nqr* in Panel F of Figures 3.1 and 3.2 (Na^+ and Li^+ at pH 8.5), as well as Panel D of Figure 3.1 and Panel B of Figure 3.4 (Na^+ at pH 6.5), demonstrating functional complementation of these double mutants with Vc-NhaA and Vc-NhaB.

3.5. Discussion

The study of bioenergetics in *V. cholerae* is necessarily clouded by the many transporters, antiporters, and symporters which are used to maintain and use the SMF

(see Table 1.1). One goal of our research is to create a strain of *V. cholerae* with a minimal set of transporters, antiporters, or symporters as a background strain against which the missing genes can be re-introduced to assess gain-of-function, much like EP432 (Pinner, *et al.*, 1993) or TO114 (Ohyama, *et al.*, 1994). To this end, we have created two strains of *V. cholerae* lacking NQR and a major antiporter (NhaA or NhaB). Initially, these strains were used to confirm the results of Herz, et al. (Herz, *et al.*, 2003), who showed the loss of function associated with loss of NQR and NhaA together by chemical inhibition of NQR with HQNO. We hypothesized that Vc-NhaA would be associated with tolerance of Na^+ in environments with a high pH, but that the activity of NQR during aerobic growth would compensate for any loss of Vc-NhaA. Indeed, loss of Vc-NhaA by in-frame deletion yielded no loss in growth fitness as a function of OD_{595} after 18 hours of aerobic growth (Figure 3.1C). Loss of NQR led to a dramatic reduction in growth in liquid media (Figure 3.1A-C, Figure 3.2A-C, and Figure 3.3A-C) and on agar plates (data not shown), a growth defect which could be largely overcome by the addition of lactate to growth media (Figure 3.1D-F, Figure 3.2D-F, and Figure 3.3D-F). Upon addition of lactate to growth media, the double mutant O395N1Δ*nqr*Δ*nhaA* was also observed to grow better than in the absence of lactate. At pH 8.5 the difference in growth yield between O395N1Δ*nqr*Δ*nhaA* and O395N1Δ*nqr* was wider in the presence of lactate than in the absence for all concentrations of Na^+ tested (Figure 3.1F), demonstrating the central role that NhaA plays in tolerance to Na^+ at pH 8.5 in *V. cholerae*. Unexpectedly, the

O395N1Δ*nqr*Δ*nhaA* strain also exhibited sensitivity to Li^+ at pH 6.5, which is outside the previously described activity range of Vc-NhaA.

Vc-NhaB was also assayed in this system (Figures 3.4-3.6) and found to be insensitive to Na^+ or K^+ (Fig 3.4 and 3.6, respectively). In the absence of lactate and in the presence of 0-300 mM Li^+, however, O395N1Δ*nhaB* outperformed the parent strain. Complementing this data, expression of Vc-NhaB in the O395N1Δ*nqr*Δ*nhaB* background hindered growth in the presence of 100-450 mM Li+ at pH 6.5. A similar resistance to Li^+ was found to be mediated by mutation of Vc-NhaP2 (Resch*, et al.*, 2010), which was best explained by Li^+/K^+ antiport, so a similar mechanism may be utilized by Vc-NhaB. Clearly, additional work needs to be performed to resolve these Li^+ phenotypes of Vc-NhaB.

The activity of Vc-NhaA has not been previously linked to any antiporter activity at pH 6.5 *in vivo* or *in vitro*. Our system, which assesses antiporter function in the absence of NQR, overcomes the respiratory inhibition caused by loss of NQR by feeding electrons into the quinone pool through lactate dehydrogenase, allowing cells to respire in a SMF-inhibited environment. This permitted the direct observation of the modest inhibition of growth caused by Li^+ in the absence of Vc-NhaA at pH 6.5 (Figure 3.2D), a growth defect which was complemented by expression of Vc-NhaA *in trans*. (Figure 3.7C). This interaction of Li^+ and Vc-NhaA is novel, warranting further investigation *in vitro* via measurement of rate kinetics in right-side out vesicles adjusted to acidic external pH.

Prior to this study, the relative contribution of NQR to antiporter function in *V. cholerae* had been partly addressed by the use of chemical inhibitors. The results presented herein confirm and expand upon those of Herz and colleagues. In addition, the bacterial strains generated can be used to assess the function of genes that have already been removed from the genome (*nqr*, *nhaA*, and *nhaB*) as well as overexpression of the other transporters, antiporters, or symporters outlined in Figure 1.1. Such a sensitive system is necessary to fully characterize the remaining antiporters (for instance, Vc-NhaC1, Vc-NhaC2, Vc-NhaC3, Vc-NhaC4, or Vc-NhaP3), which are not expected to contribute to SMF maintenance as robustly as Vc-NhaA or Vc-NhaB. Additionally, the expression profiles of these antiporter genes under a range of osmotic conditions will add to our understanding of which antiporters are recruited, when, and to what extent. The effect of antiporter mutation on virulence factor expression, notably *ctx* and *toxT*, will also be important to study. These expression studies are already underway in our lab (Y. Minato, personal communication).

Even though NhaA, NhaB, and NQR have been studied for many years in several model systems, the role of these and other SMF-creating and SMF-using proteins are still incompletely understood. The large library of such proteins (Table 1.1) explains, in part, why it is so difficult to examine their roles in physiology and virulence. Innovative research techniques combined with basic bacterial genetic methods permitted the construction of a model system wherein the interactions of the proteins in Table 1.1 can be examined in more detail *in vivo* than previously possible.

In particular, the examination of *V. cholerae* antiporters in an O395N1Δ*nqr*Δ*nhaA* background, the concept of which was shown to be feasible by the expression of Vc-NhaA, will be a useful tool to characterize the other contributors to *V. cholerae* bioenergetics.

3.6. Acknowledgements

Y. Minato provided helpful and critical feedback on the manuscript and experiment design. This research was supported by a grant from the National Institutes of Health (no. AI-063121-02).

3.7. Tables and Figures

Table 3.1. Primers used in this study.

Vc-NhaA, 5' region	5'-GGGGGGGATCCGTGATTAATG GCAAGAAAGTGAG-3'
	5'-GACTGACTGACTGACTGACTGACT CATAGGTTTGTCCTTAAATTATG-3'
Vc-NhaA, 3' region	5'-AGTCAGTCAGTCAGTCAGTCAGTC TAATCATTTCATCAGGCTTTGAAC-3'
	5'-GGGGGGAGCTCCGATGGGCCACA GAACTGGATCACAC-3'
Vc-NhaB, 5' region	5'-GGGGGGGATCCCTCAGCGAAACCG GCTGGGCTT-3'
	5'-AGTCAGTCAGTCAGTCAGTCAGTC CATGATGATTACTCTTTAACTG-3'
Vc-NhaB, 3' region	5'-AGTCAGTCAGTCAGTCAGTCAGTC TAAATTTCAATTGAAACTGAAAC-3'
	5'-GGGGGGAGCTCAACGGTAATCGTG ATGTATTGGC-3'
Vc-NhaD, 5' region	5'-GGGGGGGATCCCTATGGTGGCACC TGCAGAGAATTGG-3'
	5'-AGTCAGTCAGTCAGTCAGTCAGTCC ATAACAAAACTCCTGTTGATATCC-3'
Vc-NhaD, 3' region	5'-AGTCAGTCAGTCAGTCAGTCAGTCT AACATGTCTGATTGAAGCTGCTAC-3'
	5'-GGGGGGAGCTCCAGATCCGTAATA ACTCCAAAG-3'
Vc-NhaA expression	5'-GAAGAATAATAAATGTCTGACATGA TTCGAGA-3'
	5'-TTATTACGCTTTTTTGAGCGGCAGA GAGAG-3'
Vc-NhaB expression	5'-GAAGAATAATAAATGCCGATGTCC CTCG-3'
	5'-TTATTATTAGTGGCCACTTTGCAGT-AGT-3'

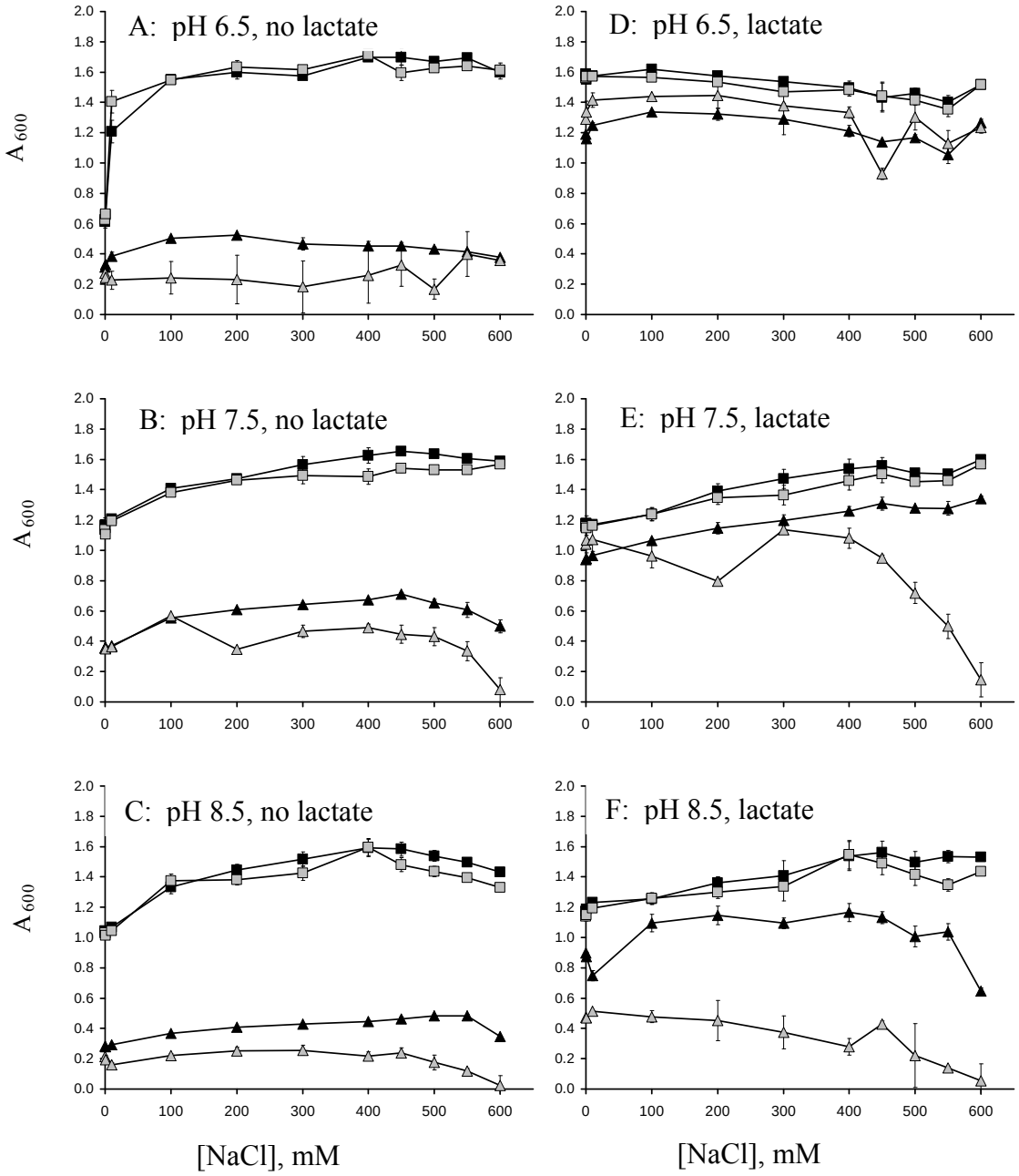

Figure 3.1. NaCl growth experiments of Δ*nqr*, Δ*nhaA*, and Δ*nqr*Δ*nhaA*. O395N1 (black squares: ■) and its mutant derivatives Δ*nqr* (black triangles: ▲), Δ*nhaA* (gray squares: ■), and Δ*nqr*Δ*nhaA* (gray triangles: ▲)were grown for 18 hours in non-cationic LB base buffered with 60 mM BTP to pH 6.5, 7.5, or 8.5 in the absence (left panels) or presence (right panels) of 33 mM lactate with 0-600 mM NaCl. Reported are the mean OD_{595} of each strain grown in duplicate under the given conditions. Error bars represent the standard deviation. Experiments were repeated three times.

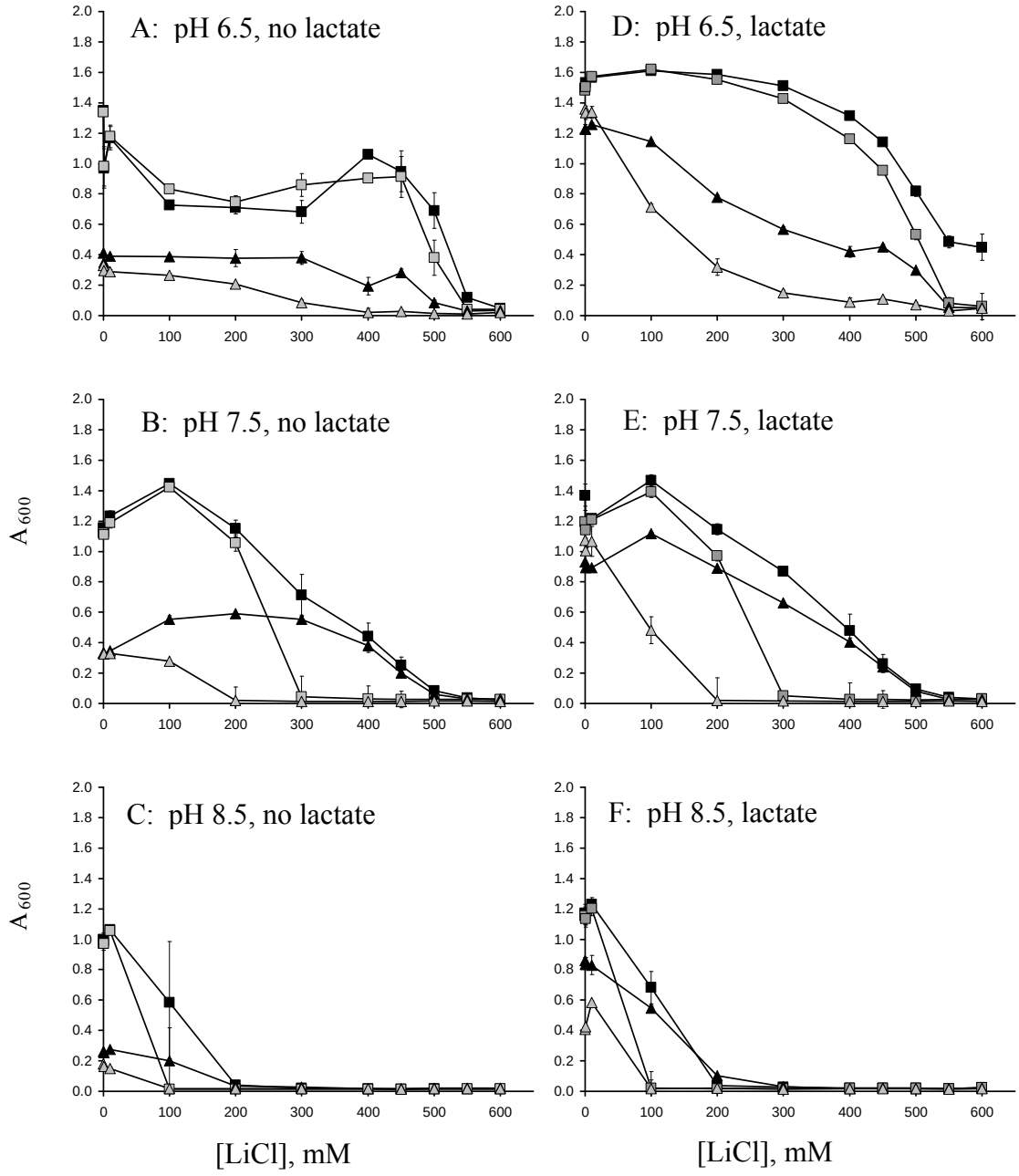

Figure 3.2. LiCl growth experiments of Δ*nqr*, Δ*nhaA*, and Δ*nqr*Δ*nhaA*. O395N1 (black squares: ■) and its mutant derivatives Δ*nqr* (black triangles: ▲), Δ*nhaA* (gray squares: ■), and Δ*nqr*Δ*nhaA* (gray triangles: ▲) were grown for 18 hours in non-cationic LB base buffered with 60 mM BTP to pH 6.5, 7.5, or 8.5 in the absence (left panels) or presence (right panels) of 33 mM lactate with 0-600 mM LiCl. Reported are the mean OD_{595} of each strain grown in duplicate under the given conditions. Error bars represent the standard deviation. Experiments were repeated three times.

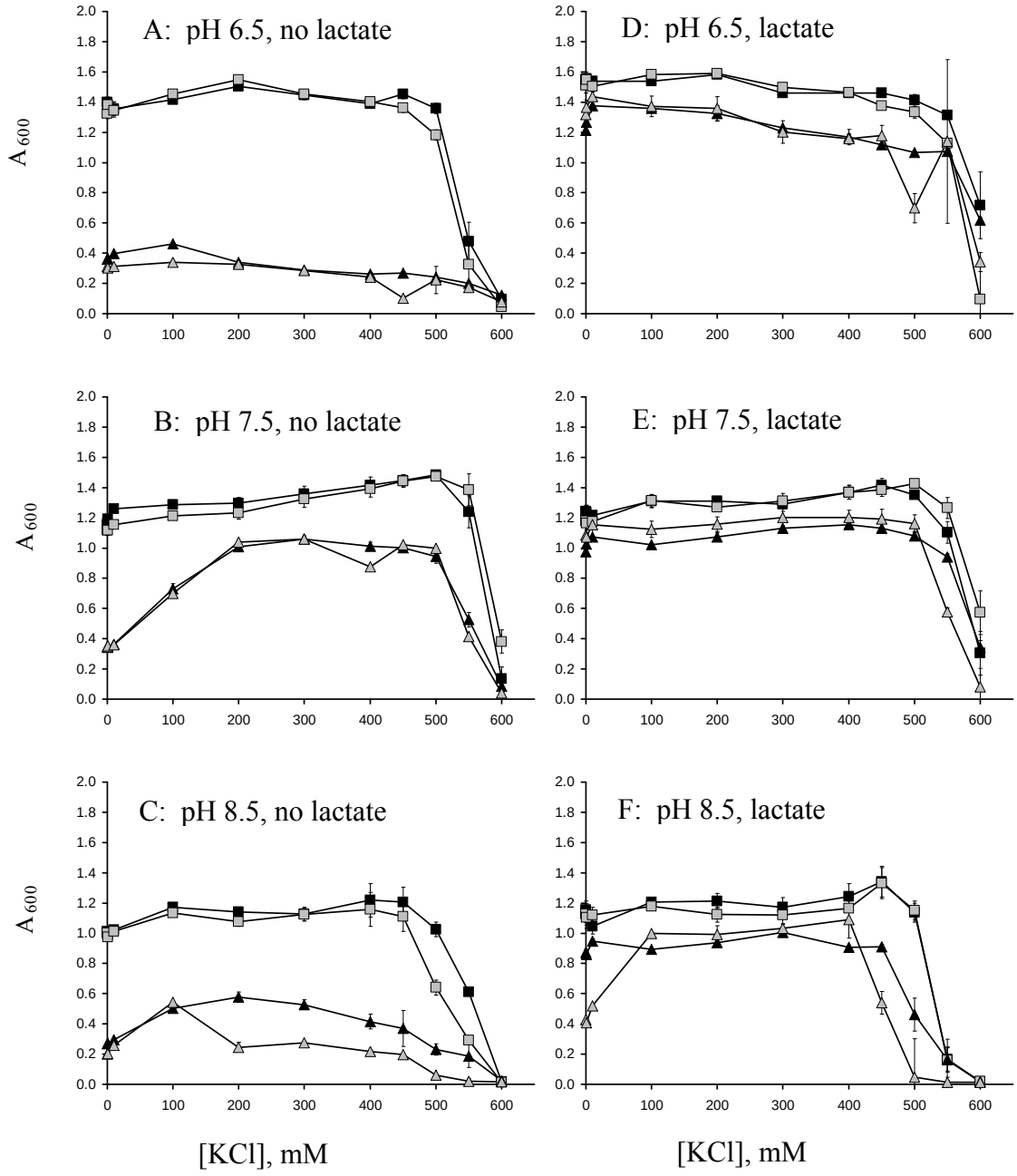

Figure 3.3. KCl growth experiments of Δ*nqr*, Δ*nhaA*, and Δ*nqr*Δ*nhaA*. O395N1 (black squares: ■) and its mutant derivatives Δ*nqr* (black triangles: ▲), Δ*nhaA* (gray squares: ■), and Δ*nqr*Δ*nhaA* (gray triangles: ▲) were grown for 18 hours in non-cationic LB base buffered with 60 mM BTP to pH 7.5 or 8.5 in the absence (left panels) or presence (right panels) of 33 mM lactate with 0-600 mM KCl. Reported are the mean OD_{595} of each strain grown in duplicate under the given conditions. Error bars represent the standard deviation. Experiments were repeated three times.

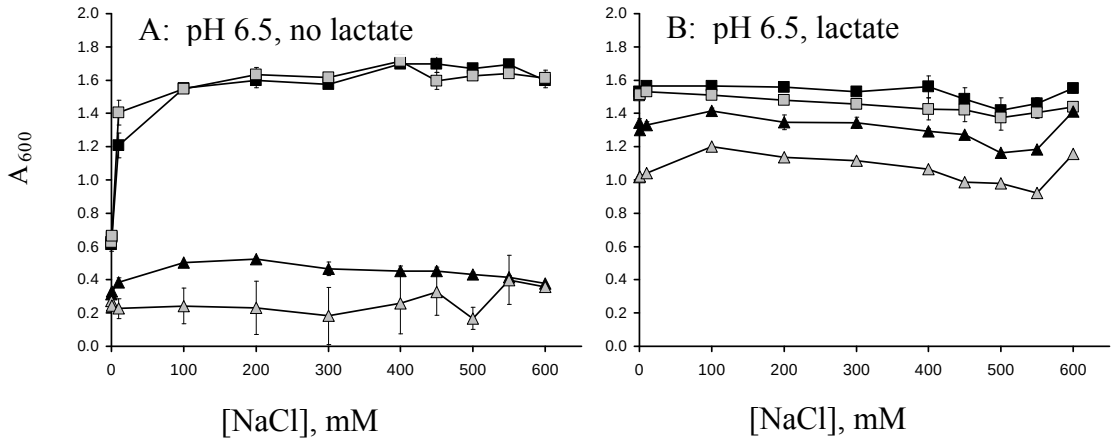

Figure 3.4. NaCl growth experiments of Δ*nqr*, Δ*nhaB*, and Δ*nqr*Δ*nhaB*. O395N1 (black squares: ■) and its mutant derivatives Δ*nqr* (black triangles: ▲), Δ*nhaB* (gray squares: ■), and Δ*nqr*Δ*nhaB* (gray triangles: ▲) were grown for 18 hours in non-cationic LB base buffered with 60 mM BTP to pH 6.5 in the absence (left panels) or presence (right panels) of 33 mM lactate with 0-600 mM NaCl. Reported are the mean OD_{595} of each strain grown in duplicate under the given conditions. Error bars represent the standard deviation. Experiments were repeated three times.

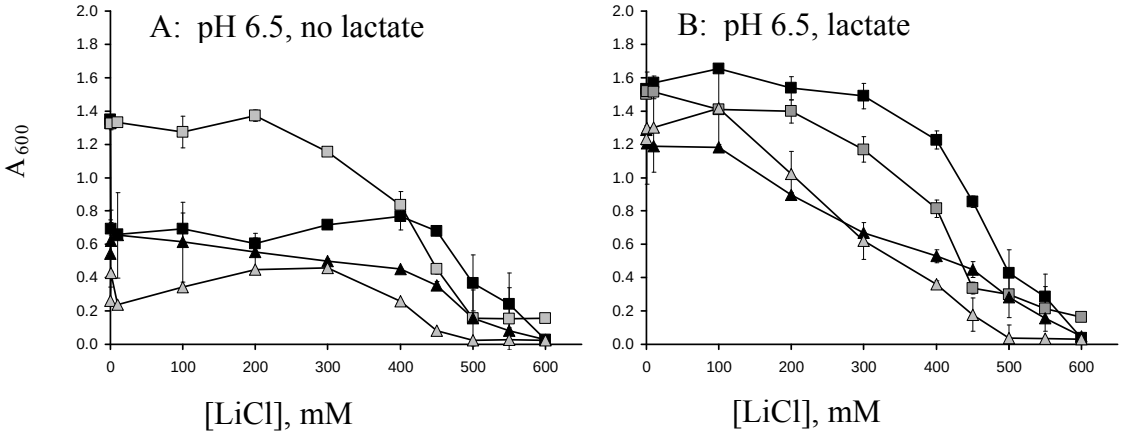

Figure 3.5. LiCl growth experiments of Δ*nqr*, Δ*nhaB*, and Δ*nqr*Δ*nhaB*. O395N1 (black squares: ■) and its mutant derivatives Δ*nqr* (black triangles: ▲), Δ*nhaB* (gray squares: ■), and Δ*nqr*Δ*nhaB* (gray triangles: ▲) were grown for 18 hours in non-cationic LB base buffered with 60 mM BTP to pH 6.5 in the absence (left panels) or presence (right panels) of 33 mM lactate with 0-600 mM LiCl. Reported are the mean OD_{595} of each strain grown in duplicate under the given conditions. Error bars represent the standard deviation. Experiments were repeated three times.

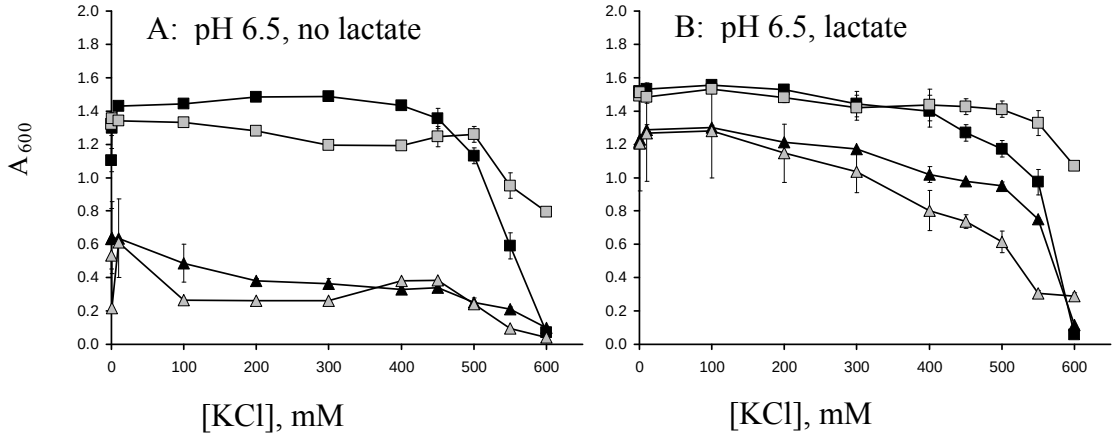

Figure 3.6. KCl growth experiments of Δ*nqr*, Δ*nhaB*, and Δ*nqr*Δ*nhaB*. O395N1 (black squares: ■) and its mutant derivatives Δ*nqr* (black triangles: ▲), Δ*nhaB* (gray squares: ■), and Δ*nqr*Δ*nhaB* (gray triangles: ▲) were grown for 18 hours in non-cationic LB base buffered with 60 mM BTP to pH 6.5 in the absence (left panels) or presence (right panels) of lactate with 0-600 mM KCl. Reported are the mean OD_{595} of each strain grown in duplicate under the given conditions. Error bars represent the standard deviation. Experiments were repeated three times.

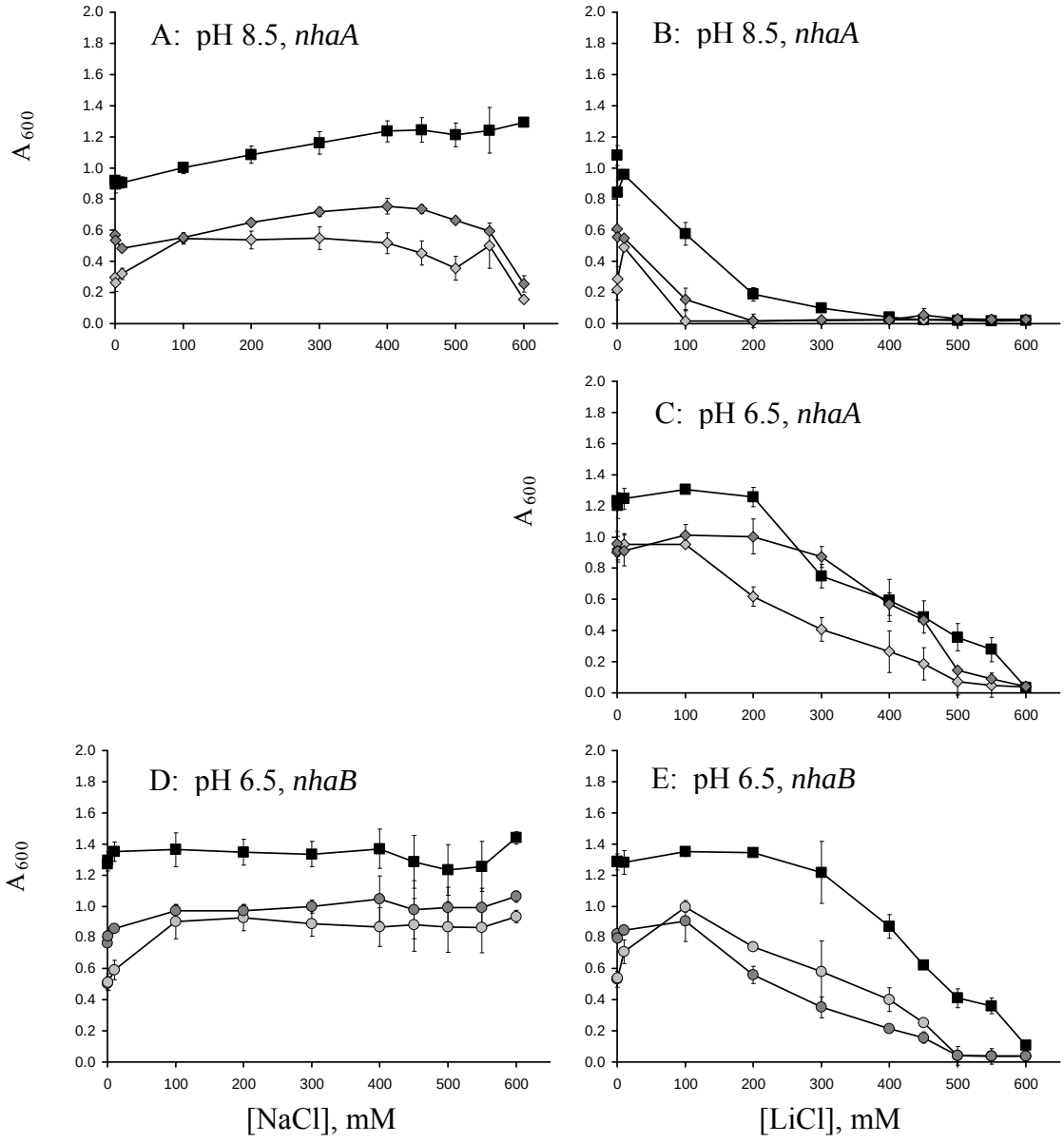

Figure 3.7. Complementation of O395N1Δ*nqr*Δ*nhaA* and O395N1Δ*nqr*Δ*nhaB*. O395N1pBAD 24 (black squares: ■) and its mutant derivatives Δ*nqr*Δ*nhaA*pBAD24 (light gray diamonds: ♦), Δ*nqr*Δ*nhaA*pBAD*nhaA* (dark gray diamonds: ♦), Δ*nqr*Δ*nhaB*pBAD24 (light gray circles: ●), and Δ*nqr*Δ*nhaB*pBAD*nhaB* (dark gray circles: ●)were grown for 18 hours in non-cationic LB base buffered with 60 mM BTP to pH 6.5, 7.5, or 8.5 in the absence (left panels) or presence (right panels) of lactate with 0-600 mM KCl. Reported are the mean OD_{595} of each strain grown in duplicate under the given conditions. Error bars represent the standard deviation. Experiments were repeated three times.

4. Use of a Defined Transposon Library to Correlate Chemical Stimuli with Methyl-Accepting Chemotaxis Protein Sensors in *Vibrio cholerae*

Matthew J. Quinn, EmilyKate McDonough, Andrew Camilli, Claudia Häse

4.1. Abstract

Methyl-accepting chemotaxis proteins (MCPs) are a family of conserved bacterial signaling proteins that sense a stimulus specific to chemotaxis, a process of changing the direction of bacterial motility in response to that stimulus. Few bacteria have as many MCPs as the pathogen *V. cholerae*, a bacterium that inhabits both human and aquatic reservoirs, using chemotaxis within both niches. Because of the link between chemotaxis and virulence in *V. cholerae*, we sought to correlate potential chemotaxis stimuli with cognate MCP receptors. The homology of MCP sensory domains among *Vibrionaceae* demonstrated a subset that were unique to *V. cholerae*. Of these unique MCPs, transposon insertion in VC0098 significantly reduced chemotaxis swarm diameter towards Na^+ and K^+. Additionally, the MCP VCA0663 was shown, by transposon mutagenesis and complementation, to direct chemotaxis towards N-acetyl-glucosamine. Additional observations are described concerning the chemotaxis defects incurred by transposon mutagenesis of MCPs *in vitro* towards mucin, bile, or L-serine. None of the observed chemotaxis defects showed complete loss of chemotaxis by transposon mutagenesis, in line with the hypothesis that the large number of MCPs encoded by *V. cholerae* result in redundant chemotaxis sensory functions. MCP strains were also tested *in vivo* for 4 and 24 hours in the infant mouse model of infection, but no significant changes in virulence were observed, which is in accordance with the redundancy hypothesis. This research is an important exposition of MCP:chemoattractant pairing, which will add to the understanding of MCP sensory function within the lifecycle of *V. cholerae*.

4.2. Introduction

V. cholerae is the bacterium which causes cholera, which continues to kill thousands of people in the developing world each year (Enserink, 2010). One of the primary virulence factors associated with *V. cholerae* is motility, which the bacterium achieves by use of a sodium motive force (SMF)-powered flagellum (Kojima, *et al.*, 1999) with characteristically fast rotation, in excess of 100,000 RPM (Magariyama, *et al.*, 1994), which propels the bacterium at over 60 μm per second (Atsumi, *et al.*, 1992; Atsumi, *et al.*, 1996). When motility is mediated by chemical stimuli, the process is called chemotaxis. The distinction between motility and chemotaxis is important because, in *V. cholerae*, motile but non-chemotactic bacteria have been shown to be hyperinfectious in mice (Butler and Camilli, 2004), implying that chemotaxis is a detriment to *V. cholerae* during at least the initial stages of colonization of the small intestine. Additionally, it has long been known that motile bacteria can be seen in the rice water stool of infected individuals (Keen and Bujalski, 1992). More recently, *V. cholerae* were also shown to be capable of forming a biofilm when isolated from the stool of infected individuals (Faruque, *et al.*, 2006), which is noteworthy because biofilm community bacteria typically downregulate the expression of motility genes, like the flagellum (Watnick, *et al.*, 2001; Liang, *et al.*, 2007). However, during the late stage of infection the starvation-associated RNA polymerase σ factor RpoS, in cooperation with the quorum sensing regulator HapR, was found to increase expression of chemotaxis genes and motility (Nielsen, *et al.*, 2006). From these observations, it is obvious that chemotaxis in *V. cholerae* during

infection is complex and dynamic. Further investigation into the role chemotaxis plays in virulence will contribute to a better understanding of this important pathogen.

Research into the chemotaxis of *V. cholerae* necessarily builds on that of more robustly studied systems, such as *Escherichia coli* (Falke*, et al.*, 1997), *Salmonella typhimurium* (Falke*, et al.*, 1997), and *Helicobacter pylori* (Spohn, 2001). From these studies, it appears that the general order of events leading from sensory stimulus to directional motility is conserved among chemotactic bacteria. Stimuli are sensed by bacteria through methylating chemotaxis proteins (MCPs), which are a highly conserved family of transmembrane proteins (Alexander and Zhulin, 2007) dedicated to sensing stimuli and, in turn, coordinating flagellum-mediated motility up or down a concentration gradient of that stimulus.

MCPs ensure that chemotaxis progresses up a concentration gradient. The sensitivity of MCPs toward their stimulus is continually modified by methylation (Sourjik and Berg, 2002), which reduces the binding affinity of the stimulus to the MCP, thereby making only progressively higher concentrations an attractant. The cytosolic protein CheR aids in methylation, and is recruited to action upon binding of a cognate stimulus (Springer and Koshland, 1977), in this manner ensuring that only higher concentrations of the stimulus will induce directional motility. CheB aids in demethylation, and in this way balances the actions of CheR by re-sensitizing the MCP to lower concentrations of chemotactic stimuli (Yonekawa*, et al.*, 1983). MCPs are noted for having a cytosolic autophosphorylating tail, which induce autophosphorylation in CheA, a soluble cytosolic intermediate, in response to MCP

stimulation (Falke and Hazelbauer, 2001). CheA phosphorylates CheY, which binds to the FliG flagellar subunit and switches the direction of flagellar rotation (Boin*, et al.*, 2004).

The switch in direction of flagellar rotation that changes direction of motility: counterclockwise rotation propels the bacterium forward, and clockwise rotation initiates a change in bacterial orientation. In *E. coli*, the "reverse" direction causes the bacterium to tumble briefly and re-orient randomly in a new direction (Berg and Brown, 1972); however, in *V. alginolyticus* the "reverse" direction causes the flagellum to flick the bacterium around into a new random direction (Xie*, et al.*, 2011). These differences in phenotype, though caused by similar mechanism, underscore the shortcoming of using bioinformatics alone to inform our understanding of chemotaxis in *V. cholerae*, as there are certainly more and greater differences.

The differences between the model system of *E. coli* and the pathogen *V. cholerae* are encompassed mostly by the multitude of paralogues possessed by the latter. *E. coli* possesses only five MCPs, which exhibit a small degree of redundancy (reviewed in (Wadhams and Armitage, 2004)), but in *V. cholerae* there are 45 predicted MCPs, which have the potential for some redundancy as well (Boin*, et al.*, 2004). Similarly, *E. coli* has one paralogue of the intermediates CheA, CheY, CheB, and CheR, but *V. cholerae* possesses 3 CheA paralogues, 5 CheY paralogues, 3 CheB paralogues, and 3 CheR paralogues (Boin*, et al.*, 2004). Interestingly, *in vitro* chemotaxis in *V. cholerae* has been shown to require only one paralogue of CheA (Gosink*, et al.*, 2002) and CheY (Hyakutake*, et al.*, 2005), the genes for which are

both located in the same cluster of chemotaxis genes (Boin, *et al.*, 2004). Study of the MCPs in *V. cholerae* is markedly more difficult than in other organisms such as *E. coli*, because functional redundancy is expected to confound any attempt to mutate sensory proteins and ectopic expression can be inhibited if CheA, CheB, or CheR have any reduced affinity to the non-native MCP.

While many motile bacteria have MCPs for sensory-directed motility, only the signal transduction portion (a hairpin turn of 2 parallel alpha helices located within the cytosol) is highly conserved: 1,915 MCPs sequences from 312 bacterial species were found to be homologous in this region (Alexander and Zhulin, 2007). Therefore, little is known about the specificity of any of the MCPs of *V. cholerae*, in spite of the work done in less complex bacterial systems (Adler, 1969; Springer, *et al.*, 1977; Clarke and Koshland, 1979; Boyd, *et al.*, 1983; Russo and Koshland, 1983; Jeffery and Koshland, 1993; Bespalov, *et al.*, 1996; Yeh, *et al.*, 1996; Bibikov, *et al.*, 1997; Liu and Parales, 2008). As mentioned in Chapter 1, three MCPs have been named due to their involvement in virulence: TcpI (Harkey, *et al.*, 1994), AcfB (Everiss, *et al.*, 1994), and HlyB (Alm and Manning, 1990). A double mutant of two of these virulence-associated MCPs (*acfB* and *tcpI*) was attenuated for infection in the mouse model (Chaparro, *et al.*, 2010), but their cognate stimuli are still unknown. However, stimuli of the MCPs VC0449 and Aer-2 (VCA0658) have been determined as chitin (an oligomer of *N*-acetyl-glucosamine, or GlcNAc) (Meibom, *et al.*, 2004) and oxygen (Boin and Hase, 2007), respectively. Chemotaxis of *V. cholerae* towards chitin is expected, as chitin is ubiquitous and most often the major carbon source in aquatic

environments, especially amongst the plankton which *V. cholerae* colonizes in its hypothesized infectious reservoir (Chapter 1). The MCP Aer-2 was predicted to bind a FAD prosthetic group by sequence analysis and experimentally determined to direct motility towards O_2 (Boin and Hase, 2007).

Prior to this work, the stimuli of the remaining 43 MCPs in *V. cholerae* had not been determined. Therefore, we sought to determine chemoattractants relevant to *V. cholerae* in a pathogenic or planktonic lifestyle, and to identify the MCP sensors that respond to these stimuli. Using a defined transposon library, we assessed the transposon-induced loss of function correlated with loss (or gain) of motility in a chemotaxis assay system. This library was assayed against the chemoattractants L-serine, K^+, Na^+, bile, mucin, and GlcNAc in soft agar swarm plates, as well as *in vivo*. This research represents an important and novel contribution to our understanding of chemotaxis in *V. cholerae*.

4.3. Materials and Methods

4.3.1. Bacterial Strains and Culture Conditions. *V. cholerae* O1 serogroup El Tor biotype strain C6706 was used to generate the transposon library (MCP::Tn*Mar*), kindly provided by J. Mekalanos (Cameron, *et al.*, 2008). The clones from this library that were used in this study are listed in Table 4.1. For routine cloning and plasmid construction, DH5α (*supE*44 *hsdR*17 *recA*1 *endA*1, *gyrA*96 *thi*-1 *relA*1) (U.S. Biochemical Corp.) or TOP10 [F- *mcr*A Δ(*mrr-hsd*rms-*mcr*BC) Δ80*lacZ*ΔM15 Δ*lac*X74 *rec*A1 *ara*D139 Δ(*ara leu*) 7697 *gal*U *gal*K *rps*L (Str^R) *end*A1 *nup*G]

(Invitrogen) was used as the host. For normal growth and cloning, strains were grown on LB agar. C6706 strains were grown with 100 μg/mL streptomycin, and *E. coli* strains were grown in the absence of antibiotics. Both the pBAD and pWM91 vectors, mentioned below, were maintained by addition of 100 μg/mL ampicillin. Chemotaxis swarm agar studies were conducted at 30°C using minimal media soft agar plates, containing M9 salts (disodium phosphate, 6.78 g/L; monopotassium phosphate, 3 g/L; sodium chloride, 0.5 g/L; ammonium chloride, 1 g/L), thiamine (1 μg/mL), magnesium sulfate (2 mM), sodium succinate (50 mM), calcium chloride (100 μg/mL), streptomycin (100 μg/mL), and agar (0.28% w/v); 25 μg/mL kanamycin was added during Illumina experiments (below). Chemoattractants were added to their specified concentration (see Results).

4.3.2. Phylogenetic Analysis of MCP Amino Acid Sequences. The amino acid sequence of each MCP from the *V. cholerae* El Tor N16961 database was obtained (listed in Table 4.1), as well as that of the *E. coli* K-12 serine-sensitive MCP, Tsr (b4355). The N-terminus was identified by locating the conserved cytosolic signaling domain, then locating the amino acid approximately 150 amino acids upstream (designated as the putative HAMP domain) and removing the amino acids within the sequence between the putative HAMP domain and the C terminus. The remaining amino acid sequence was treated as the N terminus (or MCP sensory portion). The resulting N-termini were aligned by ClustalW within the program MEGA4 (Tamura, *et al.*, 2007), which was also used to construct the phylogenetic tree in Figure 4.2. Individual Vc-MCP N-termini sequences were compared to the genomes of the

Vibrionaceae (taxid:641) using NCBI/BLASTp (Altschul*, et al.*, 1997). The alignment of these MCP N-termini sequences was used to create a phylogenetic tree using maximum parsimony analysis, which was subjected to a bootstrap test of phylogeny to determine accuracy of the analysis.

4.3.3. In-Frame Deletion of VC1898, aer2, *and* VCA1031. Chromosomal deletion of the genes VC1898, *aer2* (VCA0658), and VCA1031 were conducted by homologous recombination. A defined mutant construct was made using overlap extension PCR (Ho*, et al.*, 1989). A 1 kb fragment upstream of the start codon and downstream of the stop codon was amplified from genomic DNA (gDNA) by PCR using the primers in Table 4.2. The DNA products of these two PCR reactions were able to anneal together due to complementary sequences engineered into primers 2 and 3 and were used as a template for a third PCR using primers 1 and 4, resulting in a 2-2.4 kb PCR product encompassing 1-1.2 kb upstream of the start codon and 1-1.2 kb downstream of the stop codon with the gene itself removed. This PCR product was cloned into suicide vector pWM91 (Metcalf*, et al.*, 1996) by restriction sites engineered into the primers 1 and 4, creating pWM91-Δ*MCP* (for the MCPs VC1898, *aer-2*, or VCA1031) and the mutant allele was introduced into the chromosome of *V. cholerae* C6706 following conjugation with the *E. coli* strain SM10λpir hosting the vector. Using sucrose selection as previously described (Metcalf*, et al.*, 1996), the in-frame deletion of the ORF was introduced into the chromosome of *V. cholerae* strain C6706.

Selected MCP::Tn*Mar* mutations were complemented by expression of the native ORF *in trans* using the pBAD-TOPO expression vector (Invitrogen). The putative MCP ORF was amplified by high-fidelity polymerase chain reaction (PCR), using chromosomal DNA of *V. cholerae* C6706 as a template and directly cloned into the pBAD-TOPO vector under the arabinose-induced promoter (P_{BAD}). Clone sequences were verified by the Oregon State University Center for Genome Research and Biocomputing. Clones of WT-MCPs expressed on pBAD-TOPO were transformed into competent cells of the cognate MCP::Tn*Mar* strain. The vectors were maintained by addition of ampicillin (100 μg/mL), and expression was induced by the addition of arabinose (0.02% final concentration) to media.

4.3.4. Soft Agar Swarm Plate Assays. Individual strains from the MCP transposon library were grown for 7 hours at 37°C on LB plates with streptomycin (100 μg/mL). A sterile toothpick was used to sample a region of growth and stabbed into soft agar swarm plates containing M9 media alone or supplemented with chemoattractants, including L-serine, mucin, bile salts (a ~1:1 mixture of cholic acid and deoxycholic acid Na^+ salts), GlcNAc, K^+, or Na^+. The plates were incubated at 30°C for 18-48 hours. Plates were photographed using a UVP BioDocIt imaging station. Swarm diameters were measured using IMAGEJ ANALYSIS software (http://rsb.info.nih.gov/ij/). Data are presented as the ratio of mutant swarm diameter to parent swarm diameter for each chemoattractant as well as swarm media lacking chemoattractant. Relative swarm size, the ratio of mutant:parent swarm areas, was compared with and without chemoattractant, a relationship termed relative chemotaxis

fitness. Data are presented as the average of at least three experiments. Statistical significance was calculated by 1-tailed paired Student's t-test for each MCP, comparing relative swarm size in the presence and absence of chemoattractant.

4.3.5. Illumina-based Quantification of Mixed Transposon Library Population. The protocol was adapted from van Opijnen, *et al.* (van Opijnen, *et al.*, 2009) Each C6706 MCP::Tn*Mar* clone was grown on LB overnight at 30°C. Biomass was resuspended in LBB to a final OD_{600} of 1.0 and pooled. After vigorous agitation, 1 mL aliquots of the pooled library were mixed with glycerol (final concentration of 15%) and stored at -80°C.

For each *in vitro* experiment, a mixed aliquot was thawed and diluted into 20 mL LB, and allowed to outgrow to mid-exponential phase (2-3 hours). After outgrowth, cells were treated in multiple ways. Cells were washed once with PBS and resuspended in 10 mL PBS. Half of this volume was used to isolate gDNA using the Qiagen Tissue and Blood DNA preparation kit. A 5 μL volume of the outgrowth was inoculated into 5 mL LB with streptomycin (100 μg/mL) and kanamycin (25 μg/mL) and grown in parallel at 37°C for 18 hours. 100 μL of the remaining outgrowth was used to seed square chemotaxis plates, formed from M9 soft agar minimal media (as in section 4.3.4) in 6 inch square polystyrene Petri dishes (Fisher), with a 4 inch line cut in the center of the plate with a sterile razor blade. Plates were incubated for 18 hours at 30°C. A 2 mm band 4 inches long, encompassing the leading edge of the swarm biomass, was excised and gDNA was isolated, as described above.

For each *in vivo* experiment, a mixed frozen aliquot was grown in 20 mL LB with streptomycin (100 μg/mL) and kanamycin (25 μg/mL) at 37°C for 1-2 hours to early-exponential phase. Cells were pelleted and resuspended in 10 mL PBS; half of this volume was used to measure gDNA, as before, and the remaining volume was diluted in PBS to an OD_{600} = 0.01. Five day old CD1 mice were starved for 2 hours, then inoculated by gavage with 50 μL of the cell suspension; 4 hours or 24 hours after infection, mice were euthanized and small intestines were isolated, homogenized, and microbial gDNA was isolated as previously described. Colony forming units (CFU) present in the infected intestine were analyzed by plating homogenates on LB with streptomycin (100 μg/mL) and kanamycin (25 μg/mL) and enumerating after 18 hours growth at 37°C. A 5 μL volume of the outgrowth was inoculated into 5 mL LB with streptomycin (100 μg/mL) and kanamycin (25 μg/mL) and grown in parallel at 37°C for 18 hours, from which gDNA was isolated, as previously described.

gDNA from each sample was sheared by sonication to achieve 100-300 bp fragments, which were checked by measuring an aliquot of each sample by gel electrophoresis. The remaining volume was cleaned (Qiagen gel purification kit) and the ends were blunted (NEB QuickBlunt kit). 3'-A overhangs were added with the NEB Klenow Fragment (3'-5' exo-) and dATP. Each sample was then ligated with one of 9 unique adapters, each sharing a common sequence for binding to the Illumina Genome Analyzer flow-cell and each bearing a unique 4 base pair bar code identifier (underlined in Table 4.2); excess adapters were removed with the Qiagen Gel Extraction Kit. Hybrid DNA was amplified using primers OLJ373 (complementary to

adapter) and MAREC2 (complementary to the Mariner transposon). This PCR was product was subject to a second round of low cycle number PCR using the MarOut and OLJ245 primers, and the final reaction was cleaned using EdgeBio columns. Equimolar amounts of each sample were pooled such that each pool contained samples having unique DNA barcodes. Pooled samples were sequenced using the Illumina Genome Analyzer, which counted the number of amplicons of each gene per barcode in each pool, and genes were identified by homology to the sequenced *V. cholerae* genome (Heidelberg, *et al.*, 2000).

To control for potential polar effects of tranposon insertion on growth fitness, relative chemotaxis fitness (Illumina) was calculated for each chemoattractant condition *in vitro* as follows: first, the proportion of DNA copies (Illumina reads) of each MCP were calculated as a proportion of the total number of reads, then this proportion was compared to the same proportion in a parallel LB broth outgrowth using the same MCP mutant pool. Relative chemotaxis fitness (Illumina) for each chemoattractant was expressed as a fraction of fitness with chemoattractant divided by fitness without chemoattractant. Relative chemotaxis fitness *in vivo* was calculated as the proportion of MCP reads as a fraction of total reads in the pooled intestinal homogenate compared to the same fraction in the contemporary LB outgrowth.

4.3.6. Animal Care and Use. All animals used in this study were handled according to the guidelines set forth in Dr. Camilli's Tufts University IACUC protocol.

4.4. Results

4.4.1. In silico *analysis of* V. cholerae *MCPs.* The state of known MCP substrate specificity prior to this study is summarized in Table 4.1. We hypothesized that, among the *Vibrionaceae*, MCPs belonging solely to *V. cholerae* would be more associated with motility traits linked to virulence or environmental persistence, using known virulence-associated MCPs (TcpI, AcfB and HlyB) as controls. Since the cytoplasmic signaling domain of MCPs is highly conserved, we only compared the N-terminal signal-receiving domain. The results of our phylogenetic analysis of the MCPs of *Vibrionaceae* in respect to those of *V. cholerae* can be found in Figure 4.1. Homology is expressed as the negative-powered exponent of the Expect score, which represents the chance that the reference sequence and target sequence are related by chance. Ten *V. cholerae* MCP amino acid sequences were found to have very low similarity to any other *Vibrio* MCPs measured (Fig. 4.1A): VC0098, TcpI, AcfB, VC1394, VC1403, VC1405, VC1643, VCA0031, VCA0979, and VCA1088. Two MCPs (VC1967 and HlyB) matched only the non-pathogenic *V. cholerae* strain MZO-2. These initial results appeared to support our hypothesis, showing that the three known virulence associated MCP genes were likely harbored only by *V. cholerae*.

We also sought to identify MCP genes that are conserved amongst *Vibrio* species (Figure 4.1B), to identify which MCPs sense environmental cues versus which may sense pathogenic cues. Eight MCP genes were found to be conserved amongst *Vibrio* species regardless of pathogenicity, having an E score negative exponent of 50 or higher: VC1289, VC1898, VC2161, VCA0008, Aer-2, VCA0923, VCA0974, and

VCA1069. Notably, *aer-2* has previously been described as an aerotaxis gene in *V. cholerae*, as discussed (Boin and Hase, 2007). To further investigate the relationship between MCPs encoded in the *V. cholerae* genome, the similarity of the amino acid sequence of the N-terminal (sensory) portion of each MCP in the N16961 database was compared by maximum parsimony (Figure 4.2). The bootstrap test of phylogeny showed that the tree was unlikely to be correct, as all nodes failed to achieve the 95% threshold of the bootstrap test. Therefore, it is unlikely that paralogues with *V. cholerae* arose independent of other *Vibrio* species. Rather, it is possible that the lineage which gave rise to the *Vibrionaceae* contained many of these MCPs, some which were lost with evolutionary time in some lineages. An alternate explanation is the possible horizontal transfer of genetic material; for example, it is known that *tcpI* and *acfB* are part of the *Vibrio* pathogenicity island 1 (VPI-1; see also section 1.6), as association which clouds their evolutionary history.

4.4.2. MCP association in vitro. To determine which MCPs were putatively associated with specific chemoattractants, the swarming response of single MCP::Tn*Mar* mutants were measured by soft agar swarm plate assay the following chemoattractants: 0.5 mM L-serine, mucin (200 mg/L), 0.5 mM bile salts, and 0.5 mM GlcNAc, 200 mM KCl, and 200 mM NaCl. Selected MCPs, transposon mutagenesis of which was shown to be linked to a change of relative chemotaxis fitness of at least 20%, are shown in Figure 4.3A-F; the relative chemotaxis fitness of all MCP:chemoattractant pairings measured using this assay can be found in Table 4.4.

Chemotaxis of the MCP::Tn*Mar* strains was assayed towards the amino acids L-serine, chosen as a potential chemoattactant because *V. cholerae* has demonstrated chemotaxis towards all 20 amino acids (Freter and O'Brien, 1981), and L-serine has been a well characterized chemoattractant in *E. coli* (Adler, 1966; Adler, 1969; Springer, *et al.*, 1977). Identification of such an L-serine sensitive MCP in *V. cholerae* would allow comparison with the known serine-sensing MCP in *E. coli* (Tsr). Eight MCP::Tn*Mar* strains showed a chemotaxis defect of at least 20% towards L-serine (Fig 4.3A), two of which were significantly reduced in relative swarm size in L-serine supplemented swarm plates (VC2439 and VCA0031, $p < 0.05$) and one of which was significantly increased (VCA0268).

GlcNAc was chosen as a chemoattractant because, as a soluble component of chitin, it represents an environmental factor *V. cholerae* is expected to encounter. Transposon-associated defects in chemoattraction towards GlcNAc are shown in Figure 4.3B. Ten genes showed at least a 20% reduction in swarm size upon transposon-mediated mutagenesis as compared to the parent, four of which were significant (VC0449, VC2439, VCA0031, and VCA0663, $p < 0.05$) while transposon mutagenesis of four MCP strains show increased chemotaxis.

Mucin was assessed as a chemoattractant because its ubiquity in the digestive tract suggests that mucin would play a central role in chemotaxis during infection, which has been corroborated by the work of Freter and O'Brien (Freter and O'Brien, 1981). Five genes were found to be associated with chemotaxis of *V. cholerae* towards mucin (Figure 4.3C): VC1406, VC2439, VCA0031, VCA0268, and

VCA1069. Mutagenesis of all but VCA0031 resulted in an increase in relative swarm size. However, no difference was found to be significant.

Bile is an intriguing possibility as a chemoattractant because it would seem to be a repellent, yet the gall bladder of Cholera Dolores was the site of colonization by V. *cholerae* which allowed subsequent asymptomatic shedding of the bacterium for four years (See Chapter 1). Transposon-associated defects in chemoattraction towards bile are shown in Figure 4.3D. Transposon insertion into 11 genes were associated with loss of chemotaxis swarm diameter size of at least 20% as compared to the parent, including VC0282, VC1394, VC1406, VC1868, VC1898, VCA0008, VCA0658 (*aer-2*), VCA0663, VCA0923, and VCA1031. VC0282 was significantly reduced in swarm diameter in M9 swarm media containing bile as compared to M9 swarm media alone, and VC1898 and VCA0008 was significantly increased in swarm diameter under the same conditions ($p < 0.05$).

Sodium and potassium represent central cations that play a role in bioenergetics of *V. cholerae*, already discussed (Section 1.6.6 and Chapters 2 and 3). Therefore, it was of interest to assess these cations as potential chemoattractants. Chemotaxis of selected MCP::Tn*Mar* strains in response to 200 mM KCl can be found in Figure 4.3E. Only two MCPs were significantly reduced in chemotaxis when media was supplemented with KCl, VC0098 and VC1313. Chemotaxis in response to KCl was not as robust as that for NaCl (Figure 4.3F). Addition of 200 mM NaCl to M9 swarm media produced significantly reduced chemotaxis in VC0098::Tn*Mar*; in

contrast, the transposon--mutants of VC0449, VC1289, VC1868, VCA0923, and VCA0988 were significantly hypermotile ($p < 0.05$).

4.4.3. Complementation of MCP defects. Transposon mutagenesis is sometimes associated with polar phenotypes due to polarity and not directly associated with the disrupted gene. For this reason, some of the MCP mutants were complemented *in trans* by cloning the nucleotide sequence of the disrupted gene into the pBAD expression vector. MCP mutants were chosen based upon the observed reduction in swarm diameter in Figure 4.3 for a given chemoattractant, and included VC0098 (NaCl, KCl), VC0449 (GlcNAc), *tcpI* (multiple), VCA0031 (mucin), and VCA0663 (GlcNAc). Complementation of VC0098::Tn*Mar*, VC0449::Tn*Mar*, *tcpI*::Tn*Mar*, or VCA0031::Tn*Mar* with the cognate WT ORF did not lead to observable restoration of swarm diameter (data not shown). Thus, either polarity was the cause of the original phenotype or else expression of the MCP from the pBAD vector was too low or too high to complement the gene mutation. The effect of complementation of VCA0663::Tn*Mar* is presented in Figure 4.4. Upon addition of GlcNAc to swarm plates, the swarm diameter of the parent increased from 0.59 ± 0.04 cm to 1.71 ± 0.21 cm, similar to that of VCA0663::Tn*Mar* (pBAD-VCA0663) (which increased from 0.53 ± 0.02 cm to 1.81 ± 0.19 cm), while that of the transposon mutant hosting the empty vector increased from 0.46 cm ± 0.05 cm to 0.96 ± 0.12 cm. The difference between VCA0663::Tn*Mar* hosting pBAD-VCA0663 and the same strain hosting the empty vector was significant ($p<0.005$).

4.4.4. Illumina-based analysis of chemotaxis in V. cholerae. To investigate MCP phenotypes by another method, we took advantage of the power of high-throughput sequencing to look at relative chemotaxis fitness of transposon mutants within a pooled sample (Figure 4.4A-C). Equally-mixed MCP::Tn*Mar* strains were plated on a variety of chemoattractant-containing swarm agar plates and after 18hr of growth samples were taken from the leading edge of the swarm. We hypothesized that strains harboring transposon insertions in MCPs important for movement towards a particular chemoattractant would be poorly represented at the leading edge of the swarm. Conversely, MCP mutants not important for directional motility towards the chemoattractant would be equally represented at the leading edge of the swarm. We assessed the relative proportion of each strain in the leading edge of the swarm by: 1) PCR amplifying the MCP::Tn*Mar* junctions *en masse* for the population recovered, 2) massively parallel sequencing of the amplified junctions using an Illumina Genome Analyzer, and 3) counting the number of reads of each junction and normalizing to the total number of reads in order to calculate the relative chemotaxis fitness. Of the previously tested chemoattractants, mucin (Fig. 4.5A), bile (Fig 4.4B), and serine (Fig 4.5C) were chosen to be measured in this assay; additionally, the equally mixed population of MCP strains was inoculated using the infant mouse intestine model for 4 or 24 hours (Figures 4.5D and 4.5E, respectively).

Chemoattraction towards mucin, as measured by the Illumina assay, was inhibited most by disruption of VC1298, VC1405, VCA0663, and VCA0773. Chemoattraction towards bile was most inhibited by disruption of *tcpI*, VC1298,

VC1406, VCA0663, and VCA1031. Chemoattraction towards L-serine was most reduced by disruption of VC1298, VC1406, VC2161, and VCA0923. A comparison of the two different *in vitro* methodologies, single and pooled, was also performed (Figure 4.6) to determine a consensus of MCP:chemoattractant pairings.

Chemoattraction *in vivo* is necessarily a complex system, which is not readily comparable to our previous studies in defined media. Still, motile but non-chemotactic *V. cholerae* have been observed to be hyperinfectious. Therefore, we hypothesized that if that hyperinfectious phenotype resulted from a correlation between colonization via chemotaxis and enhanced survival, such a phenotype would be observable amongst MCP::Tn*Mar* strains in the Illumina detection system. Five-day-old suckling mice (n=10) were infected with the MCP::Tn*Mar* pool for either 4 hours or 24 hours. Nine of ten animals in each group survived the infection period. After a 4 hour infection, twelve MCP mutants were under-represented in the pool extracted from the infant mouse intestines: *tcpI*, VC1405, VC1406, VC1535, VC1643, VC1898, VC1967, VC2439, VCA0008, VCA0031, *aer-2*, and VCA0988 (*aer-3*). After a 24 hour infection, only two of these MCP::Tn*Mar* strains were under-represented, VC1898 and *aer-2*, while the VCA1031::Mariner strain was over-represented 6.8 fold. The relative chemotaxis fitness of all MCP::Tn*Mar* strains used in this study can be found in Table 4.5. To further investigate the role of MCPs in the colonization phase of infection, measured as a function of survival, in-frame deletion mutants of the MCPs VC1898, *aer-2*, and VCA1031 were constructed and competed against the parent strain in the infant mouse model of infection. No difference was

observed in the relative population of mutant and parent of any of the three mutants as measured between the inoculum and the output population (data not shown).

4.5. Discussion

The complexity of MCP research in *V. cholerae* follows from the multitude of MCPs (45) encoded in the genome which we hypothesized would be functionally redundant. Our initial assessment of MCP function, through homology within the *Vibrionaceae* and in *V. cholerae* itself (Figure 4.1), did not predict overlapping function via sequence similarity, even though it did suggest that some MCPs were unique to *V. cholerae* El Tor N16961 among other species of *Vibrio* (Figure 4.1A). Assessment of the relative chemotaxis fitness of a defined MCP transposon library, however, suggested that certain MCPs indeed shared sensitivity to specific chemoattractants (Figure 4.3), as transposon insertion failed to completely inhibit chemotaxis to any of the chemoattractants measured. A similar trend was found when relative genomic prevalence was measured using an Illumina sequencer on a mixed population of MCP::Tn*Mar* clones *in vitro* (Figure 4.5 A-C). The Illumina system also allowed us to measure chemotaxis in the intestinal tract of the infant mouse model of cholera, which indicated a dramatic change in relative chemotaxis fitness correlated with disruption of the MCPs VC1898, *aer-2*, and VCA1031 (Figure 4.5 D and E). While these phenotypes were not recapitulated in in-frame deletion mutants of the same MCPs, thus complicating interpretation of their roles, complementation of VCA0663 did restore chemotaxis function. VCA0663 showed reduced chemotaxis

towards GlcNAc by as much as 80%, and for which normal chemotaxis swarm size was restored upon the expression of VCA0663 on an inducible expression vector (Figure 4.4). Several other MCP::Tn*Mar* strains were found to moderate significantly reduced chemotaxis towards GlcNAc (VC0449, VCA0031, and VC2439), L-serine (VC2439 and VCA0031), bile (VC0282), K^+ (VC0098 and VC1313), and Na^+ (VC0098). Therefore, we have provided evidence of the redundancy of MCPs, as well as elucidating which MCPs specifically sense the chitin monomer GlcNAc.

This study culminated with the successful complementation of the VCA0663::Tn*Mar* chemotaxis defect towards GlcNAc using the C6706 ORF expressed *in trans* on the pBAD inducible plasmid (Figure 4.4). One caveat to this is that the previously published defect in chemotaxis towards GlcNAc mediated by the MCP VC0449 was not amenable to complementation (data not shown), though we did observe a significant reduction in relative chemotactic fitness of that mutant ($P < 0.05$, Figure 4.3B) (Meibom*, et al.*, 2004). This previously published observation was anecdotal, though, so a qualitative comparison of our results in that light is not possible. Also, ectopic expression of pBAD-VCA0663 in UU1250, an *E. coli* strain lacking membrane bound MCPs, resulted in no chemotaxis towards GlcNAc (data not shown). This ectopic data demonstrates that, although the cytosolic tail is conserved, perhaps the methylation sites are not, or *E. coli* CheB or CheR fails to recognize methylation sites of *V. cholerae*.

Our phylogenetic analysis of N-terminal amino acid sequences of MCPs from *V. cholerae* (Figure 4.1) proved useful in identifying those chemoreceptors unique

among the *Vibrionaceae*. As expected, the MCPs that were previously annotated as being virulence associated (TcpI, AcfB, and HlyB) were unique to *V. cholerae*. Interestingly, many of the MCPs identified by this metric were found to be associated with an intestinal growth defect after 4 hours of infection (Figure 4.5D), which supports our phylogenetic grouping of MCPs.

One prediction from our phylogenetic assessment of *V. cholerae* MCPs proved surprising, in that the relative swarming fitness of VC0098::Tn*Mar* in response to Na^+ and K^+ was significantly reduced. The link between VC0098 and Na^+ is intriguing because the N terminus of VC0098 is not conserved (Table 4.3), implying a link in virulence, which is further suggested by inhibited growth of the VC0098::Tn*Mar* strain. Thus, VC0098 may represent a virulence factor through the confluence of motility and bioenergetics, so further study of this MCP is warranted. However, the chemotaxis defect was refractory to complementation (data not shown). It may be possible that the chloride ion is actually the chemoattractant, as the chloride salt of K^+ and Na^+ was used, but the different absolute swarm diameters and ratios suggest that this is not the case. The observed chemotaxis defect towards Na^+ and K^+ may have also been metabolic in nature via a polar effect on a nearby gene; VC0098 resides downstream of *glpG* and *glpE*, members of the glycerol-3-phosphate regulon. An in-frame deletion of the VC0098 ORF would allow a more robust test of chemotaxis towards cations such as Na^+ and K^+.

Notably, the in-frame deletions we constructed of the MCPs initially shown by transposon mutagenesis to play a role during infection of the infant mouse model were

shown to lack the altered output when they competed directly, and only, with the parent. The two sets of experiments, however, were different in their mode of mutagenesis as well as their metric of infectivity. Specifically, the transposon experiment was prone to polar effects not directly resulting from disruption of the gene at the insertion site. VC1898 is upstream of a hypothetical ORF having 1527 bp, with a start codon lying 205 bp inside the VC1898 3' coding region; though its function is unknown, it is out of frame with the MCP. The previously characterized MCP *aer-2* is situated downstream from the glycerol-3-phosphate dehydrogenase *glpD*, though the *glpD* and *aer-2* ORFs lie in opposite orientations with proximal 3' ends, and the stop codons of the gene pair reside 102 bp apart. A hypothetical ORF terminates 186 bp upstream from the *aer-2* start codon, but this upstream gene would not be expected to be affected by a transposon insertion downstream. VCA1031 is catalogued in GenBank as an authentic frameshift, but our analysis of this ORF through cloning from the C6706 genome (unpublished data) as well as through Illumina sequences generated by Dr. Camilli (personal communication) indicated that the ORF is not frameshifted; further, the gene immediately downstream of this ORF (which is a hypothetical protein 408 bp in size) is 125 bp away, which is out of frame as well as in the opposite orientation, and the nearest gene upstream (also hypothetical, and only 252 bp long) is 2092 bp away. An additional difference in the two experiments was the proportion of each MCP mutant to the rest of the inoculum: in the transposon mutant pool experiment, each MCP mutant represented 1/45 of the inoculum, where in the in-frame deletion competition each mutant represented ½ of

the input. Lastly, the transposon pool lacked the parent, as relative chemotaxis fitness was determined for each mutation independent of other mutations and relative only to growth of the same mutant in complex media. These differences were intended to independently show chemotaxis differences *in vivo*, so even though their differential outcome was unexpected, it is possible that a new infection metric, such as the rabbit ileal loop model or complementation of the transposon, could confirm our initial findings. This deserves further investigation.

Comparison of the MCP::Tn*Mar* strains inoculated in soft agar swarm media individually or pooled provides some insight into the consensus of which MCPs might be most linked with the chemoattractants assayed (Figure 4.6). While a consensus was not observed for reduced chemotaxis towards mucin correlated with MCP::Tn*Mar* strains, VCA1031::Tn*Mar* was hypermotile in both assays. Additional study of mucin as a chemoattractant will prove daunting, however, as the heterogenous composition of mucin provides many potential chemoattractant monomers upon hydrolysis. Further, our studies used porcine mucin, which is not identical in composition to human mucin, though chemotaxis in our studies yielded robust swarms of 2-3 cm diameter after 18 hours of swarming (unpublished observations), similar to GlcNAc (Figure 4.4). The challenges associated with studying mucin must be overcome to continue the study of *V. cholerae* chemotaxis towards mucin.

Relative chemotaxis fitness towards bile was repressed in the transposon mutants of *aer-2* and VCA1031 by at least 21% as measured by both assays. Intriguingly, bile was the only chemoattractant tested for which VCA1031 showed

reduced relative chemotaxis fitness. However, in-frame mutagenesis of each of these MCPs did not recapitulate the observed tranposon-mediated defects *in vivo* or *in vitro*, as previously mentioned.

In response to L-serine, VC1289::Tn*Mar* and VC1406::Tn*Mar* exhibited reduced relative chemotaxis fitness in both assays. VC1406 rests within a chemotaxis cluster, adjacent to two other MCPs (VC1403 and VC1405) and VC1407 (the RNA helicase *rhlE*) which is downstream in the same orientation as VC1406, together with VC1405. The promoter of the MCP VC1289 likely overlaps with that of VC1288 (*mdoG*), encoding a periplasmic glucans biosynthetic protein, and for that reason the transposon insertion into this MCP may well have polar metabolic effects.

Non-metabolic assays that do not require growth to measure chemotaxis, such as capillary assays, were also performed on selected strains. The results of these assays were inconclusive (data not shown); notably, a CheA-2::Tn*Mar* strain was observed to swim into capillary tubes containing known chemoattractants at a similar frequency as the parent, though it was expected to be non-chemotactic (Gosink*, et al.*, 2002). If this protocol could be refined, it would be a valuable mechanism to validate the data already collected in soft agar swarm plates.

The contribution of this research to the understanding of MCP receptor specificity in *V. cholerae* is multi-faceted. Our results indicate that some of the 45 MCPs are predicted to be unique to *V. cholerae*. As expected, the sensitivity of *V. cholerae* MCPs towards chemoattractants was found to be redundant, in many cases. Using Illumina sequencing as a high throughput tool we discovered MCPs which may

be associated with virulence, and using complementation we were able to show chemotaxis towards environmental signals such as GlcNAc mediated by VCA0663. Clearly, much work remains to assign chemoattractant specificity to the remaining MCPs, work which will be greatly facilitated by high-throughput methods in years to come.

4.6. Acknowledgements

D. E. Cameron and J. Mekalanos generously supplied us with the defined transposon mutants used in this study. Kip Bodi performed the Illumina sequencing.

4.7. Tables and Figures

Table 4.1. Strains of C6706 used in this study.

MCP locus	Transposon library clone	Citation	Function , or relevant research
VC0098	EC8630		
VC0216	EC16293		
VC0282	EC5563		
VC0449	EC4384	(Meibom, *et al.*, 2004)	N-acetyl-glucosamine
VC0512 (*aer-1*)	N/A		
VC0514	N/A		
VC0825 (*tcpI*)	EC9616	(Harkey, *et al.*, 1994)	Virulence association
VC0840 (*acfB*)	EC8319	(Everiss, *et al.*, 1994)	Virulence association
VC1248	EC3044		
VC1289	EC2786		
VC1298	EC20908		
VC1313	EC9352		
VC1394	EC6233		
VC1403	EC2711		
VC1405	EC14352		
VC1406	EC10115		
VC1413	EC2535		
VC1535	EC8229		
VC1643	EC23170	(Cerda-Maira, *et al.*, 2008)	Expression upregulated by bile
VC1859	EC13993		
VC1868	EC5196		
VC1898	EC14890		
VC1967	EC10626	(Shikuma and Yildiz, 2009)	Expression upregulated by osmolarity
VC2161	EC8816		
VC2439	EC18588		
VCA0008	EC13269		
VCA0031	EC4090		
VCA0068	EC2466		
VCA0176	EC16652		
VCA0220 (*hylB*)	EC859	(Alm and Manning, 1990)	Virulence association
VCA0268	EC8514		
VCA0658 (*aer-2*)	EC10173	(Boin and Hase, 2007)	Aerotaxis
VCA0663	EC19835		
VCA0773	EC662		

VCA0864	EC7926		
VCA0906	EC6583		
VCA0923	EC6832		
VCA0974	EC18598		
VCA0979	EC6271		
VCA0988 (*aer-3*)	EC5638	(Shikuma and Yildiz, 2009)	Expression upregulated by osmolarity
VCA1034	EC12017		
VCA1056	EC11593		
VCA1069	EC8937		
VCA1088	EC4304		
VCA1092	EC24241		

Table 4.2. Primers used in this study.

Primer name	Primer sequence
VC1898, 5' region	#1: 5'-GCGGCCGCCTTGGTTAGCGCGGCGCATT-3' #2 5'-TTACTAGCTAGCTAGCTCATTGTTATTAGAATTC-3'
VC1898, 3' region	#3 5'-ATGAGCTAGCTAGCTAGCTAGTAATCCGATGAACGGCT-3' #4 5'-ACTAGTCTTTGGTTTTACACTCAATA-3'
VCA0658, mutagenesis	(Boin and Hase, 2007)
VCA1031, 5' region	#1: 5'-GCGGCCGCGATGACTGGAATCGCCTCTC-3' #2: 5'-TTACTAGCTAGCTAGCTAGCTCATAAAGAGTCTGTGAC-3'
VCA1031, 3' region	#3: 5'-ATGAGCTAGCTAGCTAGCTAGTAATAGTTCGAACGAAT-3' #4: 5'-ACTCGTACTCAACCATTCGGGTCGCA-3'
VCA0663, expression	#1: 5'-GAGGAATAATAAATGAATATTCGCCATAAACTTTAT-3' #2: 5'-TCAGTCACGATTGGTGCGAAACTC-3'
tcpI, expression	#3: 5'-GAGGAATAATAAATGATAAAAAAAATAATTTCGGTT-3' #4: 5'-TTATGAAGTAAGCTCAATTTTAAA-3'
VC0098, expression	5'-GAGGAATAATAAATGGGTTTATTGGCACGTCTTTTC-3' 5'-TCAAAAACTCTCCCATTCTTCATC-3'
449, expression	5'-GAGGAATAATAAATGAAATTAAAAACCCAAGCTTAT-3' 5'-TTAACGAGTGACCTCAAAATGCGC-3'
A0031, expression	5'-GAGGAATAATAAATGAAGTTAAGCATTAGTCGTATT-3' 5'-TTAATGTGAAAGTTGCTTGAGGTT-3'
OLJ330/331	5'-GTGACTGGAGTTCAGACGTGTGCTCTTCCGATCT-3'
OLJ373	5'- AGATCGGAAGAGCACACGTCTGAACTCCAGTCAC-3'
MAREC2	5'-CACCTTCACCCTCTCCACTGACAG-3'
MarOut	5'-CGGGGACTTATCAGCCAACC-3'
OLJ244	5'-AATGATACGGCGACCACCGAGATCTACACT CTTTAGACCGGGGACTTATCAGCCAACCTGT-3'
BARCODE1	5'-CAAGCAGAAGACGGCATACGAGATCACAGT GACTGGAGTTCAGACGTGTGCTCTTCCGATCT-3'
BARCODE2	5'-CAAGCAGAAGACGGCATACGAGATCATCGT GACTGGAGTTCAGACGTGTGCTCTTCCGATCT-3'
BARCODE3	5'-CAAGCAGAAGACGGCATACGAGATCTCTGT GACTGGAGTTCAGACGTGTGCTCTTCCGATCT-3'
BARCODE4	5'-CAAGCAGAAGACGGCATACGAGATGAGAGT GACTGGAGTTCAGACGTGTGCTCTTCCGATCT-3'
BARCODE5	5'-CAAGCAGAAGACGGCATACGAGATGATGGT GACTGGAGTTCAGACGTGTGCTCTTCCGATCT-3'
BARCODE6	5'-CAAGCAGAAGACGGCATACGAGATGTGTGT GACTGGAGTTCAGACGTGTGCTCTTCCGATCT-3'
BARCODE7	5'-CAAGCAGAAGACGGCATACGAGATAGCAGT GACTGGAGTTCAGACGTGTGCTCTTCCGATCT-3'
BARCODE8	5'-CAAGCAGAAGACGGCATACGAGATAGTCGT GACTGGAGTTCAGACGTGTGCTCTTCCGATCT-3'
BARCODE9	5'-CAAGCAGAAGACGGCATACGAGATAGAGGT GACTGGAGTTCAGACGTGTGCTCTTCCGATCT-3'
OLJ245	5'- ACACTCTTTAGACCGGGGACTTATCAGCCAACCTGT-3'

Table 4.3. Similarity of *V. cholerae* N16961 MCP N-terminus amino acid sequences to other *Vibrio* species. BLASTp was used to compare N-terminus (signaling) amino acid sequences to that of ORFs from sequenced *Vibrionaceae.* The resulting negative exponent of the E (expect) score is recorded; a higher number indicates a higher likelihood of common ancestry. E scores of 0 were converted to a value of 200 (equal to 1.0×10^{-200}). Representative *Vibrionaceae* are as follows: *V. fischerii* ES114 (*V.f.*), *V. harveyi* ATCC BAA-1116 (*V.h.*), *V. splendidus* 12B01 (*V.s.*), *V. alginolyticus* 12G01 (*V.a.*), *V. parahaemolyticus* AQ3810 (*V.p.*), *V. vulnificus* CMCP6 (*V.v.*), and *V. cholerae*, MZO-2 (*V.c.*).

Table 4.3

MCP	***V.f.***	***V.h.***	***V.s.***	***V.a.***	***V.p.***	***V.v.***	***V.c.***
VC0098	1	1	1	44	44	1	200
VC0216	33	33	33	76	33	90	122
VC0282	29	29	29	29	29	62	130
VC0449	61	18	18	18	18	18	18
Aer-1	58	1	42	1	57	66	1
VC0514	50	50	50	50	50	50	50
TcpI	8	8	8	8	8	8	8
AcfB	29	29	29	29	29	29	29
VC1248	28	28	28	28	28	72	28
VC1289	88	106	103	105	1	109	106
VC1298	1	1	84	83	1	86	116
VC1313	50	50	50	67	50	81	127
VC1394	1	1	1	1	19	1	1
VC1403	19	21	21	21	20	21	19
VC1405	1	1	1	1	1	1	1
VC1406	1	1	1	33	60	1	163
VC1413	28	83	28	28	106	28	135
VC1535	1	75	70	71	71	54	200
VC1643	1	1	1	1	1	1	146
VC1859	7	7	118	7	7	125	200
VC1868	1	1	1	1	1	75	1
VC1898	96	119	124	118	4	113	200
VC1967	1	1	1	1	1	1	1
VC2161	61	96	102	86	47	105	164
VC2439	24	56	69	59	67	59	103
VCA0008	55	75	65	67	47	63	200
VCA0031	1	1	1	1	1	1	1
VCA0068	41	41	41	41	41	41	41
VCA0176	84	119	132	123	122	114	118
HlyB	1	1	1	1	1	1	200
VCA0268	23	23	23	23	23	97	23
Aer-2	50	109	100	103	71	107	200
VCA0663	46	46	46	46	46	46	123
VCA0773	38	38	38	38	38	38	85
VCA0864	1	1	1	29	66	1	155
VCA0906	28	28	28	28	28	104	28
VCA0923	61	63	69	63	38	102	164
VCA0974	49	50	49	53	52	49	127
VCA0979	1	1	1	1	1	4	16
Aer-3	105	1	1	52	82	60	126
VCA1034	1	1	1	1	1	149	200
VCA1056	23	23	23	23	23	116	121
VCA1069	83	41	102	41	41	112	41
VCA1088	2	3	2	3	3	3	3
VCA1092	2	2	1	1	1	163	2

Table 4.4. Relative chemotaxis fitness of MCP::Tn*Mar* clones in chemotaxis soft agar swarm plates after 18 hours of swarming. Conditions are identical to those used in Figure 4.3.

Table 4.4.

MCP	L-Serine	GlcNAc	Mucin	Bile	KCl	NaCl
VC0098	165.00	116.07	146.80	106.29	67.05	60.17
VC0216	101.33	85.23	91.85	90.40	133.33	112.44
VC0282	113.63	90.88	133.65	75.08	94.60	120.79
VC0449	99.87	59.65	123.74	106.37	161.15	222.17
tcpI	102.96	97.54	138.82	93.79	112.77	92.44
acfB	88.69	110.36	135.83	98.42	94.89	101.45
VC1248	69.93	114.23	97.00	100.96	345.29	228.32
VC1289	62.71	87.15	95.50	91.36	168.53	189.52
VC1298	98.56	103.50	142.47	124.31	78.18	99.00
VC1313	125.65	122.47	117.00	104.01	43.48	34.12
VC1394	142.50	84.59	96.13	73.63	102.62	153.36
VC1403	137.63	54.16	92.27	N/A	105.41	102.56
VC1405	80.59	78.27	110.15	110.30	110.39	72.09
VC1406	70.80	127.80	168.93	247.35	67.35	116.62
VC1413	98.64	99.40	114.90	83.00	113.53	164.75
VC1535	106.72	74.65	95.75	87.96	105.61	97.79
VC1643	94.42	33.28	111.42	N/A	218.63	96.86
VC1859	105.93	94.57	101.13	90.55	118.11	105.82
VC1868	92.37	76.51	117.37	78.85	88.77	213.74
VC1898	131.20	91.21	148.29	153.28	137.30	107.52
VC1967	79.98	100.74	99.25	97.13	69.93	64.82
VC2161	85.47	106.97	122.13	113.64	102.41	104.21
VC2439	76.69	69.03	120.71	110.86	98.99	113.74
VCA0008	148.39	98.74	141.72	134.30	152.36	61.01
VCA0031	71.32	51.03	63.70	97.11	93.55	117.73
VCA0068	126.34	80.23	120.94	70.01	113.34	159.11
VCA0176	129.07	97.63	97.04	80.78	138.72	87.15
hlyB	89.70	53.18	86.36	N/A	115.63	83.67
VCA0268	133.46	127.42	122.99	101.74	70.51	70.25
aer-2	148.89	91.93	123.18	75.98	111.01	106.78
VCA0663	90.22	52.29	113.31	170.37	82.64	87.15
VCA0773	96.30	114.43	103.47	84.22	235.49	212.54
VCA0864	100.53	157.24	180.56	97.14	79.59	56.01
VCA0906	88.03	62.53	95.65	107.22	105.03	96.07
VCA0923	84.47	84.17	130.37	136.00	88.78	148.73
VCA0974	92.50	82.79	116.69	121.32	171.09	112.13
VCA0979	107.59	124.04	108.44	106.66	130.18	145.27
VCA0988	104.63	117.26	122.47	100.88	94.68	155.34
VCA1031	222.13	19.67	165.49	81.81	98.94	59.52
VCA1034	137.98	75.04	117.00	104.33	115.26	96.31
VCA1056	95.67	96.49	91.65	92.47	64.19	76.66
VCA1069	151.86	137.75	161.91	104.33	99.97	74.17
VCA1088	118.55	155.35	135.85	117.09	101.71	129.83
aer-3	113.67	99.80	127.22	N/A	119.69	129.20

Table 4.5. Relative chemotaxis fitness of pooled MCP::Tn*Mar* clones in chemotaxis soft agar swarm plates after 18 hours of swarming as measured by Illumina sequencing. Conditions are identical to those used in Figure 4.4. Pooled MCP::Tn*Mar* clones were cut from a 2 mm band encompassing the leading edge of the swarm in response to mucin, bile, and serine, and quantified as described in Materials and Methods. Pooled MCP::Tn*Mar* clones were isolated from the intestines of infant mice infected for 4 or 24 hours and similarly enumerated by Illumina sequencing, as described in Materials and Methods.

Table 4.5.

MCP	Mucin	Bile	L-serine	*In vivo* 4h	*In vivo* 24h
VC0098	105.90	128.48	104.33	98.00	107.05
VC0216	80.09	123.75	109.04	99.96	102.85
VC0282	119.40	144.15	113.81	80.02	107.58
VC0449	90.82	120.94	100.67	125.46	107.71
tcpI	136.30	64.37	131.37	43.73	130.23
acfB	88.10	101.11	94.07	88.25	86.54
VC1248	107.92	91.40	96.86	134.45	86.92
VC1289	72.53	101.43	79.23	109.23	92.99
VC1298	35.39	44.89	58.39	113.05	94.08
VC1313	85.81	90.29	105.04	138.16	101.28
VC1394	92.32	96.63	107.80	142.99	115.82
VC1403	86.05	87.13	94.65	182.47	122.32
VC1405	67.51	157.83	242.47	46.45	255.46
VC1406	102.08	32.60	52.30	62.20	153.79
VC1413	95.49	91.95	103.74	197.06	133.33
VC1535	85.46	88.55	102.13	61.55	88.46
VC1643	77.04	74.09	94.35	55.16	149.94
VC1859	95.57	101.90	98.53	106.80	92.05
VC1868	92.09	110.92	101.66	161.69	112.55
VC1898	83.71	113.35	131.93	4.29	22.27
VC1967	104.77	84.18	113.56	43.94	83.34
VC2161	82.42	114.76	77.99	144.85	80.56
VC2439	166.39	78.16	120.80	25.44	86.82
VCA0008	122.21	113.74	95.58	36.70	130.69
VCA0031	133.84	74.15	118.31	27.43	70.13
VCA0068	88.77	102.77	98.86	144.27	97.89
VCA0176	86.52	106.37	107.97	128.94	96.64
hlyB	95.65	105.87	106.68	118.66	76.91
aer-2	78.67	78.94	137.73	40.25	43.77
VCA0663	65.77	54.98	147.76	98.24	463.08
VCA0773	67.17	82.18	76.54	142.07	104.54
VCA0864	103.75	98.84	105.79	120.45	80.76
VCA0906	86.55	81.89	89.71	83.19	126.92
VCA0923	94.06	89.83	55.25	129.49	85.91
VCA0974	83.98	103.06	109.19	146.11	91.38
VCA0979	88.76	101.90	98.94	176.11	106.23
VCA0988	92.86	99.35	93.71	63.27	80.88
VCA1031	2256.90	48.69	135.95	104.75	681.89
VCA1034	166.04	72.89	118.68	87.60	140.81
VCA1056	93.16	106.68	99.30	97.41	95.32
VCA1069	97.92	113.02	117.64	86.37	108.93
VCA1088	110.99	130.56	139.19	97.56	96.48
aer-3	93.43	117.33	130.69	118.30	78.87

Figure 4.1. Alignment of selected MCP N-termini within representative strains of *Vibrionaceae*. The amino acid sequence of the N-termini of each MCP from *V. cholerae* N16961 was compared by BLASTp against published genomes of the *Vibrionaciae*, including, from front to back, *V. fischerii* ES114 (thick hatched bars, light gray), *V. harveyi* ATCC BAA-1116 (Thin hatched bars, light gray), *V. splendidus* 12B01 (solid bars, light gray), *V. alginolyticus* 12G01 (thick hatched bars, dark gray), *V. parahaemolyticus* AQ3810 (thin hatched bars, dark gray), *V. vulnificus* CMCP6 (solid bars, dark gray), and a non-pathogenic strain of *V. cholerae*, MZO-2 (solid dark bars). Panel A shows unique *V. cholerae* MCP sequences, having at most 1 homologous sequence with an inverse negative E score of 50 or less; Panel B shows conserved *V. cholerae* MCP sequences, having an inverse negative E score of 50 or more amongst at least 4 other *Vibrio* species.

Figure 4.1

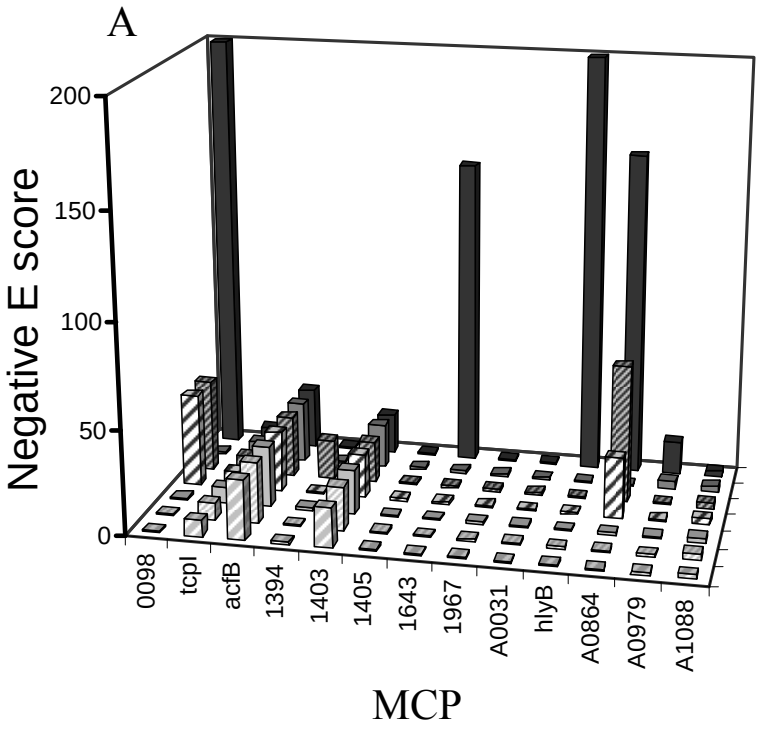
A
200
150
100
50
0
Negative E score
0098
tcpI
acfB
1394
1403
1405
1643
1967
A0031
hlyB
A0864
A0979
A1088
MCP

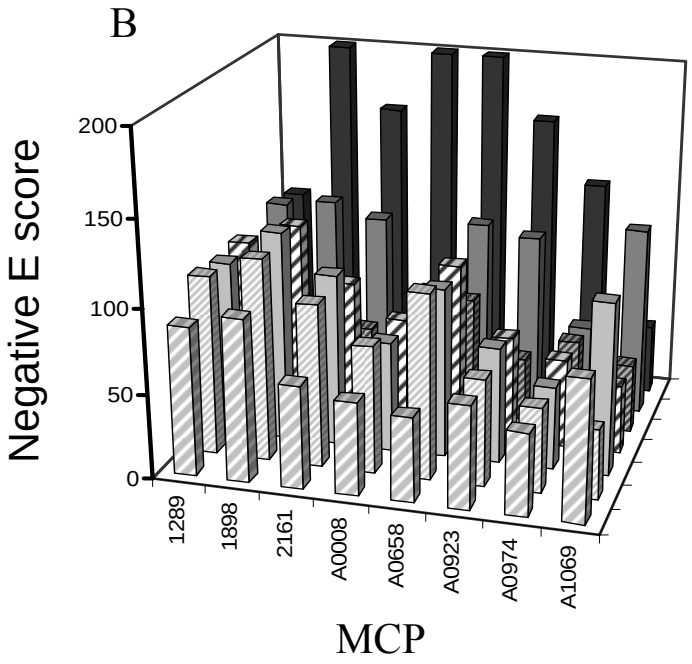
B
200
150
100
50
0
Negative E score
1289
1898
2161
A0008
A0658
A0923
A0974
A1069
MCP

Figure 4.2. Phylogeny of *V. cholerae* and *E. coli* MCP N-termini. Sequence similarity and putative evolutionary origin of each MCP was calculated by the maximum parsimony method within the program MEGA4 (Tamura*, et al.*, 2007) using the N-terminus of each amino acid sequence. The reliability of the tree was assessed by the bootstrap method, indicated at each node.

Figure 4.2.

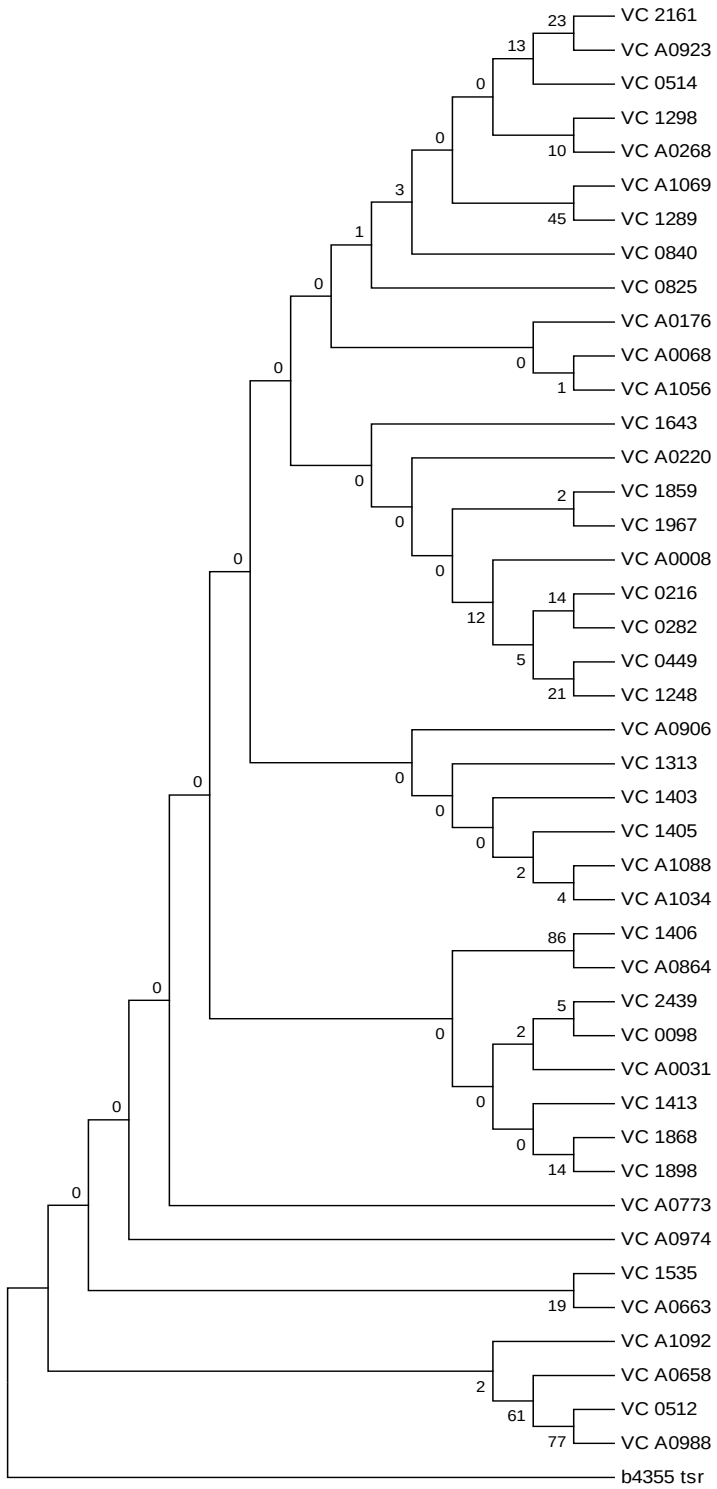
VC 2161
VC A0923
VC 0514
VC 1298
VC A0268
VC A1069
VC 1289
VC 0840
VC 0825
VC A0176
VC A0068
VC A1056
VC 1643
VC A0220
VC 1859
VC 1967
VC A0008
VC 0216
VC 0282
VC 0449
VC 1248
VC A0906
VC 1313
VC 1403
VC 1405
VC A1088
VC A1034
VC 1406
VC A0864
VC 2439
VC 0098
VC A0031
VC 1413
VC 1868
VC 1898
VC A0773
VC A0974
VC 1535
VC A0663
VC A1092
VC A0658
VC 0512
VC A0988
b4355 tsr

Figure 4.3. *In vitro* chemotaxis of single *V. cholerae* N16961 MCP::Tn*Mar* strains in defined media. Chemotaxis of individual MCP::Tn*Mar* strains was measured by soft agar swarm assay. M9 minimal media plates soft agar plates were used, with a 0.28% agar content, supplemented vehicle (deionized water—light gray bar) or chemoattractant (black bars): 0.5 mM L-serine (Figure 4.3A), 0.5 mM N-acetyl-glucosamine (Figure 4.3B), 200 mg/L mucin (Figure 4.3C), 10 mM bile (Figure 4.3D), 200 mM KCl (Figure 4.3E), and 200 mM NaCl (Figure 4.3F). Bacteria were allowed to swarm for 18 hours (Panels A-D) or 48 hours (Panels E and F). Chemotaxis swarms were normalized as a function of parent swarm size (relative swarm size). A relative swarm size of 100 indicates no change in swarm ratio between the parent and the mutant for the given condition. MCP::Tn*Mar* strains for which the relative chemotaxis fitness was less than 80 or more than 120 are graphed; strains which were significantly different than the parent ($P<0.05$, Student's t-test) are marked by an asterisk.

Figure 4.3

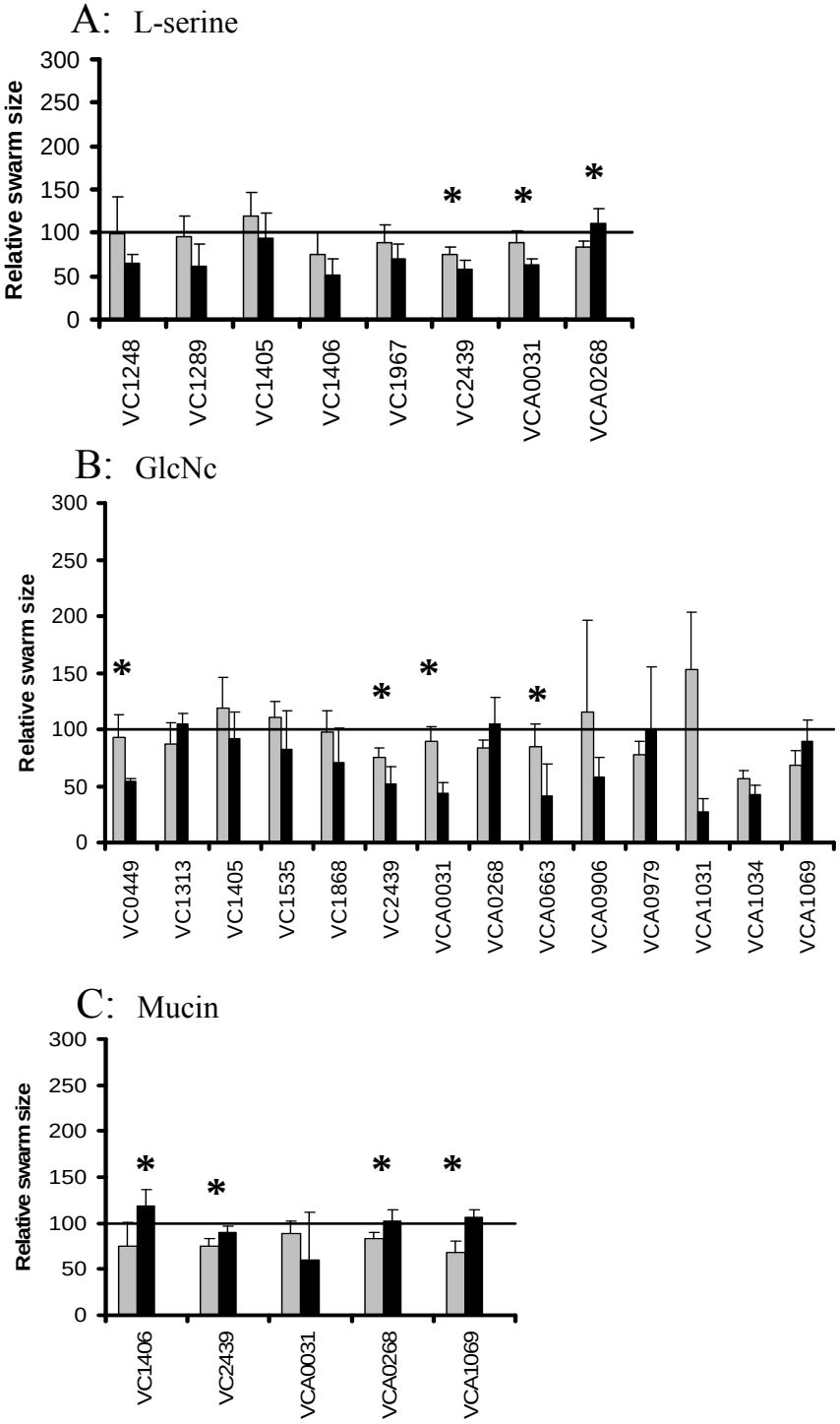
A: L-serine
Relative swarm size
300
250
200
150
100
50
0
VC1248
VC1289
VC1405
VC1406
VC1967
VC2439
VCA0031
VCA0268
B: GlcNc
Relative swarm size
VC0449
VC1313
VC1405
VC1535
VC1868
VC2439
VCA0031
VCA0268
VCA0663
VCA0906
VCA0979
VCA1031
VCA1034
VCA1069
C: Mucin
Relative swarm size
VC1406
VC2439
VCA0031
VCA0268
VCA1069

Figure 4.3, continued

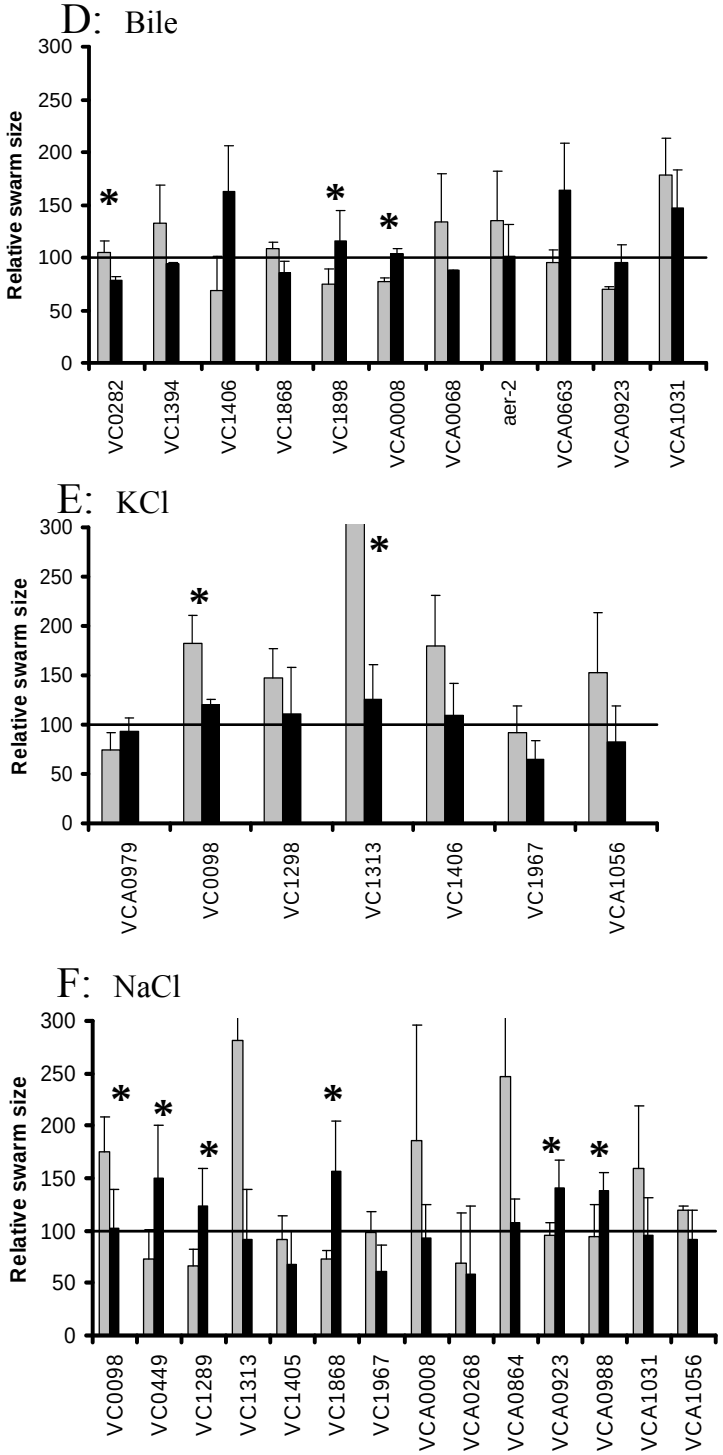

Figure 4.4. Complementation of VCA0663 chemotaxis towards GlcNAc. Panel A: C6706 (pBAD24) (solid bars), C6706 VCA0663::Tn*Mar* (pBAD24) (gray bars), and C6706 VCA0663::Tn*Mar* (pBAD-VCA0663) (hatched bars) were allowed to swarm in soft agar swarm plates with ampicillin (100 μg/mL) and arabinose (0.002%) containing no chemoattractant (null) or 0.5 mM GlcNAc. Shown are the averages of six experiments. Panel B: Representative experiment showing 18 hour swarm diameter in minimal media swarm agar containing GlcNAc of C6706 (pBAD24), C6706 VCA0663::Tn*Mar* (pBAD24), and C6706 VCA0663::Tn*Mar* (pBAD-VCA0663).

Figure 4.4.

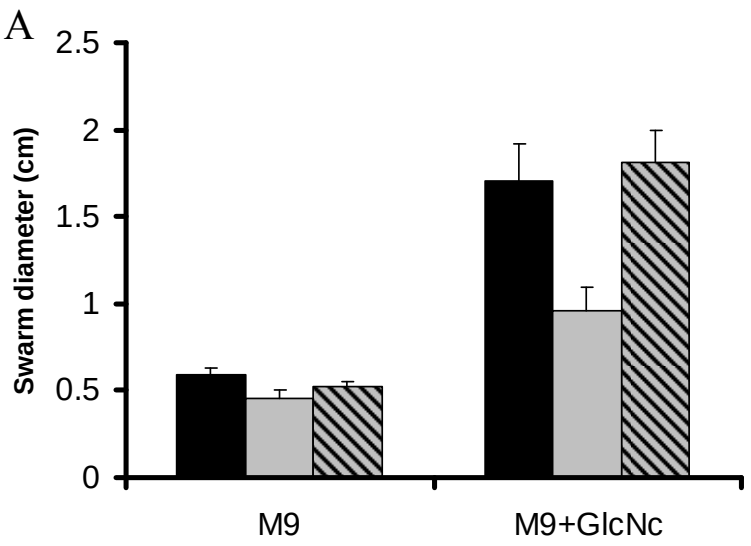
A
2.5
2
1.5
1
0.5
0
Swarm diameter (cm)
M9
M9+GlcNc

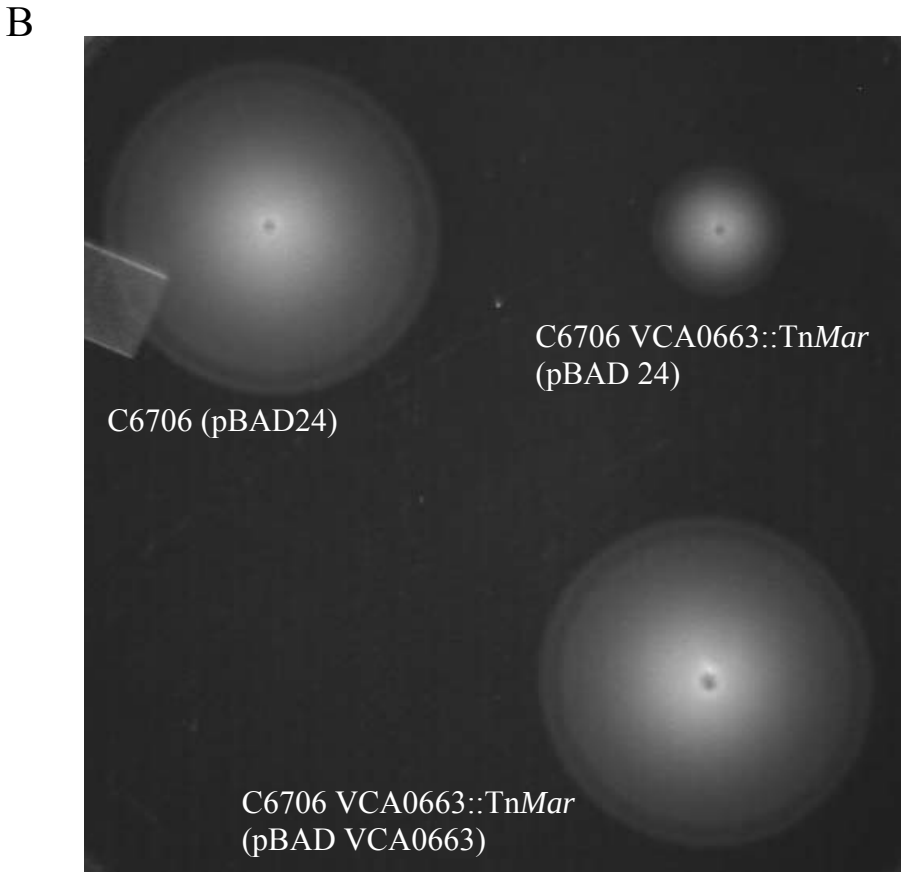
B
C6706 VCA0663::Tn*Mar*
(pBAD 24)
C6706 (pBAD24)
C6706 VCA0663::Tn*Mar*
(pBAD VCA0663)

Figure 4.5. Mixed MCP::transposon pool measured by Illumina sequencing. *V. cholerae* N16961 MCP::Tn*Mar* strains were pooled and assayed by Illumina sequencing for representative contribution of each strain to the leading edge of the swarm *in vitro* in defined soft agar swarm plates containing 200 mg/mL mucin (Panel A), 0.5 mM bile (Panels B), 0.5 mM L-serine (Panel C), or *in vivo* in the infant mouse model after infection for 4 hours (Panel D) or 24 hours (Panel E). Data for each MCP strain are represented as the relative proportion of total reads as compared to a parallel outgrowth of each experimental input in LB (*in vitro* competition), with 1 being equal to no change from *in vitro* competition.

Figure 4.5.

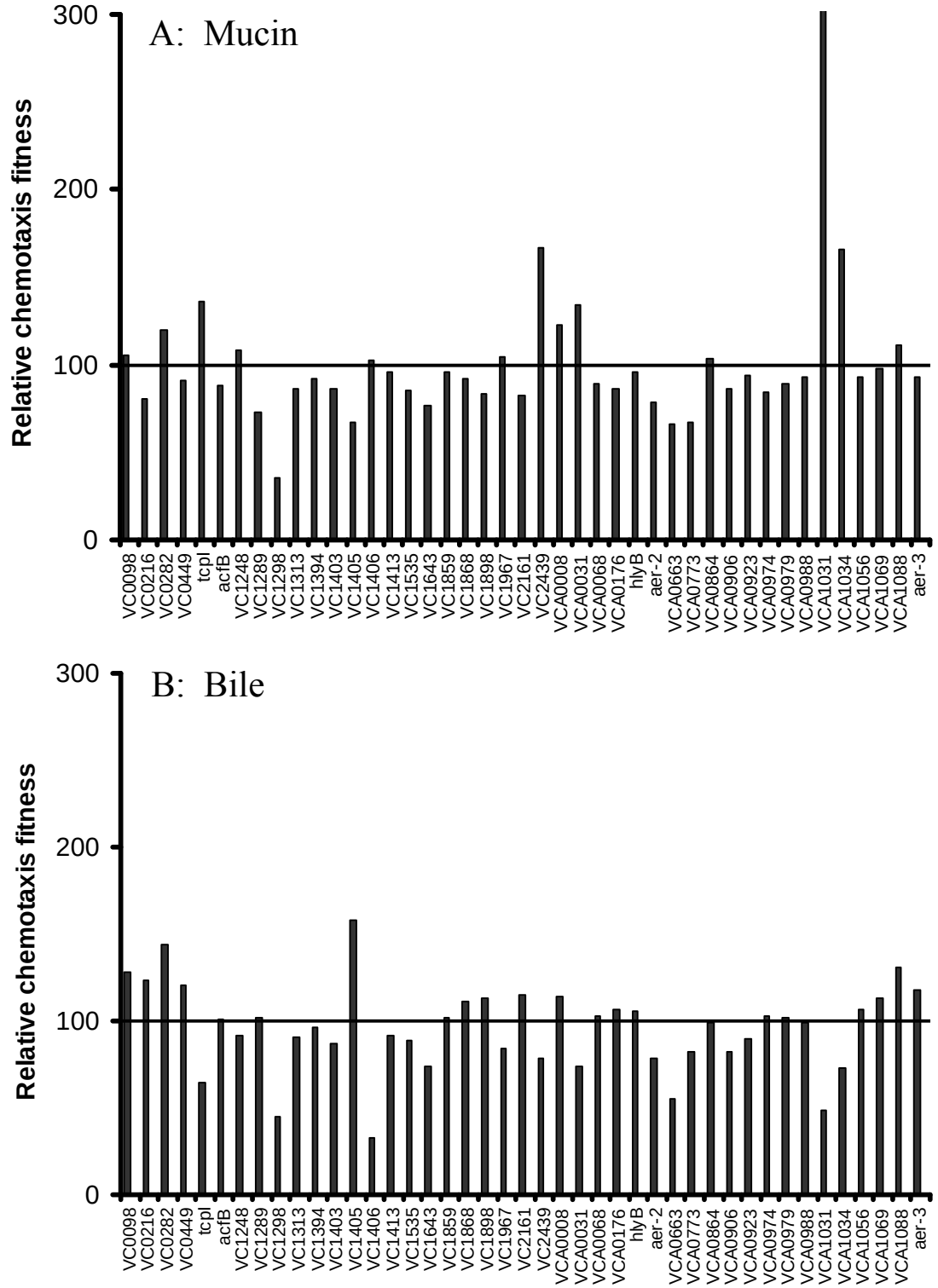
A: Mucin
B: Bile
Relative chemotaxis fitness
300
200
100
0
VC0098
VC0216
VC0282
VC0449
tcpI
actB
VC1248
VC1289
VC1298
VC1313
VC1394
VC1403
VC1405
VC1406
VC1413
VC1535
VC1643
VC1859
VC1868
VC1898
VC1967
VC2161
VC2439
VCA0008
VCA0031
VCA0068
VCA0176
hlyB
aer-2
VCA0663
VCA0773
VCA0864
VCA0906
VCA0923
VCA0974
VCA0979
VCA0988
VCA1031
VCA1034
VCA1056
VCA1069
VCA1088
aer-3

Figure 4.5, continued

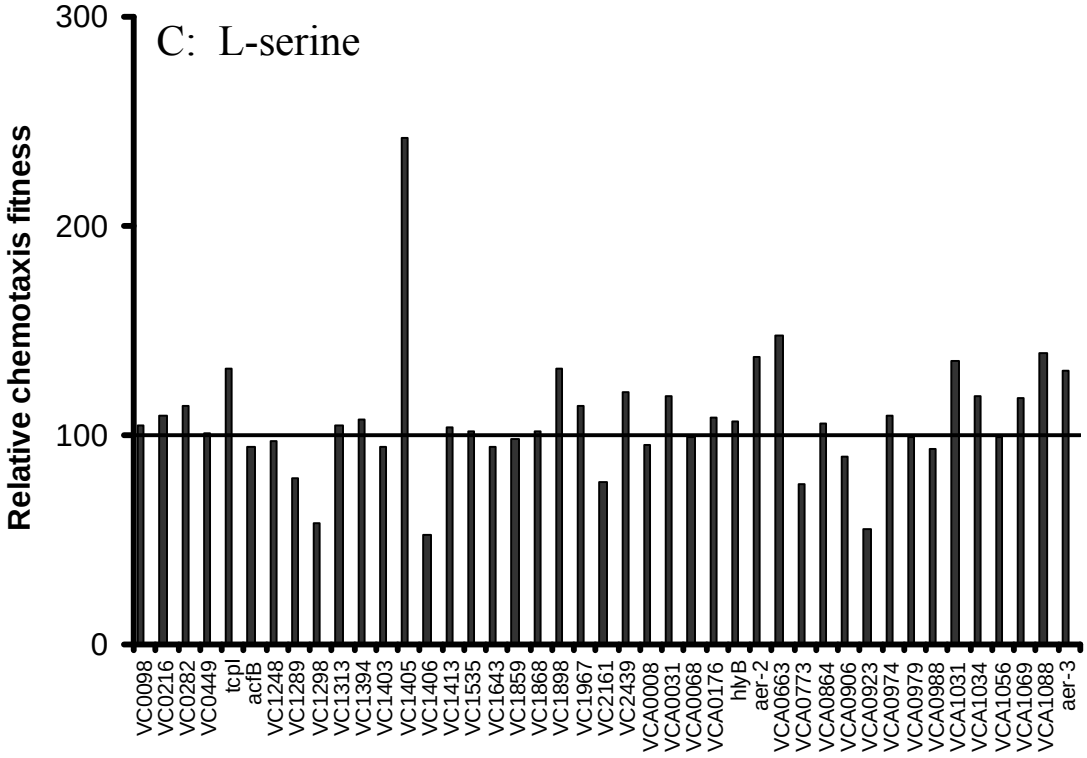

Figure 4.5, continued

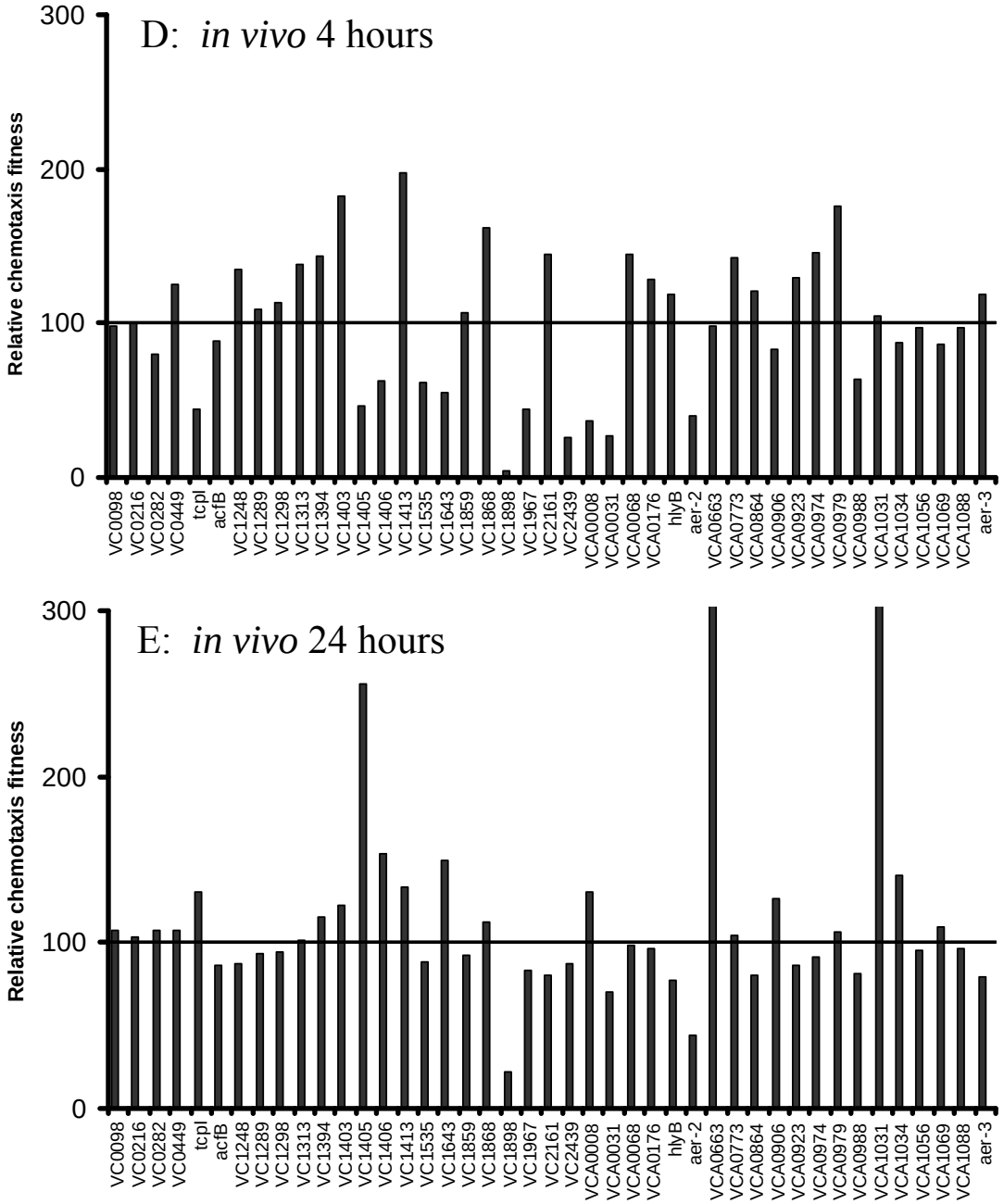

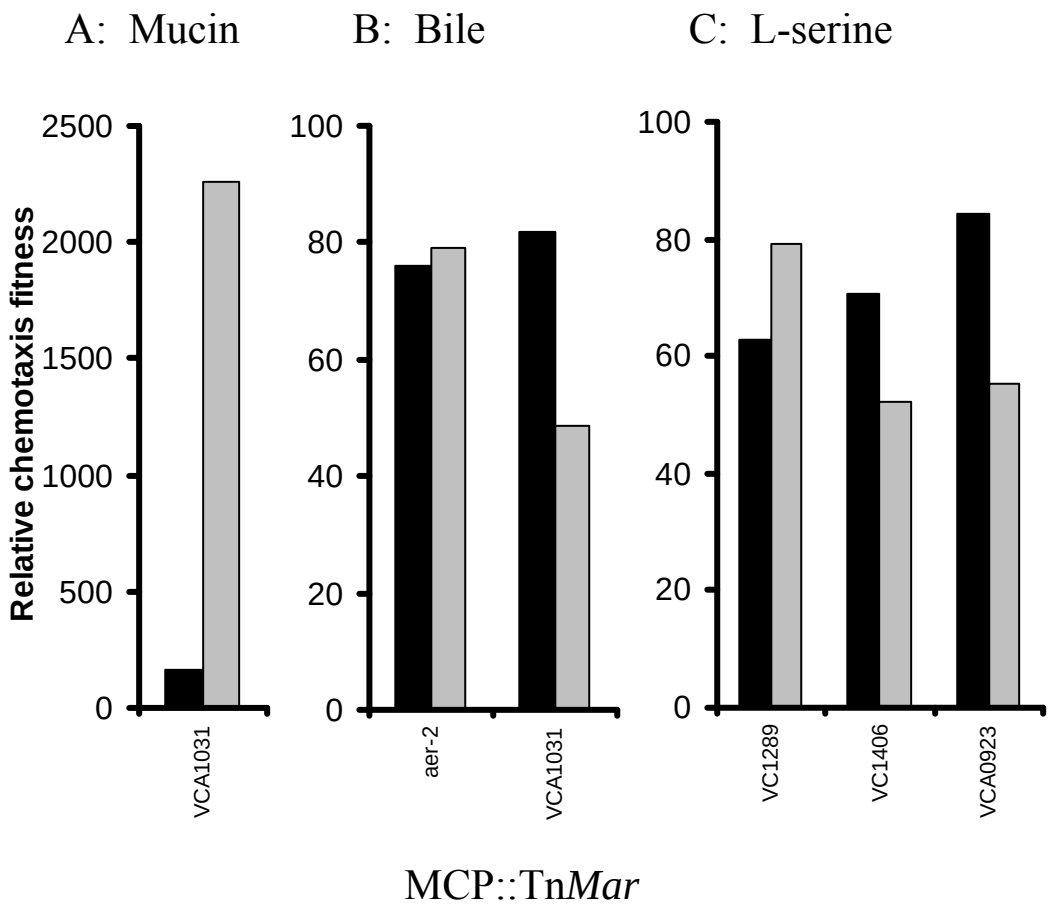

Figure 4.6. Comparison of single and pooled MCP::Tn*Mar* chemotaxis. Relative chemotaxis fitness of each MCP::Tn*Mar* clone was compared when assayed individually (data from Table 4.4, black bars) or when pooled and assayed by Illumina-based relative genomic enumeration (data from Table 4.5, gray bars) for 200 mg/L mucin (Panel A), 10 mM bile (Panel B), or 0.5 mM L-serine (Panel C).

5. Concluding Remarks

The pathogen *V. cholerae* uses cations as a primary currency of virulence, using gradients of those cations to move, acquire nutrients, and control virulence gene expression. Such dependence on salinity almost certainly stems from the aquatic origins of this microorganism. Even the introduction of cholera toxin by the *ctx* phage was likely evolutionarily selected for, as it would benefit a microbe that, normally associated with the chitin of marine organisms that humans eat, could use the toxin to recapitulate a saline environment within the intestines of a human host. Because cations play such a central role in metabolism which is, in turn, linked to virulence, we sought to better understand the physiological role these cations played in the survival of *V. cholerae* as a function of growth, gene expression, and chemotaxis.

Each chapter within this volume has contributed to understanding the intersection of bioenergetics and physiology in *V. cholerae*. Chapter 2 illustrated the central role that Vc-NhaP1 plays in survival of acidic conditions. Chapter 3 further examined the overlapping roles that Vc-NhaA, Vc-NhaB, and NQR play in survival of *V. cholerae* in the presence of environmental (Na^+ and K^+) and toxic (Li^+) cations. Chapter 4 studied cations as chemoattractants, and further examined the physiological role of all chemotaxis sensory proteins (MCPs) with additional chemoattractants.

Vc-NhaP1 was found to play a role in K^+ tolerance at acidic pH. Perhaps most intriguingly, deletion of this antiporter led to growth inhibition in complex media even in the absence of K^+ (Figure 2.1A), which suggested that Vc-NhaP1 normally played a role in surviving hypo-osmotic stress or in regulation of cytosolic pH. Measurement of cytosolic pH demonstrated that, in acidic conditions, K^+ (but not Na^+) is necessary

to regulate cytosolic pH (Figure 2.3C), and that removal of Vc-NhaP1 leads to a disregulation of cytosolic pH even in the presence of K^+ (Figure 2.3A). Although it may not act directly on cytosolic pH regulation, Vc-NhaP1 clearly plays a role in such regulation, and additional research is necessary to demonstrate what, exactly, that role is. The most likely candidates would have been the paralogues Vc-NhaP2 and Vc-NhaP3, but data suggests that each antiporter plays a distinct role under low cation concentrations (data not shown). Instead, an active K^+ transport system may be involved (for example, Trk, Ktr, or Kdp are known to act in *E. coli*, and may well act in *V. cholerae* as well). *In vitro* analysis of Vc-NhaP1 activity demonstrates it functions as an electroneutral $K^+(Na^+)/H^+$ antiporter at cytosolic pH optimum of 8.5. The next step in the study of Vc-NhaP1 is to compare its activity to that of the remaining paralogues Vc-NhaP2 and Vc-NhaP3. In particular, site directed mutagenesis could theoretically change the binding and transport specificity of any of the NhaP antiporters. This work is currently under way in the Dibrov laboratory.

The generation of a *V. cholerae* bioenergetics model system, comprised of a *V. cholerae* strain lacking both the *nqr* operon and the ORFs of *Vc-nhaA* or *Vc-nhaB* tested with and without lactate, allowed a detailed examination of the roles of NQR, Vc-NhaA, and Vc-NhaB in *V. cholerae*. These double mutant strains, along with the single mutants of *nqr*, *Vc-nhaA*, and *Vc-nhaB*, were assessed for aerobic growth as a function of media pH and cation concentration (Na^+, Li^+, or K^+). The effect of loss of Vc-NhaA and, to a lesser extent, Vc-NhaB, was better observed when NQR was absent but lactate was added to facilitate replenishment of the quinone pool. Loss of

Vc-NhaA in this background inhibited growth most at basic pH under increasing Na^+ and Li^+ conditions, and loss of Vc-NhaB in this background inhibited was most severe in acidic conditions in the presence of 0-100 mM Na^+ or Li^+, as demonstrated by complementation of the O395N1Δ*NQR*Δ*nhaB* strain with *nhaB*. We also observed the growth inhibition of Vc-NhaA in the absence of NQR and in the presence of lactate and 100-450 mM Li^+, which has not been previously reported. These growth defects were restored upon expression of the cognate gene on an inducible expression vector.

Regarding MCP receptor specificity in *V. cholerae*, it was found that 13 MCPs had no more than one identifiable homologue within the *Vibrionaceae*, and even among known MCPs their function was redundant, as expected. Interestingly, the 13 unique MCPs were either already associated with virulence (Section 1.6.7), or were shown to have some loss of function *in vivo* (Figure 4.5D) when disrupted by a Mariner transposon variant. Our results indicate that some of the 45 MCPs are predicted to be unique to *V. cholerae*. Complementation of the transposon-disrupted MCP VCA0663 rescued the swarming defect towards GlcNc in that mutant; chemotaxis towards the hybrid environmental/virulence chemoattractants Na^+ and K^+ was mediated by VC0098, though this defect was not able to be complemented. In each case, the mutant had residual chemotactic fitness, indicating other MCPs may play a redundant role. In frame deletion mutants of these, and other, MCPs will be necessary to assess which are specific to Na^+, GlcNc, mucin, and other environmental- and virulence-associated MCPs. Biochemical investigation of the cognate MCP binding sites, as well as screening of potential chemical inhibitors of binding, may yet

reveal drugs that inhibit chemotaxis in the environment or during infection. Clearly, much work remains to assign chemoattractant specificity to the remaining MCPs, work which will be greatly facilitated by high-throughput methods in years to come.

Future studies should capitalize on the results presented in this dissertation by further probing the interaction of *V. cholerae* bioenergetics and physiology. These include site directed mutagenesis of NhaP paralogues, complementation and overexpression of antiporter genes in an O395N1ΔnqrΔnhaA (or nhaB) background, and in-frame deletion of VCA0663 to validate its chemotaxis defect toward GlcNc. Ultimately, such research may help uncover environmental conditions which promote the survival of *V. cholerae* in an environmental reservoir. As we examine the biochemistry of MCPs and antiporters in more detail, drug design that inhibits the function of such proteins will become more feasible, and may represent a pharmacokinetic treatment option of *V. cholerae*.

6. Bibliography

Adler, J. (1966). "Effect of amino acids and oxygen on chemotaxis in Escherichia coli." *J Bacteriol* **92**(1): 121-129.

Adler, J. (1969). "Chemoreceptors in bacteria." *Science* **166**(3913): 1588-1597.

Alam, M., N. A. Hasan, A. Sadique, N. A. Bhuiyan, K. U. Ahmed, S. Nusrin, G. B. Nair, A. K. Siddique, R. B. Sack, D. A. Sack, A. Huq and R. R. Colwell (2006). Seasonal Cholera Caused by Vibrio cholerae Serogroups O1 and O139 in the Coastal Aquatic Environment of Bangladesh. **72:** 4096-4104.

Alam, M., M. Sultana, G. B. Nair, A. K. Siddique, N. A. Hasan, R. B. Sack, D. A. Sack, K. U. Ahmed, A. Sadique, H. Watanabe, C. J. Grim, A. Huq and R. R. Colwell (2007). Viable but nonculturable Vibrio cholerae O1 in biofilms in the aquatic environment and their role in cholera transmission. **104:** 17801-17806.

Albert, M. J., M. Neira and Y. Motarjemi (1997). "The role of food in the epidemiology of cholera." *World Health Stat Q* **50**(1-2): 111-118.

Albert, M. J., A. K. Siddique, M. S. Islam, A. S. Faruque, M. Ansaruzzaman, S. M. Faruque and R. B. Sack (1993). "Large outbreak of clinical cholera due to Vibrio cholerae non-O1 in Bangladesh." *Lancet* **341**(8846): 704.

Alexander, R. P. and I. B. Zhulin (2007). "Evolutionary genomics reveals conserved structural determinants of signaling and adaptation in microbial chemoreceptors." *Proc Natl Acad Sci U S A* **104**(8): 2885-2890.

Alm, R. A. and P. A. Manning (1990). "Characterization of the hlyB gene and its role in the production of the El Tor haemolysin of Vibrio cholerae O1." *Mol Microbiol* **4**(3): 413-425.

Altschul, S. F., T. L. Madden, A. A. Schaffer, J. Zhang, Z. Zhang, W. Miller and D. J. Lipman (1997). "Gapped BLAST and PSI-BLAST: a new generation of protein database search programs." *Nucleic Acids Res* **25**(17): 3389-3402.

Atsumi, T., Y. Maekawa, T. Yamada, I. Kawagishi, Y. Imae and M. Homma (1996). "Effect of viscosity on swimming by the lateral and polar flagella of Vibrio alginolyticus." *J Bacteriol* **178**(16): 5024-5026.

Atsumi, T., L. McCarter and Y. Imae (1992). "Polar and lateral flagellar motors of marine Vibrio are driven by different ion-motive forces." *Nature* **355**(6356): 182-184.

Azurin, J. C., A. Cruz, T. P. Pesigan, M. Alvero, T. Camena, R. Suplido, L. Ledesma and C. Z. Gomez (1967). "A controlled field trial of the effectiveness of cholera and cholera El Tor vaccines in the Philippines." *Bull World Health Organ* **37**(5): 703-727.

Azurin, J. C., K. Kobari, D. Barua, M. Alvero, C. Z. Gomez, J. J. Dizon, E. I. Nakano, R. Suplido and L. Ledesma (1967). "A long-term carrier of cholera: cholera Dolores." *Bull World Health Organ* **37**(5): 745-749.

Bakker, E. P. and W. E. Mangerich (1981). "Interconversion of components of the bacterial proton motive force by electrogenic potassium transport." *J Bacteriol* **147**(3): 820-826.

Barquera, B., P. Hellwig, W. Zhou, J. E. Morgan, C. C. Hase, K. K. Gosink, M. Nilges, P. J. Bruesehoff, A. Roth, C. R. Lancaster and R. B. Gennis (2002). "Purification and characterization of the recombinant Na(+)-translocating NADH:quinone oxidoreductase from Vibrio cholerae." *Biochemistry* **41**(11): 3781-3789.

Barquera, B., M. J. Nilges, J. E. Morgan, L. Ramirez-Silva, W. Zhou and R. B. Gennis (2004). "Mutagenesis study of the 2Fe-2S center and the FAD binding site of the Na(+)-translocating NADH:ubiquinone oxidoreductase from Vibrio cholerae." *Biochemistry* **43**(38): 12322-12330.

Barquera, B., W. Zhou, J. E. Morgan and R. B. Gennis (2002). "Riboflavin is a component of the Na+-pumping NADH-quinone oxidoreductase from Vibrio cholerae." *Proc Natl Acad Sci U S A* **99**(16): 10322-10324.

Bart, K. J., Z. Huq, M. Khan and W. H. Mosley (1970). "Seroepidemiologic studies during a simultaneous epidemic of infection with El Tor Ogawa and classical Inaba Vibrio cholerae." *J Infect Dis* **121**: Suppl 121:117+.

Barua, D. (1992). History of cholera. Cholera. (Current topics in infectious disease). D. Barua, Greenbough III, W.D. New York, NY, Plenum Publishing Corporation**:** 1-36.

Barua, D. and A. S. Paguio (1977). ABO blood groups and cholera. **4:** 489-492.

Baudry, B., A. Fasano, J. Ketley and J. B. Kaper (1992). "Cloning of a gene (zot) encoding a new toxin produced by Vibrio cholerae." *Infect Immun* **60**(2): 428-434.

Beck, N. A., E. S. Krukonis and V. J. DiRita (2004). "TcpH influences virulence gene expression in Vibrio cholerae by inhibiting degradation of the transcription activator TcpP." *J Bacteriol* **186**(24): 8309-8316.

Benenson, A. S. (1990). Cholera. Control of Communicable Diseases in Man. A. S. Benenson. Washington, D. C., American Public Health Association**:** 89-94.

Bentivoglio, M. and P. Pacini (1995). "Filippo Pacini: A determined observer." *Brain Research Bulletin* **38**(2): 161-165.

Berg, H. C. and D. A. Brown (1972). "Chemotaxis in Escherichia coli analysed by three-dimensional tracking." *Nature* **239**(5374): 500-504.

Bespalov, V. A., I. B. Zhulin and B. L. Taylor (1996). "Behavioral responses of Escherichia coli to changes in redox potential." *Proc Natl Acad Sci U S A* **93**(19): 10084-10089.

Bibikov, S. I., R. Biran, K. E. Rudd and J. S. Parkinson (1997). "A signal transducer for aerotaxis in Escherichia coli." *J Bacteriol* **179**(12): 4075-4079.

Bogachev, A. V., Y. V. Bertsova, E. K. Ruuge, M. Wikstrom and M. I. Verkhovsky (2002). "Kinetics of the spectral changes during reduction of the Na+-motive NADH:quinone oxidoreductase from Vibrio harveyi." *Biochim Biophys Acta* **1556**(2-3): 113-120.

Boin, M. A., M. J. Austin and C. C. Hase (2004). "Chemotaxis in Vibrio cholerae." *FEMS Microbiol Lett* **239**(1): 1-8.

Boin, M. A. and C. C. Hase (2007). "Characterization of Vibrio cholerae aerotaxis." *FEMS Microbiol Lett* **276**(2): 193-201.

Bott, M., K. Pfister, P. Burda, O. Kalbermatter, G. Woehlke and P. Dimroth (1997). "Methylmalonyl-CoA decarboxylase from Propionigenium modestum--cloning and sequencing of the structural genes and purification of the enzyme complex." *Eur J Biochem* **250**(2): 590-599.

Boyd, A., K. Kendall and M. I. Simon (1983). "Structure of the serine chemoreceptor in Escherichia coli." *Nature* **301**(5901): 623-626.

Bren, A. and M. Eisenbach (2001). "Changing the direction of flagellar rotation in bacteria by modulating the ratio between the rotational states of the switch protein FliM." *J Mol Biol* **312**(4): 699-709.

Brown, R. C. and R. K. Taylor (1995). "Organization of tcp, acf, and toxT genes within a ToxT-dependent operon." *Mol Microbiol* **16**(3): 425-439.

Burnette, W. N. (1994). "AB5 ADP-ribosylating toxins: comparative anatomy and physiology." *Structure* **2**(3): 151-158.

Burrus, V., J. Marrero and M. K. Waldor (2006). "The current ICE age: biology and evolution of SXT-related integrating conjugative elements." *Plasmid* **55**(3): 173-183.

Butler, S. M. and A. Camilli (2004). "Both chemotaxis and net motility greatly influence the infectivity of Vibrio cholerae." *Proc Natl Acad Sci U S A* **101**(14): 5018-5023.

Cameron, D. E., J. M. Urbach and J. J. Mekalanos (2008). "A defined transposon mutant library and its use in identifying motility genes in Vibrio cholerae." *Proc Natl Acad Sci U S A* **105**(25): 8736-8741.

Carpenter, C. C. (1971). "Cholera: diagnosis and treatment." *Bull N Y Acad Med* **47**(10): 1192-1203.

Cash, R. A., S. I. Music, J. P. Libonati, M. J. Snyder, R. P. Wenzel and R. B. Hornick (1974). "Response of man to infection with Vibrio cholerae. I. Clinical, serologic, and bacteriologic responses to a known inoculum." *J Infect Dis* **129**(1): 45-52.

Cerda-Maira, F. A., C. S. Ringelberg and R. K. Taylor (2008). "The bile response repressor BreR regulates expression of the Vibrio cholerae breAB efflux system operon." *J Bacteriol* **190**(22): 7441-7452.

Champion, G. A., M. N. Neely, M. A. Brennan and V. J. DiRita (1997). "A branch in the ToxR regulatory cascade of Vibrio cholerae revealed by characterization of toxT mutant strains." *Mol Microbiol* **23**(2): 323-331.

Chaparro, A. P., S. K. Ali and K. E. Klose (2010). "The ToxT-dependent methyl-accepting chemoreceptors AcfB and TcpI contribute to Vibrio cholerae intestinal colonization." *FEMS Microbiol Lett* **302**(2): 99-105.

Chatterjee, S. N. and K. Chaudhuri (2003). "Lipopolysaccharides of Vibrio cholerae. I. Physical and chemical characterization." *Biochim Biophys Acta* **1639**(2): 65-79.

Chaudhuri, A. and C. R. DasAdhikary (1978). "Possible role of blood-group secretory substances in the aetiology of cholera." *Transactions of the Royal Society of Tropical Medicine and Hygiene* **72**(6): 664-665.

Chiavelli, D. A., J. W. Marsh and R. K. Taylor (2001). "The mannose-sensitive hemagglutinin of Vibrio cholerae promotes adherence to zooplankton." *Appl Environ Microbiol* **67**(7): 3220-3225.

Childers, B. M. and K. E. Klose (2007). Regulation of virulence in Vibrio cholerae: the ToxR regulon. **2:** 335-344.

Chun, J., A. Huq and R. R. Colwell (1999). "Analysis of 16S-23S rRNA intergenic spacer regions of Vibrio cholerae and Vibrio mimicus." *Appl Environ Microbiol* **65**(5): 2202-2208.

Clarke, S. and D. E. Koshland, Jr. (1979). "Membrane receptors for aspartate and serine in bacterial chemotaxis." *J Biol Chem* **254**(19): 9695-9702.

Clemens, J. D., D. A. Sack, J. R. Harris, J. Chakraborty, M. R. Khan, S. Huda, F. Ahmed, J. Gomes, M. R. Rao, A. M. Svennerholm and et al. (1989). "ABO blood groups and cholera: new observations on specificity of risk and modification of vaccine efficacy." *J Infect Dis* **159**(4): 770-773.

Cohen, M. B., R. A. Giannella, G. A. Losonsky, D. R. Lang, S. Parker, J. A. Hawkins, C. Gunther and G. A. Schiff (1999). "Validation and characterization of a human volunteer challenge model for cholera by using frozen bacteria of the new Vibrio cholerae epidemic serotype, O139." *Infect Immun* **67**(12): 6346-6349.

Colwell, R. R. (1996). "Global climate and infectious disease: the cholera paradigm." *Science* **274**(5295): 2025-2031.

Colwell, R. R., P. Brayton, D. Herrington, B. Tall, A. Huq and M. M. Levine (1996). "Viable but non-culturable <i>Vibrio cholerae</i> O1 revert to a cultivable state in the human intestine." *World Journal of Microbiology and Biotechnology* **12**(1): 28-31.

Colwell, R. R., A. Huq, M. S. Islam, K. M. A. Aziz, M. Yunus, N. H. Khan, A. Mahmud, R. B. Sack, G. B. Nair, J. Chakraborty, D. A. Sack and E. Russek-Cohen (2003). Reduction of cholera in Bangladeshi villages by simple filtration. **100:** 1051-1055.

Colwell, R. R. H., A. (1994). Vibrios in the environment: Viable but Non-Culturable *Vibrio cholerae*. Vibrio cholerae and Cholera: Molecular to Global Perspectives. I. B. Wachsmuth, P.; Olsvik, O. Washington, D.C., ASM Press**:** 117-133.

Corratge-Faillie, C., M. Jabnoune, S. Zimmermann, A. A. Very, C. Fizames and H. Sentenac (2010). "Potassium and sodium transport in non-animal cells: the Trk/Ktr/HKT transporter family." *Cell Mol Life Sci* **67**(15): 2511-2532.

Csonka, L. N. (1989). "Physiological and genetic responses of bacteria to osmotic stress." *Microbiol Rev* **53**(1): 121-147.

De, S. N. (1959). "Enterotoxicity of bacteria-free culture-filtrate of Vibrio cholerae." *Nature* **183**(4674): 1533-1534.

Dhar, U., M. L. Bennish, W. A. Khan, C. Seas, E. Huq Khan, M. J. Albert and M. Abdus Salam (1996). "Clinical features, antimicrobial susceptibility and toxin production in Vibrio cholerae O139 infection: comparison with V. cholerae O1 infection." *Trans R Soc Trop Med Hyg* **90**(4): 402-405.

Dibrov, P. (2005). "The sodium cycle in vibrio cholerae: riddles in the dark." *Biochemistry (Mosc)* **70**(2): 150-153.

Dorlencourt, F., D. Legros, C. Paquet, M. Neira, B. Ivanoff and E. Le Saout (1999). "Effectiveness of mass vaccination with WC/rBS cholera vaccine during an epidemic in Adjumani district, Uganda." *Bull World Health Organ* **77**(11): 949-950.

Duffy, E. B. and B. Barquera (2006). "Membrane topology mapping of the Na+-pumping NADH: quinone oxidoreductase from Vibrio cholerae by PhoA-green fluorescent protein fusion analysis." *J Bacteriol* **188**(24): 8343-8351.

Dufresne, A., M. Salanoubat, F. Partensky, F. Artiguenave, I. M. Axmann, V. Barbe, S. Duprat, M. Y. Galperin, E. V. Koonin, F. Le Gall, K. S. Makarova, M. Ostrowski, S. Oztas, C. Robert, I. B. Rogozin, D. J. Scanlan, N. Tandeau de Marsac, J. Weissenbach, P. Wincker, Y. I. Wolf and W. R. Hess (2003). "Genome sequence of the cyanobacterium Prochlorococcus marinus SS120, a nearly minimal oxyphototrophic genome." *Proc Natl Acad Sci U S A* **100**(17): 10020-10025.

Dutta, N. K., M. V. Panse and D. R. Kulkarni (1959). "Role of cholera a toxin in experimental cholera." *J Bacteriol* **78**: 594-595.

Dzioba-Winogrodzki, J., O. Winogrodzki, T. A. Krulwich, M. A. Boin, C. C. Hase and P. Dibrov (2009). "The *Vibrio cholerae* Mrp system: cation/proton antiport properties and enhancement of bile salt resistance in a heterologous host." *J Mol Microbiol Biotechnol* **16**(3-4): 176-186.

Dzioba, J., C. C. Hase, K. Gosink, M. Y. Galperin and P. Dibrov (2003). "Experimental verification of a sequence-based prediction: F(1)F(0)-type ATPase of Vibrio cholerae transports protons, not Na(+) ions." *J Bacteriol* **185**(2): 674-678.

Dzioba, J., E. Ostroumov, A. Winogrodzki and P. Dibrov (2002). "Cloning, functional expression in *Escherichia coli* and primary characterization of a new Na+/H+ antiporter, NhaD, of *Vibrio cholerae*." *Mol Cell Biochem* **229**(1-2): 119-124.

Enserink, M. No Vaccines in the Time of Cholera. **329:** 1462-1463.

Enserink, M. (2010). "Public health. No vaccines in the time of cholera." *Science* **329**(5998): 1462-1463.

Epstein, W. and B. S. Kim (1971). "Potassium transport loci in *Escherichia coli* K-12." *J Bacteriol* **108**(2): 639-644.

Everiss, K. D., K. J. Hughes, M. E. Kovach and K. M. Peterson (1994). "The Vibrio cholerae acfB colonization determinant encodes an inner membrane protein that is related to a family of signal-transducing proteins." *Infect Immun* **62**(8): 3289-3298.

Falke, J. J., R. B. Bass, S. L. Butler, S. A. Chervitz and M. A. Danielson (1997). "The two-component signaling pathway of bacterial chemotaxis: a molecular view of signal transduction by receptors, kinases, and adaptation enzymes." *Annu Rev Cell Dev Biol* **13**: 457-512.

Falke, J. J. and G. L. Hazelbauer (2001). "Transmembrane signaling in bacterial chemoreceptors." *Trends Biochem Sci* **26**(4): 257-265.

Faruque, A. S., D. Mahalanabis, S. S. Hoque and M. J. Albert (1994). "The relationship between ABO blood groups and susceptibility to diarrhea due to Vibrio cholerae 0139." *Clin Infect Dis* **18**(5): 827-828.

Faruque, S. M., Asadulghani, M. Kamruzzaman, R. K. Nandi, A. N. Ghosh, G. B. Nair, J. J. Mekalanos and D. A. Sack (2002). "RS1 element of Vibrio cholerae can propagate horizontally as a filamentous phage exploiting the morphogenesis genes of CTXphi." *Infect Immun* **70**(1): 163-170.

Faruque, S. M., K. Biswas, S. M. Udden, Q. S. Ahmad, D. A. Sack, G. B. Nair and J. J. Mekalanos (2006). "Transmissibility of cholera: in vivo-formed biofilms and their relationship to infectivity and persistence in the environment." *Proc Natl Acad Sci U S A* **103**(16): 6350-6355.

Fasano, A., B. Baudry, D. W. Pumplin, S. S. Wasserman, B. D. Tall, J. M. Ketley and J. B. Kaper (1991). "Vibrio cholerae produces a second enterotoxin, which affects intestinal tight junctions." *Proc Natl Acad Sci U S A* **88**(12): 5242-5246.

Felsenfeld, O. (1965). "Notes on food, beverages and fomites contaminated with Vibrio cholerae." *Bull World Health Organ* **33**(5): 725-734.

Finkelstein, R. A. (1996). Cholera, *Vibrio cholerae* O1 and O139, and Other Pathogenic Vibrios. Medical Microbiology. S. Baron. Galveston, University of Texas Medical Branch at Galveston.

Finkelstein, R. A., M. Boesman-Finkelstein, Y. Chang and C. C. Hase (1992). "Vibrio cholerae hemagglutinin/protease, colonial variation, virulence, and detachment." *Infect Immun* **60**(2): 472-478.

Finkelstein, R. A., M. Boesman-Finkelstein and P. Holt (1983). "Vibrio cholerae hemagglutinin/lectin/protease hydrolyzes fibronectin and ovomucin: F.M. Burnet revisited." *Proc Natl Acad Sci U S A* **80**(4): 1092-1095.

Finkelstein, R. A. and J. J. LoSpalluto (1969). "Pathogenesis of experimental cholera. Preparation and isolation of choleragen and choleragenoid." *J Exp Med* **130**(1): 185-202.

Finn, T. M., J. Reiser, R. Germanier and S. J. Cryz, Jr. (1987). "Cell-associated hemagglutinin-deficient mutant of Vibrio cholerae." *Infect Immun* **55**(4): 942-946.

Franceschini, P. (1971). " Filippo Pacini e il colera." *Physis (Rio de Janiero, Brazil)* **13**: 324-332.

Franzon, V. L., A. Barker and P. A. Manning (1993). "Nucleotide sequence encoding the mannose-fucose-resistant hemagglutinin of Vibrio cholerae O1 and construction of a mutant." *Infect Immun* **61**(7): 3032-3037.

Franzon, V. L. and P. A. Manning (1986). "Molecular cloning and expression in Escherichia coli K-12 of the gene for a hemagglutinin from Vibrio cholerae." *Infect Immun* **52**(1): 279-284.

Freter, R. and P. C. O'Brien (1981). "Role of chemotaxis in the association of motile bacteria with intestinal mucosa: chemotactic responses of Vibrio cholerae and description of motile nonchemotactic mutants." *Infect Immun* **34**(1): 215-221.

Furrer, E. M., M. F. Ronchetti, F. Verrey and K. M. Pos (2007). "Functional characterization of a NapA Na(+)/H(+) antiporter from Thermus thermophilus." *FEBS Lett* **581**(3): 572-578.

Gardel, C. L., J. J. Mekalanos and P. M. B. Virginia L. Clark (1994). [41] Regulation of cholera toxin by temperature, pH, and osmolarity. Methods in Enzymology, Academic Press. **Volume 235:** 517-526.

Gerchman, Y., Y. Olami, A. Rimon, D. Taglicht, S. Schuldiner and E. Padan (1993). "Histidine-226 is part of the pH sensor of NhaA, a Na+/H+ antiporter in Escherichia coli." *Proc Natl Acad Sci U S A* **90**(4): 1212-1216.

Gil, A. I., V. R. Louis, I. N. G. Rivera, E. Lipp, A. Huq, C. F. Lanata, D. N. Taylor, E. Russek-Cohen, N. Choopun, R. B. Sack and R. R. Colwell (2004). "Occurrence and distribution of Vibrio cholerae in the coastal environment of Peru." *Environmental Microbiology* **6**(7): 699-706.

Goldberg, H., P. Clayman and K. Skorecki (1988). "Mechanism of Li inhibition of vasopressin-sensitive adenylate cyclase in cultured renal epithelial cells." *Am J Physiol* **255**(5 Pt 2): F995-1002.

Gómez-Puyou, A., and Gómez-Lojero, C. (1977). The use of ionophores and channel formers in the study of the function of biological membranes.

. Current Topic in Bioenergetics

D. Rao Sanadi. New York, Academic Press. **6:** 221-257.

Gosink, K. K., R. Kobayashi, I. Kawagishi and C. C. Hase (2002). "Analyses of the roles of the three cheA homologs in chemotaxis of Vibrio cholerae." *J Bacteriol* **184**(6): 1767-1771.

Graves, P. M., J. J. Deeks, V. Demicheli and T. Jefferson "Vaccines for preventing cholera: killed whole cell or other subunit vaccines (injected)." *Cochrane Database Syst Rev*(8): CD000974.

Griffith, D. C., L. A. Kelly-Hope and M. A. Miller (2006). "Review of reported cholera outbreaks worldwide, 1995-2005." *Am J Trop Med Hyg* **75**(5): 973-977.

Guffanti, A. A., J. Cheng and T. A. Krulwich (1998). "Electrogenic antiport activities of the Gram-positive Tet proteins include a Na+(K+)/K+ mode that mediates net K+ uptake." *J Biol Chem* **273**(41): 26447-26454.

Gupta, S. and R. Chowdhury (1997). "Bile affects production of virulence factors and motility of Vibrio cholerae." *Infect Immun* **65**(3): 1131-1134.

Hamaide, F., D. J. Kushner and G. D. Sprott (1983). "Proton motive force and Na+/H+ antiport in a moderate halophile." *J Bacteriol* **156**(2): 537-544.

Hamashima, H., M. Iwasaki and T. Arai (1995). "A simple and rapid method for transformation of *Vibrio* species by electroporation." *Methods Mol Biol* **47**: 155-160.

Harkey, C. W., K. D. Everiss and K. M. Peterson (1994). "The Vibrio cholerae toxin-coregulated-pilus gene tcpI encodes a homolog of methyl-accepting chemotaxis proteins." *Infect Immun* **62**(7): 2669-2678.

Hase, C. C. and B. Barquera (2001). "Role of sodium bioenergetics in Vibrio cholerae." *Biochim Biophys Acta* **1505**(1): 169-178.

Hase, C. C., N. D. Fedorova, M. Y. Galperin and P. A. Dibrov (2001). "Sodium ion cycle in bacterial pathogens: evidence from cross-genome comparisons." *Microbiol Mol Biol Rev* **65**(3): 353-370, table of contents.

Hase, C. C. and J. J. Mekalanos (1998). "TcpP protein is a positive regulator of virulence gene expression in Vibrio cholerae." *Proc Natl Acad Sci U S A* **95**(2): 730-734.

Hase, C. C. and J. J. Mekalanos (1999). "Effects of changes in membrane sodium flux on virulence gene expression in Vibrio cholerae." *Proc Natl Acad Sci U S A* **96**(6): 3183-3187.

Heidelberg, J. F., J. A. Eisen, W. C. Nelson, R. A. Clayton, M. L. Gwinn, R. J. Dodson, D. H. Haft, E. K. Hickey, J. D. Peterson, L. Umayam, S. R. Gill, K. E. Nelson, T. D. Read, H. Tettelin, D. Richardson, M. D. Ermolaeva, J. Vamathevan, S. Bass, H. Qin, I. Dragoi, P. Sellers, L. McDonald, T. Utterback, R. D. Fleishmann, W. C. Nierman, O. White, S. L. Salzberg, H. O. Smith, R. R. Colwell, J. J. Mekalanos, J. C. Venter and C. M. Fraser (2000). "DNA sequence of both chromosomes of the cholera pathogen Vibrio cholerae." *Nature* **406**(6795): 477-483.

Hemp, J., H. Han, J. H. Roh, S. Kaplan, T. J. Martinez and R. B. Gennis (2007). "Comparative genomics and site-directed mutagenesis support the existence of only one input channel for protons in the C-family (cbb3 oxidase) of heme-copper oxygen reductases." *Biochemistry* **46**(35): 9963-9972.

Herrington, D. A., R. H. Hall, G. Losonsky, J. J. Mekalanos, R. K. Taylor and M. M. Levine (1988). "Toxin, toxin-coregulated pili, and the toxR regulon are essential for Vibrio cholerae pathogenesis in humans." *J Exp Med* **168**(4): 1487-1492.

Herz, K., S. Vimont, E. Padan and P. Berche (2003). "Roles of NhaA, NhaB, and NhaD Na+/H+ antiporters in survival of Vibrio cholerae in a saline environment." *J Bacteriol* **185**(4): 1236-1244.

Higgins, R. M. (1979). "The 1832 cholera epidemic in East London." *East London Record* **2**.

Hilpert, W., B. Schink and P. Dimroth (1984). "Life by a new decarboxylation-dependent energy conservation mechanism with Na as coupling ion." *Embo J* **3**(8): 1665-1670.

Hisatsune, K., S. Kondo, Y. Isshiki, T. Iguchi, Y. Kawamata and T. Shimada (1993). "O-antigenic lipopolysaccharide of Vibrio cholerae O139 Bengal, a new epidemic strain for recent cholera in the Indian subcontinent." *Biochem Biophys Res Commun* **196**(3): 1309-1315.

Ho, S. N., H. D. Hunt, R. M. Horton, J. K. Pullen and L. R. Pease (1989). "Site-directed mutagenesis by overlap extension using the polymerase chain reaction." *Gene* **77**(1): 51-59.

Hochhut, B., Y. Lotfi, D. Mazel, S. M. Faruque, R. Woodgate and M. K. Waldor (2001). "Molecular analysis of antibiotic resistance gene clusters in vibrio cholerae O139 and O1 SXT constins." *Antimicrob Agents Chemother* **45**(11): 2991-3000.

Holmgren, J., I. Lonnroth, J. Mansson and L. Svennerholm (1975). "Interaction of cholera toxin and membrane GM1 ganglioside of small intestine." *Proc Natl Acad Sci U S A* **72**(7): 2520-2524.

Holmner, A., A. Mackenzie and U. Krengel "Molecular basis of cholera blood-group dependence and implications for a world characterized by climate change." *FEBS Lett* **584**(12): 2548-2555.

Hood, M. A. and G. E. Ness (1982). Survival of Vibrio cholerae and Escherichia coli in estuarine waters and sediments. **43:** 578-584.

Hood, M. A., G. E. Ness, G. E. Rodrick and N. J. Blake (1983). "Distribution of<i>Vibrio cholerae</i> in two Florida estuaries." *Microbial Ecology* **9**(1): 65-75.

Hsiao, A., Z. Liu, A. Joelsson and J. Zhu (2006). "Vibrio cholerae virulence regulator-coordinated evasion of host immunity." *Proc Natl Acad Sci U S A* **103**(39): 14542-14547.

Hsiao, A., K. Toscano and J. Zhu (2008). "Post-transcriptional cross-talk between pro- and anti-colonization pili biosynthesis systems in Vibrio cholerae." *Mol Microbiol* **67**(4): 849-860.

Hung, D. T. and J. J. Mekalanos (2005). "Bile acids induce cholera toxin expression in Vibrio cholerae in a ToxT-independent manner." *Proc Natl Acad Sci U S A* **102**(8): 3028-3033.

Hung, D. T., E. A. Shakhnovich, E. Pierson and J. J. Mekalanos (2005). "Small-molecule inhibitor of Vibrio cholerae virulence and intestinal colonization." *Science* **310**(5748): 670-674.

Huq, A., E. B. Small, P. A. West, M. I. Huq, R. Rahman and R. R. Colwell (1983). "Ecological relationships between Vibrio cholerae and planktonic crustacean copepods." *Appl Environ Microbiol* **45**(1): 275-283.

Huq, A., P. A. West, E. B. Small, M. I. Huq and R. R. Colwell (1984). "Influence of water temperature, salinity, and pH on survival and growth of toxigenic Vibrio cholerae serovar 01 associated with live copepods in laboratory microcosms." *Appl Environ Microbiol* **48**(2): 420-424.

Huq, A. S., E.; West, P.; Colwell, R. (1984). The role of planktonic copepods in the survival and multiplication of *Vibrio cholerae* in the environment. *Vibrio cholerae* in the environment. R. R. Colwell. New York, NY, John Wiley & Sons.

Hyakutake, A., M. Homma, M. J. Austin, M. A. Boin, C. C. Hase and I. Kawagishi (2005). "Only one of the five CheY homologs in Vibrio cholerae directly switches flagellar rotation." *J Bacteriol* **187**(24): 8403-8410.

Inaba, K., T. Kuroda, T. Shimamoto, T. Kayahara, M. Tsuda and T. Tsuchiya (1994). "Lithium toxicity and Na+(Li+)/H+ antiporter in Escherichia coli." *Biol Pharm Bull* **17**(3): 395-398.

Jeffery, C. J. and D. E. Koshland, Jr. (1993). "Three-dimensional structural model of the serine receptor ligand-binding domain." *Protein Sci* **2**(4): 559-566.

Jobling, M. G. and R. K. Holmes (1997). "Characterization of hapR, a positive regulator of the Vibrio cholerae HA/protease gene hap, and its identification as

a functional homologue of the Vibrio harveyi luxR gene." *Mol Microbiol* **26**(5): 1023-1034.

Jonson, G., J. Holmgren and A. M. Svennerholm (1991). "Identification of a mannose-binding pilus on Vibrio cholerae El Tor." *Microb Pathog* **11**(6): 433-441.

Jonson, G., M. Lebens and J. Holmgren (1994). "Cloning and sequencing of Vibrio cholerae mannose-sensitive haemagglutinin pilin gene: localization of mshA within a cluster of type 4 pilin genes." *Mol Microbiol* **13**(1): 109-118.

Kaneko, T. and R. R. Colwell (1973). Ecology of Vibrio parahaemolyticus in Chesapeake Bay. **113:** 24-32.

Kanungo, S., A. Paisley, A. L. Lopez, M. Bhattacharya, B. Manna, D. R. Kim, S. H. Han, S. Attridge, R. Carbis, R. Rao, J. Holmgren, J. D. Clemens and D. Sur (2009). "Immune responses following one and two doses of the reformulated, bivalent, killed, whole-cell, oral cholera vaccine among adults and children in Kolkata, India: A randomized, placebo-controlled trial." *Vaccine* **27**(49): 6887-6893.

Kaper, J. B., J. G. Morris, Jr. and M. M. Levine (1995). "Cholera." *Clin Microbiol Rev* **8**(1): 48-86.

Karaolis, D. K., J. A. Johnson, C. C. Bailey, E. C. Boedeker, J. B. Kaper and P. R. Reeves (1998). "A Vibrio cholerae pathogenicity island associated with epidemic and pandemic strains." *Proc Natl Acad Sci U S A* **95**(6): 3134-3139.

Karpel, R., T. Alon, G. Glaser, S. Schuldiner and E. Padan (1991). "Expression of a sodium proton antiporter (NhaA) in Escherichia coli is induced by Na+ and Li+ ions." *J Biol Chem* **266**(32): 21753-21759.

Kassis, S., J. Hagmann, P. H. Fishman, P. P. Chang and J. Moss (1982). Mechanism of action of cholera toxin on intact cells. Generation of A1 peptide and activation of adenylate cyclase. **257:** 12148-12152.

Keen, M. F. and L. Bujalski (1992). "The diagnosis and treatment of cholera." *Nurse Pract* **17**(12): 53-56.

Khwaif, J. M., A. H. Hayyawi and T. I. Yousif "Cholera outbreak in Baghdad in 2007: an epidemiological study." *East Mediterr Health J* **16**(6): 584-589.

King, A. A., E. L. Ionides, M. Pascual and M. J. Bouma (2008). "Inapparent infections and cholera dynamics." *Nature* **454**(7206): 877-880.

King, C. A. and W. E. Van Heyningen (1973). "Deactivation of cholera toxin by a sialidase-resistant monosialosylganglioside." *J Infect Dis* **127**(6): 639-647.

Kiørboe, T. N., T.G. (1994). "Regulation of zooplankton biomass and production in a temperate, coastal ecosystem. I. Copepods." *Limnol. Oceanogr.* **39**: 493-507.

Kitko, R. D., R. L. Cleeton, E. I. Armentrout, G. E. Lee, K. Noguchi, M. B. Berkmen, B. D. Jones and J. L. Slonczewski (2009). "Cytoplasmic acidification and the benzoate transcriptome in *Bacillus subtilis*." *PLoS One* **4**(12): e8255.

Kitko, R. D., J. C. Wilks, G. M. Garduque and J. L. Slonczewski (2010). "Osmolytes contribute to pH homeostasis of *Escherichia coli*." *PLoS One* **5**(4): e10078.

Kluge, C., W. Laubinger and P. Dimroth (1992). "The Na(+)-translocating ATPase of Propionigenium modestum." *Biochem Soc Trans* **20**(3): 572-577.

Koch, R. (1884). "An Address on Cholera and its Bacillus." *Br Med J* **2**(1236): 453-459.

Kojima, S., K. Yamamoto, I. Kawagishi and M. Homma (1999). "The polar flagellar motor of Vibrio cholerae is driven by an Na+ motive force." *J Bacteriol* **181**(6): 1927-1930.

Kovacikova, G., W. Lin and K. Skorupski (2004). "Vibrio cholerae AphA uses a novel mechanism for virulence gene activation that involves interaction with the LysR-type regulator AphB at the tcpPH promoter." *Mol Microbiol* **53**(1): 129-142.

Kovacikova, G. and K. Skorupski (1999). "A Vibrio cholerae LysR homolog, AphB, cooperates with AphA at the tcpPH promoter to activate expression of the ToxR virulence cascade." *J Bacteriol* **181**(14): 4250-4256.

Kovacikova, G. and K. Skorupski (2002). "Regulation of virulence gene expression in Vibrio cholerae by quorum sensing: HapR functions at the aphA promoter." *Mol Microbiol* **46**(4): 1135-1147.

Kroll, R. G. and I. R. Booth (1981). "The role of potassium transport in the generation of a pH gradient in *Escherichia coli*." *Biochem J* **198**(3): 691-698.

Kroll, R. G. and I. R. Booth (1983). "The relationship between intracellular pH, the pH gradient and potassium transport in *Escherichia coli*." *Biochem J* **216**(3): 709-716.

Krukonis, E. S. and V. J. DiRita (2003). "DNA binding and ToxR responsiveness by the wing domain of TcpP, an activator of virulence gene expression in Vibrio cholerae." *Mol Cell* **12**(1): 157-165.

Kumar, P., P. A. Wilson, R. Bhai and S. Thomas "Characterization of an SXT variant Vibrio cholerae O1 Ogawa isolated from a patient in Trivandrum, India." *FEMS Microbiol Lett* **303**(2): 132-136.

Kuroda, T., N. Fujita, J. Utsugi, M. Kuroda, T. Mizushima and T. Tsuchiya (2004). "A major Li(+) extrusion system NhaB of Pseudomonas aeruginosa : comparison with the major Na(+) extrusion system NhaP." *Microbiol Immunol* **48**(4): 243-250.

Kuroda, T., T. Mizushima and T. Tsuchiya (2005). "Physiological roles of three Na+/H+ antiporters in the halophilic bacterium Vibrio parahaemolyticus." *Microbiol Immunol* **49**(8): 711-719.

Kuroda, T., T. Shimamoto, K. Inaba, M. Tsuda and T. Tsuchiya (1994). "Properties and sequence of the NhaA Na+/H+ antiporter of Vibrio parahaemolyticus." *J Biochem* **116**(5): 1030-1038.

Legros, D., C. Paquet, W. Perea, I. Marty, N. K. Mugisha, H. Royer, M. Neira and B. Ivanoff (1999). "Mass vaccination with a two-dose oral cholera vaccine in a refugee camp." *Bull World Health Organ* **77**(10): 837-842.

Levine, M. M. (1980). Immunity to cholera as evaluated in volunteers. Cholera and related diarrheas. O. H. Ouchterlony, J. Basel, Karger**:** 195-203.

Levine, M. M. B., R. E.; Clements, M. L.; Nalin, D. R.; Cisneros, L.; Finkelstein, R. A. (1981). Volunteer studies in development of vaccines against cholera and enterotoxigenic *Escherichia coli*: A review. Acute Enteric Infections in

Children: New Prospects for Treatment and Prevention. T. H. Holme, J.; Merson, M., Molby, R. Amsterdam, Elsevier**:** 443-459.

Liang, W., A. Pascual-Montano, A. J. Silva and J. A. Benitez (2007). "The cyclic AMP receptor protein modulates quorum sensing, motility and multiple genes that affect intestinal colonization in Vibrio cholerae." *Microbiology* **153**(Pt 9): 2964-2975.

Lin, P. C., K. Turk, C. C. Hase, G. Fritz and J. Steuber (2007). "Quinone reduction by the Na+-translocating NADH dehydrogenase promotes extracellular superoxide production in Vibrio cholerae." *J Bacteriol* **189**(10): 3902-3908.

Liu, X. and R. E. Parales (2008). "Chemotaxis of Escherichia coli to pyrimidines: a new role for the signal transducer tap." *J Bacteriol* **190**(3): 972-979.

Lonnroth, I. and J. Holmgren (1973). "Subunit structure of cholera toxin." *J Gen Microbiol* **76**(2): 417-427.

Lycke, N. (2005). "Targeted vaccine adjuvants based on modified cholera toxin." *Curr Mol Med* **5**(6): 591-597.

Magariyama, Y., S. Sugiyama, K. Muramoto, Y. Maekawa, I. Kawagishi, Y. Imae and S. Kudo (1994). "Very fast flagellar rotation." *Nature* **371**(6500): 752.

Meibom, K. L., X. B. Li, A. T. Nielsen, C. Y. Wu, S. Roseman and G. K. Schoolnik (2004). "The Vibrio cholerae chitin utilization program." *Proc Natl Acad Sci U S A* **101**(8): 2524-2529.

Mekalanos, J. J., D. J. Swartz, G. D. Pearson, N. Harford, F. Groyne and M. de Wilde (1983). "Cholera toxin genes: nucleotide sequence, deletion analysis and vaccine development." *Nature* **306**(5943): 551-557.

Metcalf, W. W., W. Jiang, L. L. Daniels, S. K. Kim, A. Haldimann and B. L. Wanner (1996). "Conditionally replicative and conjugative plasmids carrying lacZ alpha for cloning, mutagenesis, and allele replacement in bacteria." *Plasmid* **35**(1): 1-13.

Miller, C. J., B. S. Drasar and R. G. Feachem (1984). "Response of toxigenic *Vibrio cholerae* 01 to physico-chemical stresses in aquatic environments." *J Hyg (Lond)* **93**(3): 475-495.

Miller, V. L., V. J. DiRita and J. J. Mekalanos (1989). Identification of toxS, a regulatory gene whose product enhances toxR-mediated activation of the cholera toxin promoter. **171:** 1288-1293.

Miller, V. L. and J. J. Mekalanos (1988). A novel suicide vector and its use in construction of insertion mutations: osmoregulation of outer membrane proteins and virulence determinants in Vibrio cholerae requires toxR. **170:** 2575-2583.

Mitchell, P. (1961). "Coupling of phosphorylation to electron and hydrogen transfer by a chemi-osmotic type of mechanism." *Nature* **191**: 144-148.

Moorthy, S. and P. I. Watnick (2004). "Genetic evidence that the Vibrio cholerae monolayer is a distinct stage in biofilm development." *Mol Microbiol* **52**(2): 573-587.

Morris, J. G., Jr., G. E. Losonsky, J. A. Johnson, C. O. Tacket, J. P. Nataro, P. Panigrahi and M. L. Myron (1995). "Clinical and Immunologic Characteristics

of Vibrio cholerae O139 Bengal Infection in North American Volunteers." *J Infect Dis* **171**(4): 903-908.

Mosley, W. H., K. M. Aziz, A. S. Mizanur Rahman, A. K. Alauddin Chowdhury, A. Ahmed and M. Fahimuddin (1972). "Report of the 1966-67 cholera vaccine trial in rural East Pakistan." *Bull World Health Organ* **47**(2): 229-238.

Mosley, W. H., K. M. Aziz, A. S. Rahman, A. K. Chowdhury and A. Ahmed (1973). "Field trials of monovalent Ogawa and Inaba cholera vaccines in rural Bangladesh--three years of observation." *Bull World Health Organ* **49**(4): 381-387.

Moss, J. and M. Vaughan (1977). "Mechanism of action of choleragen. Evidence for ADP-ribosyltransferase activity with arginine as an acceptor." *J Biol Chem* **252**(7): 2455-2457.

Mukerjee, S., U. K. Roy and B. C. Rudra (1963). "Studies on Typing of Cholera Vibrios by Bacteriophage. V. Geographical Distribution of Phage-Types of Vibrio Cholerae." *Ann Biochem Exp Med* **23**: 523-530.

Nakamura, T., S. Kawasaki and T. Unemoto (1992). "Roles of K+ and Na+ in pH homeostasis and growth of the marine bacterium *Vibrio alginolyticus*." *J Gen Microbiol* **138**(6): 1271-1276.

Nakamura, T., H. Tokuda and T. Unemoto (1982). "Effects of pH and monovalent cations on the potassium ion exit from the marine bacterium, Vibrio alginolyticus, and the manipulation of cellular cation contents." *Biochimica et Biophysica Acta (BBA) - Biomembranes* **692**(3): 389-396.

Nakamura, T., H. Tokuda and T. Unemoto (1984). "K+/H+ antiporter functions as a regulator of cytoplasmic pH in a marine bacterium, *Vibrio alginolyticus*." *Biochim Biophys Acta* **776**(2): 330-336.

Nelson, E. (2009). "Beyond cholera-the Zimbabwe health crisis." *Lancet Infect Dis* **9**(10): 587-588.

Nielsen, A. T., N. A. Dolganov, G. Otto, M. C. Miller, C. Y. Wu and G. K. Schoolnik (2006). "RpoS controls the Vibrio cholerae mucosal escape response." *PLoS Pathog* **2**(10): e109.

NOAA. (2005, Feb. 23, 2005). "El Nino Definition." NOAA News Online Retrieved November 12, 2011, from http://www.nws.noaa.gov/ost/climate/STIP/ElNinoDef.htm.

Ohyama, T., K. Igarashi and H. Kobayashi (1994). "Physiological role of the chaA gene in sodium and calcium circulations at a high pH in Escherichia coli." *J Bacteriol* **176**(14): 4311-4315.

Organization, W. H. (2009). "Cholera outbreak--southern Sudan, 2007." *MMWR Morb Mortal Wkly Rep* **58**(13): 337-341.

Padan, E., N. Maisler, D. Taglicht, R. Karpel and S. Schuldiner (1989). "Deletion of ant in *Escherichia coli* reveals its function in adaptation to high salinity and an alternative Na+/H+ antiporter system(s)." *J Biol Chem* **264**(34): 20297-20302.

Padan, E., D. Zilberstein and S. Schuldiner (1981). "pH homeostasis in bacteria." *Biochim Biophys Acta* **650**(2-3): 151-166.

Pascual, M., X. Rodo, S. P. Ellner, R. Colwell and M. J. Bouma (2000). Cholera Dynamics and El Nino-Southern Oscillation. **289:** 1766-1769.

Pearson, G. D., V. J. DiRita, M. B. Goldberg, S. A. Boyko, S. B. Calderwood and J. J. Mekalanos (1990). "New attenuated derivatives of Vibrio cholerae." *Res Microbiol* **141**(7-8): 893-899.

Pearson, G. D., A. Woods, S. L. Chiang and J. J. Mekalanos (1993). "CTX genetic element encodes a site-specific recombination system and an intestinal colonization factor." *Proc Natl Acad Sci U S A* **90**(8): 3750-3754.

Pesigan, T. P., J. Plantilla and M. Rolda (1967). "Applied studies on the viability of El Tor vibrios." *Bull World Health Organ* **37**(5): 779-786.

Pierce, N. F. (1973). "Differential inhibitory effects of cholera toxoids and ganglioside on the enterotoxins of Vibrio cholerae and Escherichia coli." *J Exp Med* **137**(4): 1009-1023.

Pinner, E., Y. Kotler, E. Padan and S. Schuldiner (1993). "Physiological role of nhaB, a specific Na+/H+ antiporter in Escherichia coli." *J Biol Chem* **268**(3): 1729-1734.

Pollitzer, R., S. Swaroop and W. Burrows (1959). "Cholera." *Monogr Ser World Health Organ* **58**(43): 1001-1019.

Popova, L. G., G. A. Shumkova, I. M. Andreev and Y. V. Balnokin (2005). "Functional identification of electrogenic Na+-translocating ATPase in the plasma membrane of the halotolerant microalga Dunaliella maritima." *FEBS Lett* **579**(22): 5002-5006.

Qadri, F., M. I. Chowdhury, S. M. Faruque, M. A. Salam, T. Ahmed, Y. A. Begum, A. Saha, A. Al Tarique, L. V. Seidlein, E. Park, K. P. Killeen, J. J. Mekalanos, J. D. Clemens and D. A. Sack (2007). "Peru-15, a live attenuated oral cholera vaccine, is safe and immunogenic in Bangladeshi toddlers and infants." *Vaccine* **25**(2): 231-238.

Radchenko, M. V., R. Waditee, S. Oshimi, M. Fukuhara, T. Takabe and T. Nakamura (2006). "Cloning, functional expression and primary characterization of *Vibrio parahaemolyticus* K+/H+ antiporter genes in Escherichia coli." *Mol Microbiol* **59**(2): 651-663.

Rahav-Manor, O., O. Carmel, R. Karpel, D. Taglicht, G. Glaser, S. Schuldiner and E. Padan (1992). "NhaR, a protein homologous to a family of bacterial regulatory proteins (LysR), regulates nhaA, the sodium proton antiporter gene in Escherichia coli." *J Biol Chem* **267**(15): 10433-10438.

Ramamurthy, T., S. Garg, R. Sharma, S. K. Bhattacharya, G. B. Nair, T. Shimada, T. Takeda, T. Karasawa, H. Kurazano, A. Pal and et al. (1993). "Emergence of novel strain of Vibrio cholerae with epidemic potential in southern and eastern India." *Lancet* **341**(8846): 703-704.

Reguera, G. and R. Kolter (2005). "Virulence and the environment: a novel role for Vibrio cholerae toxin-coregulated pili in biofilm formation on chitin." *J Bacteriol* **187**(10): 3551-3555.

Resch, C. T., J. L. Winogrodzki, C. C. Hase and P. Dibrov (2010). "Insights into the biochemistry of the ubiquitous NhaP family of cation/H+ antiporters." *Biochem Cell Biol* **89**(2): 130-137.

Resch, C. T., J. L. Winogrodzki, C. T. Patterson, E. J. Lind, M. J. Quinn, P. Dibrov and C. C. Hase (2010). "The putative Na+/H+ antiporter of *Vibrio cholerae*, Vc-NhaP2, mediates the specific K+/H+ exchange in vivo." *Biochemistry* **49**(11): 2520-2528.

Russo, A. F. and D. E. Koshland, Jr. (1983). "Separation of signal transduction and adaptation functions of the aspartate receptor in bacterial sensing." *Science* **220**(4601): 1016-1020.

Sack, D. A., R. B. Sack, G. B. Nair and A. K. Siddique (2004). "Cholera." *The Lancet* **363**(9404): 223-233.

Sahyoun, N. and P. Cuatrecasas (1975). "Mechanism of activation of adenylate cyclase by cholera toxin." *Proc Natl Acad Sci U S A* **72**(9): 3438-3442.

Sakuma, T., N. Yamada, H. Saito, T. Kakegawa and H. Kobayashi (1998). "pH dependence of the function of sodium ion extrusion systems in Escherichia coli." *Biochim Biophys Acta* **1363**(3): 231-237.

Sayamov, R. M. (1963). "Laboratory studies on the El Tor vibrio." *Bull World Health Organ* **28**(3): 311-325.

Schuldiner, S. and E. Padan (1993). "Molecular analysis of the role of Na+/H+ antiporters in bacterial cell physiology." *Int Rev Cytol* **137C**: 229-266.

Sepulveda, J., H. Gomez-Dantes and M. Bronfman (1992). "Cholera in the Americas: an overview." *Infection* **20**(5): 243-248.

Sharma, C., G. B. Nair, A. K. Mukhopadhyay, S. K. Bhattacharya, R. K. Ghosh and A. Ghosh (1997). "Molecular characterization of Vibrio cholerae O1 biotype El Tor strains isolated between 1992 and 1995 in Calcutta, India: evidence for the emergence of a new clone of the El Tor biotype." *J Infect Dis* **175**(5): 1134-1141.

Shijuku, T., H. Saito, T. Kakegawa and H. Kobayashi (2001). "Expression of sodium/proton antiporter NhaA at various pH values in Escherichia coli." *Biochim Biophys Acta* **1506**(3): 212-217.

Shikuma, N. J. and F. H. Yildiz (2009). "Identification and characterization of OscR, a transcriptional regulator involved in osmolarity adaptation in Vibrio cholerae." *J Bacteriol* **191**(13): 4082-4096.

Shimamoto, T., K. Inaba, P. Thelen, T. Ishikawa, E. B. Goldberg, M. Tsuda and T. Tsuchiya (1994). "The NhaB Na+/H+ antiporter is essential for intracellular pH regulation under alkaline conditions in Escherichia coli." *J Biochem* **116**(2): 285-290.

Siddique, A. K. (1994). "Cholera epidemic among Rwandan refugees: experience of ICDDR,B in Goma, Zaire." *Glimpse* **16**(5): 3-4.

Siddique, A. K., A. Salam, M. S. Islam, K. Akram, R. N. Majumdar, K. Zaman, N. Fronczak and S. Laston (1995). "Why treatment centres failed to prevent cholera deaths among Rwandan refugees in Goma, Zaire." *Lancet* **345**(8946): 359-361.

Sidley, P. (2001). "Cholera sweeps through South African province." *Bmj* **322**(7278): 71.

Singleton, F. L., R. Attwell, S. Jangi and R. R. Colwell (1982). "Effects of temperature and salinity on *Vibrio cholerae* growth." *Appl Environ Microbiol* **44**(5): 1047-1058.

Singleton, F. L., R. W. Attwell, M. S. Jangi and R. R. Colwell (1982). "Influence of salinity and organic nutrient concentration on survival and growth of *Vibrio cholerae* in aquatic microcosms." *Appl Environ Microbiol* **43**(5): 1080-1085.

Slonczewski, J. L., B. P. Rosen, J. R. Alger and R. M. Macnab (1981). "pH homeostasis in *Escherichia coli*: measurement by 31P nuclear magnetic resonance of methylphosphonate and phosphate." *Proc Natl Acad Sci U S A* **78**(10): 6271-6275.

Sourjik, V. and H. C. Berg (2002). "Receptor sensitivity in bacterial chemotaxis." *Proc Natl Acad Sci U S A* **99**(1): 123-127.

Spangler, B. D. (1992). "Structure and function of cholera toxin and the related Escherichia coli heat-labile enterotoxin." *Microbiol Rev* **56**(4): 622-647.

Spohn, G. a. S., V. (2001). Motility, Chemotaxis, and Flagella. *Helicobacter pylori*: Physiology and Genetics. H. L. T. Mobley, Mendz, G.L., Hazell, S.L. Washington (DC), ASM Press.

Springer, M. S., M. F. Goy and J. Adler (1977). "Sensory transduction in Escherichia coli: two complementary pathways of information processing that involve methylated proteins." *Proc Natl Acad Sci U S A* **74**(8): 3312-3316.

Springer, W. R. and D. E. Koshland, Jr. (1977). "Identification of a protein methyltransferase as the cheR gene product in the bacterial sensing system." *Proc Natl Acad Sci U S A* **74**(2): 533-537.

Strausak, D., M. Waser and M. Solioz (1993). "Functional expression of the Enterococcus hirae NaH-antiporter in Escherichia coli." *J Biol Chem* **268**(35): 26334-26337.

Swerdlow, D. L., E. D. Mintz, M. Rodriguez, E. Tejada, C. Ocampo, L. Espejo, T. J. Barrett, J. Petzelt, N. H. Bean, L. Seminario and et al. (1994). "Severe life-threatening cholera associated with blood group O in Peru: implications for the Latin American epidemic." *J Infect Dis* **170**(2): 468-472.

Syed, K. A., S. Beyhan, N. Correa, J. Queen, J. Liu, F. Peng, K. J. Satchell, F. Yildiz and K. E. Klose (2009). "The Vibrio cholerae flagellar regulatory hierarchy controls expression of virulence factors." *J Bacteriol* **191**(21): 6555-6570.

Tacket, C. O., G. Losonsky, J. P. Nataro, S. J. Cryz, R. Edelman, A. Fasano, J. Michalski, J. B. Kaper and M. M. Levine (1993). "Safety and immunogenicity of live oral cholera vaccine candidate CVD 110, a delta ctxA delta zot delta ace derivative of El Tor Ogawa Vibrio cholerae." *J Infect Dis* **168**(6): 1536-1540.

Taglicht, D., E. Padan and S. Schuldiner (1991). "Overproduction and purification of a functional Na+/H+ antiporter coded by nhaA (ant) from Escherichia coli." *J Biol Chem* **266**(17): 11289-11294.

Taglicht, D., E. Padan and S. Schuldiner (1993). "Proton-sodium stoichiometry of NhaA, an electrogenic antiporter from Escherichia coli." *J Biol Chem* **268**(8): 5382-5387.

Takeya, K., T. Otohuji and H. Tokiwa (1981). "FK phage for differentiating the classical and El T or groups of Vibrio cholerae." *J Clin Microbiol* **14**(2): 222-224.

Tamplin, M. L., A. L. Gauzens, A. Huq, D. A. Sack and R. R. Colwell (1990). "Attachment of Vibrio cholerae serogroup O1 to zooplankton and phytoplankton of Bangladesh waters." *Appl Environ Microbiol* **56**(6): 1977-1980.

Tamura, K., J. Dudley, M. Nei and S. Kumar (2007). "MEGA4: Molecular Evolutionary Genetics Analysis (MEGA) software version 4.0." *Mol Biol Evol* **24**(8): 1596-1599.

Taylor, R. K., V. L. Miller, D. B. Furlong and J. J. Mekalanos (1987). "Use of phoA gene fusions to identify a pilus colonization factor coordinately regulated with cholera toxin." *Proc Natl Acad Sci U S A* **84**(9): 2833-2837.

Thelen, P., T. Tsuchiya and E. B. Goldberg (1991). "Characterization and mapping of a major Na+/H+ antiporter gene of Escherichia coli." *J Bacteriol* **173**(20): 6553-6557.

Tokuda, H., T. Nakamura and T. Unemoto (1981). "Potassium ion is required for the generation of pH-dependent membrane potential and delta pH by the marine bacterium *Vibrio alginolyticus*." *Biochemistry* **20**(14): 4198-4203.

Tokuda, H. and T. Unemoto (1981). "A respiration-dependent primary sodium extrusion system functioning at alkaline pH in the marine bacterium *Vibrio alginolyticus*." *Biochem Biophys Res Commun* **102**(1): 265-271.

Tokuda, H. and T. Unemoto (1982). "Characterization of the respiration-dependent Na+ pump in the marine bacterium *Vibrio alginolyticus*." *J Biol Chem* **257**(17): 10007-10014.

Trucksis, M., J. E. Galen, J. Michalski, A. Fasano and J. B. Kaper (1993). "Accessory cholera enterotoxin (Ace), the third toxin of a Vibrio cholerae virulence cassette." *Proc Natl Acad Sci U S A* **90**(11): 5267-5271.

Turk, K., A. Puhar, F. Neese, E. Bill, G. Fritz and J. Steuber (2004). "NADH oxidation by the Na+-translocating NADH:quinone oxidoreductase from Vibrio cholerae: functional role of the NqrF subunit." *J Biol Chem* **279**(20): 21349-21355.

Van Dellen, K. L., L. Houot and P. I. Watnick (2008). "Genetic analysis of Vibrio cholerae monolayer formation reveals a key role for DeltaPsi in the transition to permanent attachment." *J Bacteriol* **190**(24): 8185-8196.

van Opijnen, T., K. L. Bodi and A. Camilli (2009). "Tn-seq: high-throughput parallel sequencing for fitness and genetic interaction studies in microorganisms." *Nat Methods* **6**(10): 767-772.

Venkatraman, K. V. R., C. S. (1941). "A preserving medium for the transmission of specimens for the isolation of *Vibrio cholerae*." *Indian J Med Res* **29**: 681-684.

Vimont, S. and P. Berche (2000). "NhaA, an Na(+)/H(+) antiporter involved in environmental survival of *Vibrio cholerae*." *J Bacteriol* **182**(10): 2937-2944.

Wadhams, G. H. and J. P. Armitage (2004). "Making sense of it all: bacterial chemotaxis." *Nat Rev Mol Cell Biol* **5**(12): 1024-1037.

Waldor, M. K. and J. J. Mekalanos (1996). "Lysogenic conversion by a filamentous phage encoding cholera toxin." *Science* **272**(5270): 1910-1914.

Waldor, M. K., H. Tschape and J. J. Mekalanos (1996). "A new type of conjugative transposon encodes resistance to sulfamethoxazole, trimethoprim, and streptomycin in Vibrio cholerae O139." *J Bacteriol* **178**(14): 4157-4165.

Watnick, P. I., K. J. Fullner and R. Kolter (1999). "A role for the mannose-sensitive hemagglutinin in biofilm formation by Vibrio cholerae El Tor." *J Bacteriol* **181**(11): 3606-3609.

Watnick, P. I., C. M. Lauriano, K. E. Klose, L. Croal and R. Kolter (2001). "The absence of a flagellum leads to altered colony morphology, biofilm development and virulence in Vibrio cholerae O139." *Mol Microbiol* **39**(2): 223-235.

Watten, R. H., F. M. Morgan, S. Yachai Na, B. Vanikiati and R. A. Phillips (1959). "Water and electrolyte studies in cholera." *J Clin Invest* **38**: 1879-1889.

Webb, D. (1939). "The sodium and potassium content of seawater." *J Exp Biol* **16**: 178-183.

Williams, S. G., O. Carmel-Harel and P. A. Manning (1998). "A functional homolog of Escherichia coli NhaR in Vibrio cholerae." *J Bacteriol* **180**(3): 762-765.

Wilson, G. (1984). Cholera. Topley and Wilson's principles of bacteriology, virology, and immunology. G. Wilson, A. Miles, M. T. Parker. Baltimore, Williams and Wilkins. **3:** 446-457.

Withey, J. H. and V. J. DiRita (2006). "The toxbox: specific DNA sequence requirements for activation of Vibrio cholerae virulence genes by ToxT." *Mol Microbiol* **59**(6): 1779-1789.

Xie, L., T. Altindal, S. Chattopadhyay and X. L. Wu (2011). "From the Cover: Bacterial flagellum as a propeller and as a rudder for efficient chemotaxis." *Proc Natl Acad Sci U S A* **108**(6): 2246-2251.

Yeh, J. I., H. P. Biemann, G. G. Prive, J. Pandit, D. E. Koshland, Jr. and S. H. Kim (1996). "High-resolution structures of the ligand binding domain of the wild-type bacterial aspartate receptor." *J Mol Biol* **262**(2): 186-201.

Yonekawa, H., H. Hayashi and J. S. Parkinson (1983). "Requirement of the cheB function for sensory adaptation in Escherichia coli." *J Bacteriol* **156**(3): 1228-1235.

Zhang, R. G., D. L. Scott, M. L. Westbrook, S. Nance, B. D. Spangler, G. G. Shipley and E. M. Westbrook (1995). "The three-dimensional crystal structure of cholera toxin." *J Mol Biol* **251**(4): 563-573.

Zhang, R. G., M. L. Westbrook, E. M. Westbrook, D. L. Scott, Z. Otwinowski, P. R. Maulik, R. A. Reed and G. G. Shipley (1995). "The 2.4 A crystal structure of cholera toxin B subunit pentamer: choleragenoid." *J Mol Biol* **251**(4): 550-562.

Zhou, W., Y. V. Bertsova, B. Feng, P. Tsatsos, M. L. Verkhovskaya, R. B. Gennis, A. V. Bogachev and B. Barquera (1999). "Sequencing and preliminary characterization of the Na+-translocating NADH:ubiquinone oxidoreductase from *Vibrio harveyi*." *Biochemistry* **38**(49): 16246-16252.

Zilberstein, D., V. Agmon, S. Schuldiner and E. Padan (1982). "The sodium/proton antiporter is part of the pH homeostasis mechanism in *Escherichia coli*." *J Biol Chem* **257**(7): 3687-3691.